Trace: Tennessee Research and Creative Exchange

Doctoral Dissertations

University of Tennessee 2010

Dynamics of the Toc GTPases: Modulation by Nucleotides and Transit Peptides Reveal a Mechanism for Chloroplast Protein Import

Lovett Evan Reddick
University of Tennessee - Knoxville, lreddick@utk.edu

Reddick, Lovett Evan, "Dynamics of the Toc GTPases: Modulation by Nucleotides and Transit Peptides Reveal a Mechanism for Chloroplast Protein Import. " PhD diss., University of Tennessee, 2010.
http://trace.tennessee.edu/utk_graddiss/743

To the Graduate Council:

I am submitting herewith a dissertation written by Lovett Evan Reddick entitled "Dynamics of the Toc GTPases: Modulation by nucleotides and transit peptides." I have examined the final electronic copy of this dissertation for form and content and recommend that it be accepted in partial fulfillment of the requirements for the degree of Doctor of Philosophy, with a major in Biochemistry and Cellular and Molecular Biology.

Barry D. Bruce, Major Professor

We have read this dissertation and recommend its acceptance:

Elias Fernandez

Beth Mullin

Andreas Nebenführ

Cynthia Peterson

Accepted for the Council:

Carolyn R. Hodges, Vice Provost and
Dean of the Graduate School

(Original signatures are on file with official student records)

Dynamics of the Toc GTPases: Modulation by Nucleotides and Transit Peptides Reveal a Mechanism for Chloroplast Protein Import

A Thesis Presented for the
Doctor of Philosophy Degree
The University of Tennessee, Knoxville

Lovett Evan Reddick

May 2010

Copyright © 2009 by Lovett Evan Reddick
All rights reserved.

ACKNOWLEDGEMENTS

First, I would like to thank my mentor and advisor, Dr. Barry D. Bruce. His unique style of motivation and training has transformed me into a young scientist; I am very fortunate indeed to have had the opportunity to be a member of his laboratory. I thank Drs. Andreas Nebenführ and Albrecht Von Arnim for our many discussions in the hallways of Hesler, and I thank the members of my committee, Drs. Elias Fernandez, Beth Mullin, Andreas Nebenführ and Cynthia Peterson. I would also like to thank past and present members of the Bruce laboratory, namely Michael Vaughn and Sarah Wright. Other members whose contributions are too great to list are Natalie Myers, Ashita Dave, Richard Simmerman, Non Chotewutmontri, Will Crenshaw, Letitia Olson and Ian “The Anion” Campbell.

Furthermore, I would like to thank the organizations who funded my research and travels: the National Science Foundation, the American Society of Plant Biologists, The Science Alliance, Sigma Xi Scientific Society and the Department of Biochemistry, Cellular and Molecular Biology.

Finally, I am forever indebted to my wife and her family for their constant encouragement and seemingly unending patience. I thank my father, Dr. Lovett. P. Reddick, MD and my sister, Alice Vickers “Polly” Reddick, for their support and encouragement, both through their words and their actions. Witnessing their own personal struggles during mine as a graduate student has been humbling. My mother passed away knowing I had been accepted to graduate school, but unfortunately she was unable to witness my transformation as a scientist. This thesis is dedicated to her memory.

ABSTRACT

The chloroplast is the green organelle in the plant cell responsible for harvesting energy from sunlight and converting it into sugars and ATP. Origins of this organelle can be traced back to an endosymbiotic event in which a primitive eukaryotic cell capable of oxidative phosphorylation engulfed a free-living cyanobacterium capable of photosynthetic respiration (1). Immediately following this event the details are not clear, however what is known is that over the course of evolution, the engulfed cyanobacteria relinquished approximately 97% of its protein coding sequences to the host cell nucleus, thus making the newly formed chloroplast reliant on its host cell (2). This resulted in the requirement of a post-translational import mechanism (3,4). Accomplishing posttranslational import are Translocons of the Outer and Inner Chloroplast membranes, or TOC and TIC complexes (5). These complexes are comprised of multiple proteins whose function is the efficient and robust recognition of chloroplast-destined preproteins and their subsequent import. Preproteins are synthesized in the cytosol with a cleavable Nterminal extension of approximately 50-150 amino acids known as a transit peptide (6-8). It is the transit peptide that is recognized by the Toc complex which facilitates the import of the preprotein (9). It is this transit peptide mediated chloroplast protein import mechanism that will be the subject of this dissertation. Presented in Chapter II is an analysis of the basal enzymology of the isolated, soluble forms of the Toc GTPases. Chapter III analyzes the homo- and heterodimeric interaction between Toc proteins and how this oligomerization can be modulated. Chapter IV presents evidence that the transit 2 peptide interacts with the Toc proteins in such a way as to increase enzymatic activity as well as bias the dimeric equilibria. Analysis of the data presented in Chapters II, III and IV allow the creation of a chloroplast protein import model, Chapter V, to potentially explain the observed phenomenon. Finally, Chapter VI presents potential future directions for this research.

TABLE OF CONTENTS

CHAPTER		PAGE
CHAPTER I		
INTRODUCTION		1
1.1	General Introduction	1
1.2	Endosymbiotic Origin of the Chloroplast	2
1.3	Chloroplast Protein Import	4
1.4	General Import Pathway	7
1.5	The Toc Core Complex	11
1.5.1	Toc34	12
1.5.2	Toc159	13
1.5.3	Toc75	15
1.6	GTPase Activity of Toc34 and Toc159	16
1.7	Tic Complex	18
1.7.1	Tic110	18
1.7.2	Tic40	19
1.7.3	Tic20 and Tic22	19
1.8	Cytosolic Factors in Chloroplast Protein Import	20
1.9	The Transit Peptide	23
1.10	Summary	26
CHAPTER II		
KINETIC CHARACTERIZATION AND BASAL ENZYMOLOGY OF THE TOC GTPASES		27
2.1	Abstract	27
2.2	Introduction	28
2.3	Materials and Methods	29
2.3.1	Expression and Purification of the Toc GTPases	29
2.3.2	Phosphate Release Assay for GTP Hydrolysis	30
2.3.3	Determination of Enzyme Velocity and Substrate Affinity	31
2.3.4	Optimization of Buffer and Storage Conditions	33
2.3.5	Effect of Cation Replacement on psToc34 Activity	34
2.3.6	Creation of psToc34 Mutants	34
2.3.7	Circular Dichroism Analysis of psToc34(R133A)	35
2.3.8	Activation Energies of the Toc GTPases	35
2.3.9	Nucleotide Binding Studies	36
2.3.10	Global Fit Analysis of Nucleotide Binding Data	38
2.4	Results	38
2.4.1	Expression and Purification of Toc and Transit Peptides	38
2.4.2	Generation of Glycerol Stabiliized IMAC-Toc34 Columns	42
2.4.3	Effects of Buffers, Storage, [Enzyme] and Metal Ions	43
2.4.4	Hydrolysis Activity of the Toc GTPases	45
2.4.5	Hydroysis Rates of the Toc GTPases are not Influenced by Concentration-Dependent Dimerization	46

2.4.6 The Mutant Protein psToc34(R133A) is Monomeric and Lacks GTPase Activity 49
2.4.7 Activation Energies of the Toc GTPases 56
2.4.8 Nucleotide Binding Activity of the Toc GTPases 56
2.4.9 Nucleotide Exchange of psToc34 is Not Stimulated by Transit Peptide 62
2.4.10 Creation of a Toc XTPase 63
2.5 Discussion 66
2.6 Summary 72

CHAPTER III
TOC PROTEIN INTERACTIONS 74
3.1 Abstract 74
3.2 Introduction 74
3.3 Materials and Methods 77
3.3.1 Generation of Lipisomes and Detergent Micelles 77
3.3.2 Homobifunctional Chemical Crosslinking 78
3.3.3 SDS-PAGE and Western Analysis of Crosslinked Proteins 80
3.3.4 Transit Peptide Crosslinking and Detection 82
3.3.5 Nucleotides and Transition-State Analogue Modulation of psToc34 82
3.4 Results 83
3.4.1 Liposomes and Detergent Micelle Modulation of psToc34 Activity 83
3.4.2 Trapping psToc34 on Lipid Membranes 87
3.4.3 Heterodimerization of psToc34 and psToc159G is Revealed by Homobifunctional Crosslinking 89
3.4.4 The Dimer of psToc34 is Modulated by Nucleotides and a Transition State Analogue 89
3.4.5 Transit Peptide Modulates Heterodimerization of psToc34 and psToc159G 93
3.5 Discussion 97
3.6 Summary 100

CHAPTER IV
TOC – TRANSIT PEPTIDE INTERACTIONS
4.1 Abstract 102
4.2 Introduction 103
4.3 Materials and Methods 105
4.3.1 Transit Peptide Mutagenesis 105
4.3.2 Protein Purification 106
4.3.3 Circular Dichroism Spectroscopy 107
4.3.4 Generation of Transit Peptide Affinity Column and Binding of psToc34 with Nucleotides and Transition State Analogues 107
4.3.5 Hydrolysis Measurements of psToc34 109

4.3.6 Effect of Transit Peptide on Nucleotide Exchange 109
4.3.7 Homobifunctional Chemical Crosslinking 110
4.3.8 Analysis of Fluorescently Labeled Transit Peptides 110
4.3.9 GEF Assay 111
4.3.10 *In Organeller* Chloroplast GTPase Assay 113
4.4 Results 114
4.4.1 Transit Peptide Mutagenesis and Purification 114
4.4.2 Induced Secondary Structure of the Transit Peptide 114
4.4.3 Nucleotides and Transition State Analogues Modulate Transit Peptide Affinity for psToc34 118
4.4.4 Hydrolysis Rate and Affinity for GTP are Stimulated by Transit Peptide 119
4.4.5 Transit Peptide Mutants Differentially Modulate psToc34 GTPase Activity and Monomer / Dimer Equilibrium 123
4.4.6 Both psToc34 and psToc159G Bind Transit Peptide with Varying Degrees of Affinity 124
4.4.7 Transit Peptide Induced Dimer to Monomer Transition is Titratable 130
4.4.8 The psToc34 Protein Interacts Primarily with the C-terminus of the Transit Peptide 134
4.4.9 Transit Peptide Bound psToc159G Acts as GEF for psToc34 140
4.4.10 *In Organeller* GTPase Assays Reveal GTP Requirement During Chloroplast Protein Import 143
4.5 Discussion 145
4.6 Summary 151

CHAPTER V
THE TOC CLOCK: THE UNIFIED MODEL OF CHLOROPLAST PROTEIN TRANSLOCATION
5.1 Abstract 153
5.2 Evolutionary Origins of the Toc Translocon 153
5.2.1 Cyanobacterial Origin of Toc75 154
5.2.2 Eukaryotic Origin of Toc34 and Toc159 155
5.3 Stoichiometry of the Toc Translocon 155
5.4 Electron Microscopy Studies of the Chloroplast Outer Membrane 157
5.5 Enzymology of the Toc Complex 159
5.6 Chloroplast Protein Import Models: The Motor and Targeting Hypotheses 159
5.6.1 The Motor Hypothesis 160
5.6.2 The Targeting Hypothesis 162
5.7 The Toc Clock 164
5.7.1 Step I 166
5.7.2 Step II 166
5.7.3 Step III 166
5.7.4 Step IV 167
5.7.5 Step V 167

5.7.6 Step VI 167
5.8 Summary 167

CHAPTER VI
CONCLUSIONS AND FUTURE DIRECTIONS
6.1 Conclusions 169
6.2 Future Directions 171

REFERENCES 174
VITA 181

LIST OF FIGURES

FIGURE	PAGE
Figure 1-1	3
Figure 1-2	5
Figure 1-3	8
Figure 1-4	14
Figure 1-5	17
Figure 1-6	21
Figure 2-1	39
Figure 2-2	44
Figure 2-3	48
Figure 2-4	50
Figure 2-5	51
Figure 2-6	53
Figure 2-7	54
Figure 2-8	55
Figure 2-9	59
Figure 2-10	60
Figure 2-11	64
Figure 2-12	65
Figure 3-1	79
Figure 3-2	85
Figure 3-3	86
Figure 3-4	88
Figure 3-5	90
Figure 3-6	92
Figure 3-7	94
Figure 4-1	115
Figure 4-2	117
Figure 4-3	120
Figure 4-4	122
Figure 4-5	125
Figure 4-6	127
Figure 4-7	131
Figure 4-8	133
Figure 4-9	136
Figure 4-10	138
Figure 4-11	142
Figure 4-12	144
Figure 5-1	158
Figure 5-2	161
Figure 5-3	163
Figure 5-4	165

CHAPTER I

Introduction

1.1 General Introduction

The chloroplast is the green organelle in the plant cell responsible for harvesting energy from sunlight and converting it into sugars and ATP. Origins of this organelle can be traced back to an endosymbiotic event in which a primitive eukaryotic cell capable of oxidative phosphorylation engulfed a free-living cyanobacterium capable of photosynthetic respiration (1). Immediately following this event the details are not clear, however what is known is that over the course of evolution, the engulfed cyanobacteria relinquished approximately 97% of its protein coding sequences to the host cell nucleus, thus making the newly formed chloroplast reliant on its host cell (2). This resulted in the requirement of a post-translational import mechanism (3,4). Accomplishing post-translational import are **T**ranslocons of the **O**uter and **I**nner **C**hloroplast membranes, or TOC and TIC complexes (5). These complexes are comprised of multiple proteins whose function is the efficient and robust recognition of chloroplast-destined preproteins and their subsequent import. Preproteins are synthesized in the cytosol with a cleavable N-terminal extension of approximately 50-150 amino acids known as a transit peptide (6-8). It is the transit peptide that is recognized by the Toc complex which facilitates the import of the preprotein (9). It is this transit peptide mediated chloroplast protein import mechanism that will be the subject of this dissertation. Presented in Chapter II is an analysis of the basal enzymology of the isolated, soluble forms of the Toc GTPases. Chapter III analyzes the homo- and heterodimeric interaction between Toc proteins and how this oligomerization can be modulated. Chapter IV presents evidence that the transit

peptide interacts with the Toc proteins in such a way as to increase enzymatic activity as well as bias the dimeric equilibria. Analysis of the data presented in Chapters II, III and IV allow the creation of a chloroplast protein import model, Chapter V, to potentially explain the observed phenomenon. Finally, Chapter VI presents potential future directions for this research.

1.2 Endosymbiotic Origin of the Chloroplast

Prior to engulfment, the ancient cyanobacterial cell presumably possessed an outer membrane exporter protein known as SynToc75, or *Synechocystis* Toc75 (3,10). It is hypothesized that this β-barrel protein was oriented in such a way that it recognized 'virulence proteins' and exported them into the extracellular mileu in order to combat other prokaryotic and/or primitive eukaryotic cells (11). After cyanobacterial engulfment by a primitive eukaryotic cell, the majority of the genome of the cyanobacterium was transferred to the host cell nucleus. The protein transporter SynToc75 retained its function as a transporter, however after DNA being reshuffled to the host cell nucleus, it was redirected to the newly formed chloroplast outer membrane where it exhibited a reversed topology (Figure 1-1) and (3,10). This topologically inverted protein (now referred to as Toc75 – *e.g.* psToc75 in the case of Toc75 protein from *Pisum sativum*) functions to alleviate a potential problem created from the lateral transfer of chloroplastic DNA to the cell nucleus. Toc75 recognizes and imports precursor proteins into the chloroplast in much the same way SynToc75 once exported proteins (12).

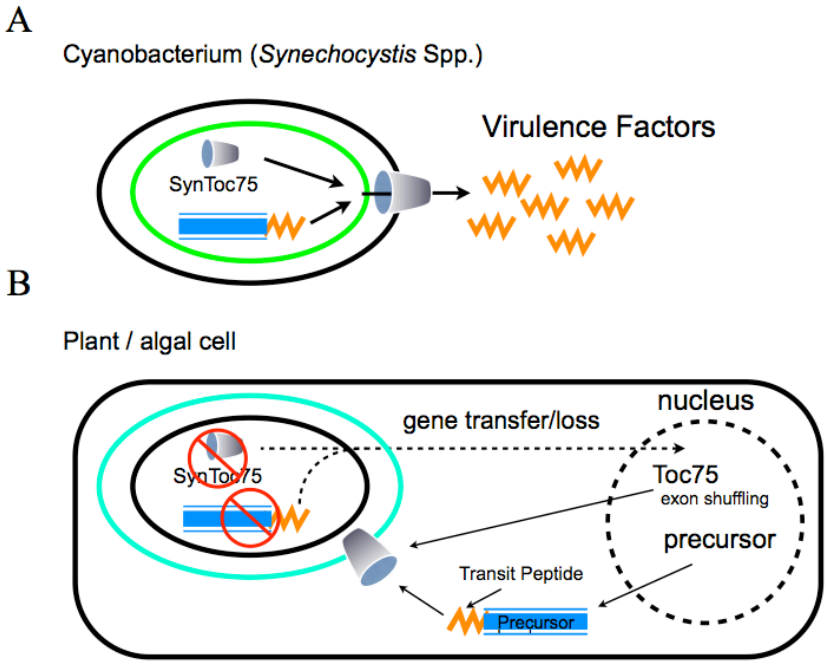


Figure 1-1. Model depicting origin of Toc75 and modern transit peptides. A, it is hypothesized that *Synechocystis* utilized the channel protein *Syn*Toc75 to export virulence factor substrates, shown in orange, into the extracellular mileu. The substrates for this may be the evolutionary origin of the modern day transit peptide. B, subsequent to engulfment of the cyanobacterium, the majority of the cyanobacterial genome was laterally transferred to the nucleus. The Toc75 protein is inserted into the plastid outer membrane such that it facilitates the directional import of proteins back into the organelle. Some of the original information recognized by SynToc75 is reorganized through exon shuffling eventually resulting in a modern transit peptide capable of directing the import of the gene products that were once transferred to the nucleus. This model is adapted from (Bruce, 2000).

1.3 Chloroplast Protein Import

The genome of the modern day plastid is approximately 150 kb encoding approximately 100 proteins, however, the proteome of the chloroplast is greater than 3000 proteins (13,14). A recent study in *Arabidopsis*, utilizing the neural network TargetP, indicated that about 2100 nuclear encoded, chloroplast destined proteins contain transit peptides and are targeted to the chloroplast (15,16). The transit peptide has been shown to be both necessary and sufficient for preprotein import; ablation of this targeting information renders the protein unable to enter the chloroplast and the generation of heterologous proteins composed of transit peptides and non-chloroplast proteins affords these proteins access to the chloroplast (17,18). The majority of chloroplast-targeted preproteins possessing an N-terminal transit peptide follow the general import pathway, Figure 1-2. Data exists to substantiate claims that other chloroplast protein import pathways may exist, *e.g.* ER to Golgi to chloroplast (19,20), however these alternative pathways require further work and are not the subject of this dissertation.

Protein import across the double membrane of the chloroplast is mediated by two multimeric protein complexes referred to as the **T**ranslocon of the **O**uter/**I**nner **C**hloroplast membranes. Individual proteins that comprise these complexes are referred to as Toc and Tic proteins, respectively, and are denoted by their apparent molecular masses. The requisite components of the translocon, referred to as the Toc Core Complex (Figure 1-3), were identified via chemical crosslinking during various stages of protein import using isolated chloroplasts from pea seedlings (21-23). This work identified two

Figure 1-2. General Import Pathway. Preproteins synthesized in the cytosol have an N-terminal transit peptide; shown here are two different classes of preproteins, each with three domains in red, green and yellow and purple, green and blue, respectively. Multiple import mechanisms exist. (1a) Interaction of the phosphorylated (black dot) transit peptide with a soluble guidance complex containing 14-3-3 protein and Hsp70. (1b) Interaction of the preprotein and soluble Toc159. (1c) Interaction of preprotein and Hsp90. (2a) Partitioning of the transit peptide onto the membrane via interactions with chloroplast-specific lipids such as MGDG (monogalactosyldiacylglycerol), SL (sphingolipid) and PG (phosphatidyl choline). Hsp70 and/or Hsp90 mediated interaction of the precursor with the Toc components (2b, 2c, 2d, 2e, 2f). Initial interaction may occur with the full-length Toc159 (2b), Toc64 (2c) or (2f), the heteroligomeric Toc translocon (2d), or guidance by soluble Toc159 to the translocon (2e). (3) Peptide/lipid interactions resulting in reciprocal changes in the transit peptide structure (green) and the possible formation of an inverted lipid micelle in the outer membrane. (4) Recognition/interaction of membrane-associated transit peptide with Toc159 receptor. (5, 6) Lateral movement and/or transfer of the transit peptide from Toc159 and/or Toc64 to Toc34 and Toc75, resulting in the assembly of a Toc translocon forming a contact site of the outer and inner chloroplast membranes. (6) The sequential or concomitant insertion and translocation of transit peptide into Toc75. (7) Translocation across outer membrane in a nucleotide-dependent manner. (8) Complete translocation of preprotein across the inner membrane requires higher levels of both GTP and ATP and utilizes stromal ATPase molecular motors. (9, 10) Upon import, the transit peptide is cleaved by SPP (stromal processing peptidase), followed by complete degradation of the transit peptide by PreP1

and PreP2 and proper folding of the mature domain. This figure is adapted from (Bruce, 2000; Wright, 2006).

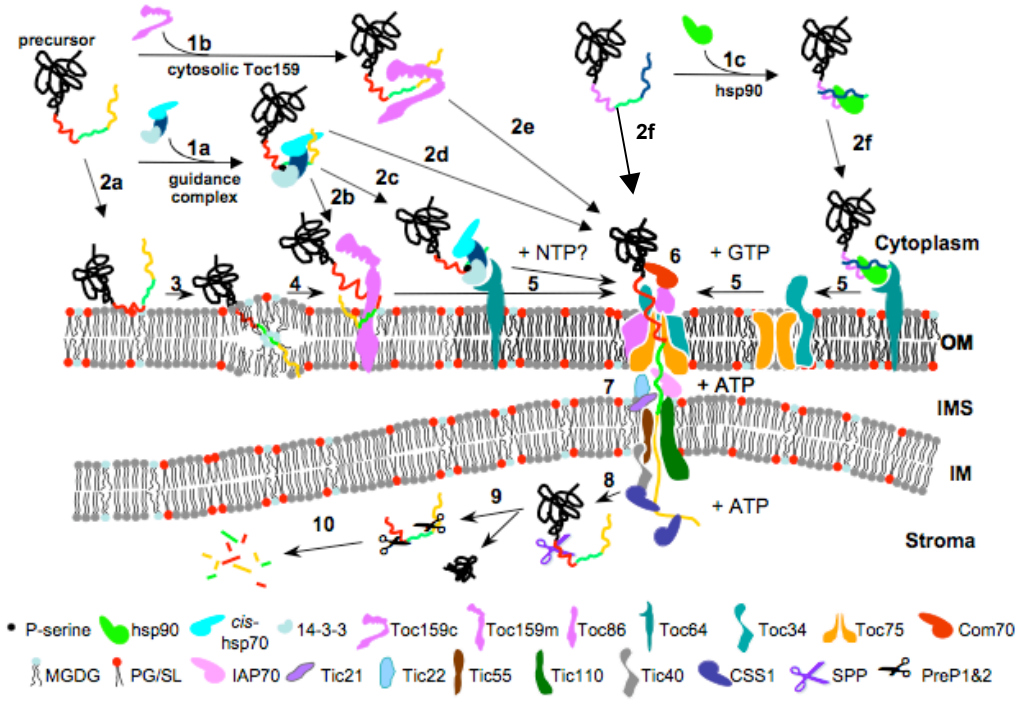

precursor
1b
cytosolic Toc159
1a
guidance complex
2a
2b
2c
2d
2e
2f
1c
hsp90
+ NTP?
+ GTP
+ ATP
+ ATP
Cytoplasm
OM
IMS
IM
Stroma
P-serine
hsp90
cis-hsp70
14-3-3
Toc159c
Toc159m
Toc86
Toc64
Toc34
Toc75
Com70
MGDG
PG/SL
IAP70
Tic21
Tic22
Tic55
Tic110
Tic40
CSS1
SPP
PreP1&2

Figure 1-2.

GTP binding proteins, later named Toc34 and Toc159, that interacted with the incoming preprotein as well as a channel protein shown to be Toc75 (24).

Additional characterization of the Toc Core Complex led to a low-resolution electron microscopy image of approximately 14 Å (Figure 1-3) and (25). This isolated Toc core complex was comprised of Toc34, Toc75 with a stoichiometry of ~4-5:4:1, respectively. It indicated that the core complex was roughly spherical with four pores surrounding a finger-like domain; the four pores are thought to correspond to Toc75 and the finger-like projection most likely represents a domain of Toc159 interacting with one of the four Toc34 molecules (25).

The inner membrane of the chloroplast harbours the Tic apparatus, responsible for translocating the incoming preprotein across the inner membrane and into the stroma. The Tic components, although not characterized as well as the Toc components, are Tic20, Tic22, Tic40, and Tic110, and are discussed further below (26-28).

1.4 The General Import Pathway

As depicted in Figure 1-2, preproteins possessing an N-terminal targeting sequence known as a transit peptide, follow the general import pathway which includes but is not limited to interaction with the membrane, interaction with soluble chaperones and putative ‘guidance complexes’, interaction with specific or various members of the Toc complex and finally import through Toc75 across the outer membrane of the chloroplast (4,11). Recent data indicate that other pathways may exist (29), however the majority of chloroplast-targeted preproteins are produced in the cytosol and follow this general import pathway.

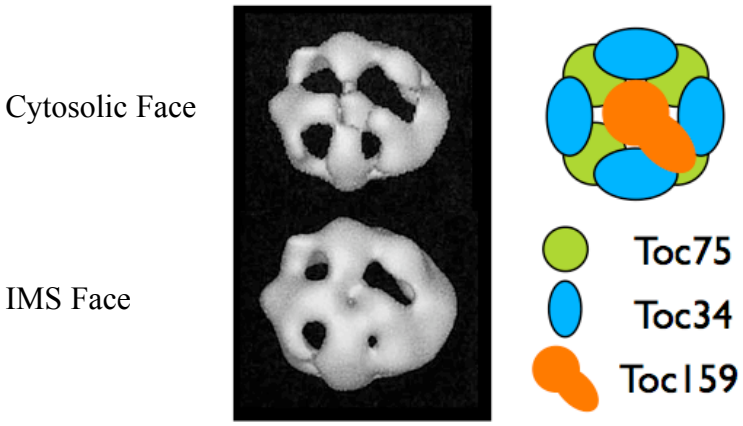


Figure 1-3. Reconstructed EM image of Toc core complex and proposed stoichimetry. The Toc core complex was isolated from young, actively greening, *Pisum sativum* chloroplast outer membranes and exhibited GTP-dependent import competence. The stoichiometry was determined to be ~4-5:4:1 between Toc34, Toc75 and Toc159, respectively, with an apparent molecular mass of 500 kDa. This image shows four channels around a central finger-like core region. Adapted from (Schleiff *et. al.*, 2003b). The top image represents the cytosolic face while the lower image represents the intermembrane space face (IMS).

After the precursor protein is synthesized and released from the ribosome, there are several possibilities for preprotein targeting from the cytosol to the outer membrane of the chloroplast, interaction with, and subsequent translocation through the Toc complex and are presented here. It is important to note that one or all of the following possibilities occur and some are more debated than others. The first, Figure 1-2, 1a, is the recognition and binding of a possibly phosphorylated transit peptide by a guidance complex comprised of (at minimum) a 14-3-3 protein and an Hsp70 chaperone which delivers the transit peptide to the Toc receptors (30). A second possibility, denoted as 1b, indicates the interaction between the preprotein with a soluble form of the Toc159 receptor. Toc159 presumably recognizes the transit peptide of the precursor proteins in the cytosol and targets them to the outer membrane where it docks with Toc34 and Toc75 molecules of the Toc Core Complex allowing import to proceed (31). A third possibility, denoted as 1c, is most likely specific to a certain class of preproteins and involves the recognition and binding by the Hsp90 chaperone. This guidance complex is targeted to Toc64 (2f), a lesser known putative member of the translocon, and is guided to Toc34 (5) which then assembles the Toc complex (32). A fourth possibility (2a) is the specific interaction of the transit peptide with chloroplast-specific lipids. These lipids include the galactolipids and sulfolipids, which can only be found in the outer membrane of the chloropast. These lipids have been shown to increase the α-helical content of the transit peptide (33,34). It is hypothesized that the induced secondary structure could facilitate an interaction with the Toc components (33). Finally, the preprotein may interact directly with the Toc complex (2f). It has been suggested that various preproteins may utilize different pathways of interaction with the Toc complex. Therefore, different targeting

mechanisms may exist due to recent findings that Toc159 and Toc33 interact with highly expressed photosynthetic protein while Toc34 and Toc120, Toc132 and Toc90 interact with 'houskeeping' chloroplast proteins (35).

Energy is required for the translocation of preproteins across the Toc/Tic apparatus. Chloroplast protein import can be divided into three stages according to the amount of energy required for each step (36). The first stage of import occurs at the outer membrane where preproteins weakly interact with the membrane and Toc components in an energy independent reversible manner (Figure 1-2, steps 5 and 6) and (21). The second stage of import requires low levels of ATP (< 100 μM) wherein early translocation intermediates are formed (Figure 1-2, step 7). GTP is also required in this step, however the concentrations required are debated (37,38). In step 7, the preprotein has begun to make contacts with the Toc75 channel protein as well as the assembled portions of the Tic apparatus (39,40). Early import formation is mainly driven by GTP in this step, probably driving translocon assembly and/or preprotein insertion into the translocation channel. Low ATP levels and GTP alone are not sufficient for complete translocation (41,42). In order to facilitate complete translocation of preproteins across the double membrane of the chloroplast, ATP is required at levels > 100 μM (Figure 1-2, step 8). This is most likely due to the involvement of Hsp70 or Hsp100, two stromal chaperones known to utilize ATP to bind and release precursor proteins facilitating import like a molecular ratchet (43,44). Upon import into the stroma of the chloroplast, the transit peptide is cleaved from the mature domain by the stromal processing peptidase (SPP) and completely degraded by the presequence protease PreP1 and PreP2 (Figure 1-2, steps 9 and 10). The folding and assembly process is initiated for the mature domain which either

gains its biological activity, or is targeted to sub-plastid compartments such as the thylakoid membrane (45,46).

1.5 The Toc Core Complex

The Toc complex is responsible for the recognition and translocation of preproteins across the outer envelope of the chloroplast double membrane. Crosslinking of early intermediates identified Toc components resulting in the isolation of the receptors Toc34 and Toc86/159/160 (21,38). Toc86, as it was first identified, is a proteolytic degradation of a larger protein, later identified as Toc160 (47). After careful proteolytic protection and rapid purification techniques, Toc160 was finally given the correct designation based on molecular mass, Toc159 (48). The β-barrel channel protein Toc75 serves as the preprotein translocation channel (3,49). A fourth member of the Toc translocon has been identified as Toc64, a protein potentially serving as a binding site for Hsp90-bound preproteins (50).

The minimal core complex, however, is composed of Toc34, Toc75 and Toc159 and is approximately 500 kDa in apparent mass and has been visualized using low resolution electron microscopy (Figure 1-3) and (25). The core complex is composed of Toc34, Toc75 and Toc159 in a ratio of ~4-5:4:1, respectively. This arrangement was supported by the observation that up to four transit peptide-nano-gold particles could be visualized bound simultaneously to the core complex (25). Furthermore, the Toc core complex has been observed using Blue Native PAGE (51).

1.5.1 Toc34

Crosslinking studies under low levels of ATP and GTP afforded the first identification of the GTPase preprotein receptor, Toc34 (22,24). As with other canonical GTP-binding proteins, Toc34 is composed of a central G-domain, which is highly similar to the Ras superfamily of GTP-binding proteins as well as Toc159 (52,53). Toc34 has a short C-terminal α-helical transmembrane domain that anchors it in the outer membrane leaving the majority of the protein cytosolically exposed (38). The cytosolic domain has been shown to specifically interact with both transit peptides and preproteins and to also possess GTPase activity, *i.e.* binding and hydrolyzing GTP (discussed in further detail below). This supports the role of Toc34 as a GTP-regulated preprotein receptor of the Toc complex (54,55).

More than one homologue of Toc34 has been found in *Arabidopsis* as well as many other plants including maize (*Z. mays*), rape seed (*B. napus*), potato (*S. tuberosum*), tomato (*L. esculentum*), poplar (*P. tremula*) and a non-vascular plant, the moss (*P. patens*) (56). In the model organism *Arabidopsis thaliana*, two genes have been identified encoding atToc33 and atToc34, however their mRNA distribution within plant tissues differs considerably. For example, atToc33 expression is significantly increased (up to 5-fold) compared to atToc34 in actively greening tissues whereas atToc34 expression is greatest in stems and roots (57,58). It was shown that some transit peptides in *Arabidopsis* bind only to one of the homologues while other transit peptides bound equally to either protein indicating that the receptors are not totally exclusive for specific preproteins but can compensate for one another to some extent (59). A mutant *Arabidopsis* lacking atToc33, termed *ppi1* for plastid protein import-deficient 1, was

identified and shown to have a decreased amount of photosynthetic proteins present in their chloroplasts as compared to wild type plants (60). Affording more in-depth analysis into both mechanism and structure-function studies on the Toc proteins, both psToc34 from garden pea (*Pisum sativum*) and and atToc33 from *Arabidopsis*, respectively, were recently crystallized (61,62). Although not all Toc proteins have solved and reported structures, due to the highly homologous nature of the Toc G-domains, structural data obtained from one Toc protein is highly applicable to other Toc proteins (62). Structural alignment 3-D models have been created for atToc34 and atToc159 (53). As observed in the crystal structure, the psToc34 protein is a dimer whose dimeric interface is involved in both protein-protein interactions as well as nucleotide binding. In fact, residues such as Arg128, Arg133, Tyr 132, Pro160 and Asp170 are involved in the nucleotide binding of the other monomer suggesting possibly involvement of nucleotide regulated dimerization in the import mechanism (Figure 1-4 A and B) and (61,63). Furthermore, the bound GDP molecules in the crystal structure appear to be unable to exchange with bulk solvent unless the Toc34 proteins monomerize.

1.5.2 Toc159

Originally identified as Toc86 due to its sensitivity to proteolysis, Toc159 is a tripartite protein composed of three domains: the A, G and M domains. The most N-terminal domain, the A domain (residues 1-727), is characterized by an acidic protein sequence, however the function of this domain is unknown (53). Ablation of the A domain to form Toc86 seems to have no bearing on protein import as chloroplasts with only Toc86 import preproteins at wild type levels (64). The middle GTP-binding, or G

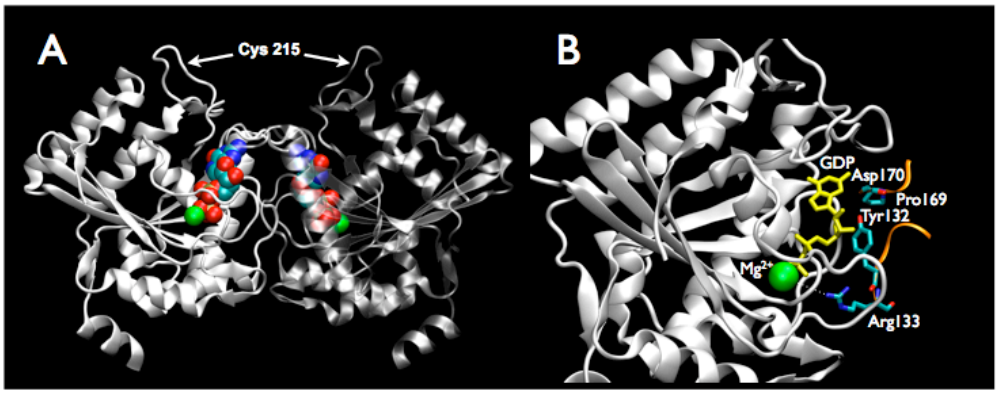


Figure 1-4. Crystal Structure of psToc34. Panel A, the psToc34 homodimer is shown such that the two monomers are white (left) and transparent silver (right). Their respective GDP molecules are shown in space filling and the Mg^{2+} cations are shown as green spheres. The location of the single cysteine, C215, is indicated. Panel B illustrates the degree to which amino acids from one monomer interact with the bound GDP of the other monomer. The psToc34 monomer, bound GDP and Mg^{2+} are white, yellow and green, respectively, with the α-carbon backbone of the other monomer shown in orange and the residues from the orange monomer acting in trans labeled accordingly.

domain (residues 728-1092), shares significant homology with Toc34 as well as the Ras superfamily of GTPases (52,53). The most C-terminal, or M domain (residues 1093-1503), represents the membrane-associated domain (53,64). The stability with which Toc159 remains integrated into the chloroplast outer membrane is debated (65-68). A soluble pool of Toc159 has been reported to be in close proximity to the chloroplast outer membrane and some authors believe Toc159 to cycle between a membrane associated form and soluble form of the protein allowing for a targeting complex (Figure 1-2 step 1b) and (65). However, other reports suggest this was an artifact (69). In either case, Toc159 has been implicated to be the primary receptor for precursor recognition, however GTP hydrolysis by Toc159 was unnecessary for plastid protein import (70). Crosslinking studies of precursor binding to the Toc Core Complex as well as reconstituted proteoliposomal assays were used to implicate Toc159 as the primary receptor for the transit peptide (70).

1.5.3 Toc75

The most abundant protein of the outer membrane of the chloroplast, Toc75, was originally identified by isolation of early preprotein import intermediates with only low levels of ATP (22). Early patch-clamp experiments indicated that Toc75 forms a pore of diameter 8-10 Å in diameter and structural studies predict a transmembrane β-barrel channel with either 16 or 18 transmembrane β-strands (25,71). Later studies were aided by a semi-folded transit peptide fused to DHFR (dihydrofolate reductase) with methotrexate bound. This construct probed the constriction site of Toc75 and indicated that the Toc75 β-barrel was approximately 15 Å in diameter (72,73).

1.6 GTPase Activity of Toc34 and Toc159

Early studies of chloroplast precursor import indicated a need for the nucleotide GTP in promoting the formation of early import intermediates (38,42). Since these early experiments, it has been shown that GTP does indeed play a role, and absence of this nucleotide abrogates protein transport (54). The crystal structure of psToc34 suggested GTP may play a role in homodimerization (61). A homodimeric equilibrium of Toc34 has been reported by several laboratories and the nucleotide loading status (*i.e.* GDP *vs* GTP) modulates this equilibrium (53,62). The affinity of Toc34 for preproteins and transit peptides is stimulated by GTP, indicating that the nucleotide may act as a switch, not uncommon with GTP-binding proteins (54,74). The involvement of GTP has also been shown to represent a commitment step in the import of preproteins (53). Incubation of preproteins and transit peptides with Toc34 have been shown to stimulate GTP hydrolysis suggesting that they also play a role in the regulation of GTPase activity (75).

The Toc GTPases share significant homology with the Ras superfamily of GTP-binding proteins, which include Ras, Ran, Rho, Rac, Rab and Arf (74). These eukaryotic GTPases, which are active with bound GTP and inactive with bound GDP, all have effectors in the forms of GTPase Activating Proteins and Guanine nucleotide Exchange Factors (GAPs and GEFs) (Figure 1-5) (76). GAPs act by causing the GTPase to hydrolyze the bound GTP to GDP inactivating the protein while GEFs act by accelerating the exchange of GDP for GTP and activating the protein. Therefore, GAPs and GEFs represent regulatory points in the cycle of the GTPase. It was first suggested that the Toc34 homodimer may represent a form of self-GAP since Arg-133 from one monomer

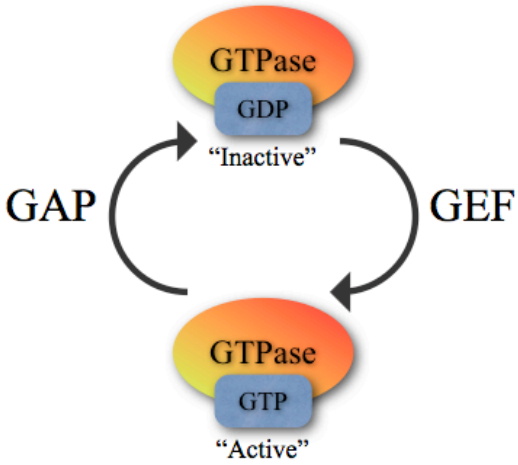


Figure 1-5. The GAP and GEF cycle of GTPases. GTPases are active in the GTP-bound form and inactive in the GDP-bound form. Cycling between the inactive and active form requires nucleotide exchange and hydrolysis, which are mediated by Guanine nucleotide Exchange Factors (GEFs) and GTPase Activating Proteins (GAPs).

extends deeply into the GTP binding pocket of the other monomer (61). However, mutation of Arg-130 in the *Arabidopsis* homologue atToc33, equivalent to the putative arginine finger in Toc34 (R133) eliminated dimerization and did not have any affect on GTPase activity, directly contradicting any function as a GAP (77). The observation that preproteins and transit peptides increase GTPase activity suggests they may serve as GAPs for the Toc GTPases (53,78).

1.7 Tic Complex

The Tic complex, or **T**ranslocon of the **I**nner **C**hloroplast membrane, receives transit peptide containing precursor proteins imported by the Toc complex and facilitates their delivery to the stroma. Unlike the Toc complex, the Tic complex is not very well characterized in part due to its dynamic organization and difficulty to purify. Freeze etch electron microscopy has shown that the outer membrane and the inner membrane of the chloroplast come together where preproteins are undergoing translocation (79). It is here that the Toc and Tic complexes interact to rapidly import precursor proteins from the cytosol to the stroma (21,80). It has been shown that preproteins can be translocated across each membrane independently, however this is only in the case of osmotically induced organelle shrinkage (81). The most studied Tic proteins include Tic110, Tic40, Tic22 and Tic20.

1.7.1 Tic110

Tic110 was isolated via crosslinking to preproteins (82). The actual role of Tic110 is a matter of debate, however, it forms pores when incorporated into proteoliposomes.

This suggests that it is the pore-forming component of the Tic complex (83); although this has not been confirmed *in vivo* (28). The large stromal domain of Tic110 has also been shown to be involved in stromal chaperone recruitment and may serve as a binding and assembly site for preproteins as they are translocated into the stroma and concomitantly folded by molecular chaperones (84,85). The knockout of Tic110 results in embryo lethality, underscoring its importance in protein import (28).

1.7.2 Tic40

Tic40 was first identified as a component of the Tic complex due to its crosslinking to arrested precursor proteins during import (27,86). Tic40 is implicated as a chaperone recruitment factor due to its association with Hsp93, and its knockout mutation results in a chlorotic phenotype indicating its importance (28,87).

1.7.3 Tic20 and Tic22

Tic20 and Tic22 were originally isolated as crosslinked products to arrested late import intermediates (24). Tic 22 is weakly associated with the inner membrane and is localized in the intermembrane space (IMS) while Tic20 is an integral membrane protein and both have been shown to interact with preproteins during transport across the inner membrane of the chloroplast (26). Knockout mutants of Tic20 result in a chlorotic phenotype indicating its importance in protein import and has been implicated as being able to form a channel, but this has not been confirmed to date (88).

1.8 Cytosolic Factors in Chloroplast Protein Import

There are many factors that may be involved in the plant cell cytosol that impact protein import, however, the key features are shown in Figure 1-6. Of these are the cytosolic guidance complex, the transit peptide itself and the lipid composition of the outer leaflet of the outer membrane. After the mRNA coding for chloroplastic proteins exits the nuclear pore complex and is translated on soluble ribosomes. The resultant transit peptide and precursor protein interacts with soluble chaperones and 14-3-3 proteins in the cytosol. It is believed that these interactions form a guidance complex that targets the newly synthesized precursor protein to the chloroplast outer membrane. In fact, over 75% of chloroplast transit peptides have been shown to possess domains for either 14-3-3 binding or Hsp70 molecular chaperones, and some have been found to possess both (89). The binding and/or interaction with 14-3-3 proteins require a phosphorylation of the substrate. Several preproteins have shown a putative phosphorylation motif $(P/G)X_n(K/R)X_n(S/T)X_n(S^P/T^P)$ where the superscript 'P' represents the predicted site of phosphorylation and n can be 0-3 residues (90). Chloroplastic preproteins translated in a wheat germ lysate were shown to have been phosphorylated and in association with a 14-3-3 and chaperone guidance complex (90). Furthermore, preproteins associated with guidance complexes are imported more readily than preproteins devoid of guidance complexes (90). Interestingly, not all chloroplast transit peptides have been shown to possess chaperone and 14-3-3 binding domains. This indicates that chaperone binding may not be required for all transit peptides; instead the presence of these binding domains may be indicative of the need to target highly expressed preproteins thus preventing their buildup in the cytosol (91).

Figure 1-6. Chloroplast protein import schematic. The mRNA encoding chloroplastic proteins exits the nuclear pore (yellow). It is translated on ribosomes into precursor proteins that have an N-terminal extension known as the transit peptide (red). The solubility and protease resistance of the precursor protein is maintained through the interaction with 14–3–3 proteins and chaperones and it is ultimately targeted it to the chloroplast Toc translocon. Interaction with the receptor GTPases Toc159 and Toc34 is mediated by the transit peptide. The precursor protein is translocated through the beta-barrel protein Toc75. There it interacts with the Tic complex. The actions of cytosolic, IMS and stromal chaperones drive the import of the precursor protein. Stromal processing peptidase cleaves the transit peptide and the precursor protein folds to its ultimate active form, or proceeds to a suborganeller location for further import/ processing. The transit peptide is degraded via the presequence processing peptidase. This figure is reproduced from Reddick, *et. al.*, 2008.

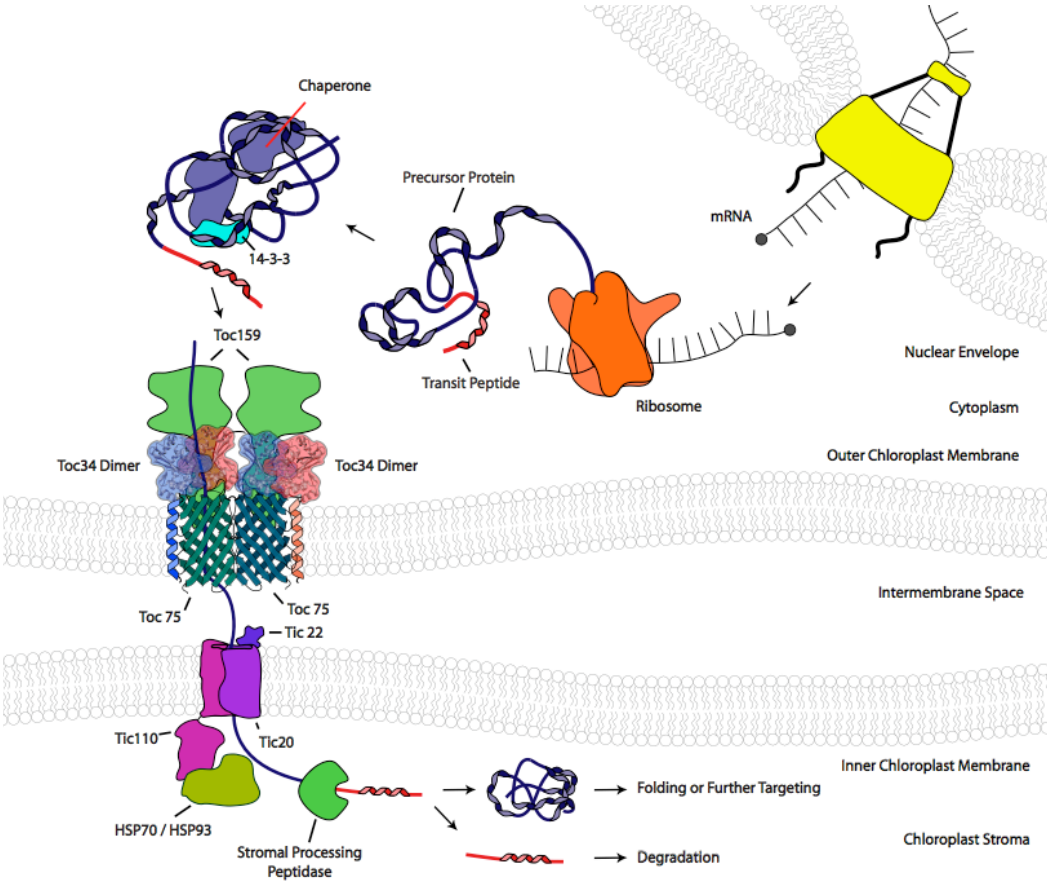

Chaperone
14-3-3
Precursor Protein
mRNA
Transit Peptide
Ribosome
Nuclear Envelope
Cytoplasm
Toc159
Toc34 Dimer
Toc34 Dimer
Outer Chloroplast Membrane
Intermembrane Space
Toc 75
Toc 75
Tic 22
Tic110
Tic20
Inner Chloroplast Membrane
HSP70 / HSP93
Stromal Processing Peptidase
Folding or Further Targeting
Degradation
Chloroplast Stroma

Figure 1-6.

As a result of its endosymbiotic origin, the chloroplast possesses two membranes, the outer and the inner. The outer membrane has a high lipid:protein ratio of 3:1 with the major lipids as follows: phosphatidyl choline (PC), 32%; monogalactosyl diacylglycerol (MGDG), 17%; digalactosyl diacylglycerol (DGDG), 29%; phosphatidyl glycerol, 10%; and a small mol fraction is represented by sulfolipids (SL) (92). The outer leaflet of the outer membrane (cytosolic side) contains PC while the inner leaflet contains PG. Furthermore, the outer membrane of the chloroplast utilizes cytosolic phospholipase D (PLD) and phosphatidic acid phosphatase (PAP) to convert PC to digalactolipids (93). A galactolipid containing outer membrane is informative and interesting as there are no other cytosolically exposed membranes in the plant cell that present galactolipids. Therefore, it is possible that galactolipids represent a unique binding interface for the transit peptide and precursor proteins. In fact, it has been shown that the transit peptide, which is unstructured in solution (94), adopts an α-helical conformation in the presence of liposomes containing galactolipids (17). Several studies have supported this idea, indicating that the transit peptide interacts with chloroplast outer membrane lipids, specifically MGDG, and forms α-helical secondary structure (33,94). It has also been shown that an *Arabidopsis* mutant defective in the plastid lipid DGDG had significantly reduced ability to import proteins into the chloroplast interior indicating that lipids play a significant role in chloroplast protein import (95).

1.9 The Transit Peptide

The transit peptide is a cleavable N-terminal extension that is both necessary and sufficient for chloroplast protein import. Precursor proteins expressed and isolated *in*

vitro devoid of transit sequences are unable to gain access to the chloroplast (8,96). Furthermore, non-chloroplastic proteins, such as GFP, heterologously expressed with an N-terminal transit peptide does become imported into the chloroplast (7,97). The GTPase components of the Toc complex, Toc34 and Toc159, have been shown to specifically interact with the transit peptide during import, and mutations to the transit peptide have been shown to abrogate chloroplast protein targeting and import (21,35,53,55,78,98-100). Furthermore, transit peptides have been shown to have affinity for liposomes with galactolipid character, suggestive of transit peptide-lipid mediated targeting (33).

With the publication of the *Arabidopsis* genome and continually increasing number of Expressed Sequence Tags (ESTs) the number of known chloroplast targeting sequences is growing rapidly. There are estimates as high as 3574 genes identified that code for proteins targeted to the chloroplast (11). Primary sequence alignments of transit peptides, which vary in length from 25-150 amino acids, generally result in poor alignment. These peptides are highly heterogenous in length, composition and organization, which make it difficult decipher the information contained that directs their targeting (101). Despite these peptides having apparently no primary sequence similarity, there are several shared features. Transit peptides tend to be enriched in hydroxylated amino acids, small nonpolar residues and are devoid of aspartate and glutamate (102). Additionally, the N-termini of transit peptides generally lack charge and have a basic central and/or C-terminal region (30).

The information contained within transit peptides may be structural rather than sequence specific. Unfortunately, little information exists to support this hypothesis. This lack of structural information is not only a result of limited investigation, but potentially

may reflect the fundamental property of transit peptides to readily change from an unstructured peptide in solution to a structured peptide in detergent micelles, liposomes or in the presence of the α-helical promoting solvent TFE (11,34,94,103). Multidimensional NMR has been utilized to determine the identity and placement of transit peptide structural elements, however due to the length of higher plant transit peptides, NMR studies have been performed on the ferredoxin and Rubisco transit peptides from the algae *Chlamydomonas* (104,105). The transit peptide for ferredoxin from *Silene* has been expressed in *E. coli* with stable isotopes in order to observe its structure via NMR NOESY (94). When this labeled transit sequence interacted with a micellar system composed of MGDG and the ionic detergent dodecylphosphoglycol, two helical domains (S_{10}-L_{13} and G_{30}-L_{34}) were elicited (94) in an otherwise unstructured peptide (example shown in Figure 4-2 D). Other observations gleaned from this experimentation indicate that the central proline rich domain (P15-P26) remained unstructured presumably to allow extreme flexibility to the two flanking α-helical domains induced upon interaction with an outer membrane mimetic environment. Circular dichroism experimentation has confirmed these results (34). It can be summarized that in aqueous solution, transit peptides are largely unstructured, however when interacting with envelope-like lipids or non-polar solvents, α-helicity is induced. Although a helix-coil-helix organization may be a universal feature of transit peptides, the degree of amphipathicity and position of these two α-helices may vary significantly (105). This plasticity of domain organization may play a role in the guidance complex and/or Toc mediated recognition of transit peptides. Recent kinetic analyses of the Toc

GTPases with and without transit peptides suggests these amphipathic peptides may play a role in the GTPase cycle (53,100,106).

1.10 Summary

The modern day plant is the result of a secondary endosymbiotic event which utilizes its prokaryotically-derived chloroplast to harvest solar energy and convert sunlight to sugars and energy supporting life on planet Earth (107). A double membrane surrounds the chloroplast, which imports the majority of its proteins from the plant cell cytosol. This has necessitated a dynamic and complex chloroplast targeting system in which an N-terminal extension known as the transit peptide directs the import of post-translationally synthesized proteins. This is accomplished, in large part, by the targeting of the transit peptide containing precursor protein to the outer membrane of the chloroplast. There it is recognized in a transit peptide and GTP-dependent manner. Facilitating this recognition are the GTPases Toc34 and Toc159 working in concert with the outer membrane translocation β-barrel channel protein Toc75. After recognition and rounds of GTP hydrolysis, the Tic complex receives the incoming protein, recruits stromal chaperones, and completes the directional import while concomitantly folding the imported protein and/or targeting it to a sub-stromal compartment. While it is known that this sequence of events occurs to facilitate chloroplast protein import, the enzymatic and mechanistic details occurring between the transit peptide and Toc components and within the Toc complex itself are poorly understood. This study provides new insight into the enzymology and mechanism of the Toc GTPases and highlights the importance for homo- and heterodimerization of the Toc translocon components.

CHAPTER II

Kinetic Characterization and Basal Enzymology of the chloroplast Toc GTPases

2.1 ABSTRACT

A unique aspect of protein transport into plastids is the coordinate involvement of two GTPases in the translocon of the outer chloroplast membrane (Toc). There are two subfamilies in Arabidopsis, the small GTPases (Toc33 and Toc34) and the large acidic GTPases (Toc90, Toc120, Toc132, and Toc159). In chloroplasts, Toc34 and Toc159 are implicated in precursor binding, yet mechanistic details are poorly understood. How the GTPase cycle is modulated by precursor binding is complex and in need of careful dissection. To this end, we have developed novel in vitro assays to quantitate nucleotide binding and hydrolysis of the Toc GTPases. Here we present the first systematic kinetic characterization of four Toc GTPases (cytosolic domains of atToc33, atToc34, psToc34, and the GTPase domain of atToc159) to permit their direct comparison. Reported are the K_M, V_{max}, and E_a values for GTP hydrolysis and the K_d value for nucleotide binding for each protein. It is demonstrated that GTP hydrolysis by psToc34 is stimulated by chloroplast transit peptides; however, this activity is not stimulated by homodimerization and is abolished by the R133A mutation. Furthermore, peptide stimulation of hydrolytic rates are not due to accelerated nucleotide exchange, indicating that transit peptides function as GTPase-activating proteins and not guanine nucleotide exchange factors in modulating the activity of psToc34.

2.2 INTRODUCTION

Despite multiple reports investigating the interaction of the Toc34 and Toc159 homologues with preproteins and transit peptides, the role of GTP binding and hydrolysis is far from understood (11,17,25,68,78,108). In fact, the few reports on GTPase activity have been primarily focused on the small GTPases and report enzymatic properties such as V_{max} and K_M values that disagree by nearly 2 orders of magnitude (61,78). In *Arabidopsis*, the two related homologues, Toc33 and Toc34, have had their nucleotide binding properties investigated, yet there have not been systematic investigations on their potentially different enzymatic properties (106). Finally, atToc159G has had only limited analysis performed on its nucleotide binding and/or hydrolysis properties (35,109).

Mechanistically, from both the crystal structure (61) and the low resolution EM structure of the Toc translocon, Figure 1-3 and (25), it is clear that the Toc GTPases may be able to form either a functional homo- or heteroligomer. The significance of this dimerization is still debated (77), yet it has been proposed that one possible explanation is that the two subunits can function as GTPase-activating proteins that may reciprocally stimulate and/or coordinate the hydrolysis of GTP (61). This dimeric, self-stimulatory interaction was first reported in the crystal structure where the presence of Arg-133 from one monomer interacting deep within the GTP-binding pocket of the other monomer can be observed. Reciprocal GAP activity is not a novel idea; for instance, reciprocal GAP activity has become an accepted model for the function of SRP54/Ffh and SRα/FtsY in protein secretion (110), the only other family of small GTPases associated with protein translocation (52).

Therefore, to enable a careful analysis of how preprotein binding, membrane

association, and homo- and heterodimerization influence the GTPase activity of the various Toc proteins, a systematic comparative kinetic analysis of the Toc34 subfamily and atToc159G is presented. We report the V_{max}, K_M, E_a, and k_{cat} values for GTP hydrolysis, as well as the K_d and K_i values of nucleotide binding for each protein. Using psToc34 as a model, we evaluated how concentration-dependent homodimerization, an "arginine finger" mutation, and transit peptide interaction affect subunit dimerization and GTP hydrolysis for psToc34.

2.3 MATERIALS AND METHODS

2.3.1 Expression and purification of the Toc GTPases

The expression clones for the Toc proteins were kindly provided by the following: psToc34, Prof. Jürgen Soll (Munich, Germany); atToc159G, Prof. Danny Schnell (Amherst, MA); and atToc33 and atToc34, Michael Gutensohn (Cologne, Germany). The cDNA encoding the truncated, cytosolic domain of psToc34, atToc33 and atToc34 was inserted into pET21d (Novagen, Madison, WI), pQE60 (Qiagen, Valencia, CA) and pQE60 (Qiagen), respectively. The transmembrane spanning regions were deleted by insertion of His tags C-terminal to residues Asp-243, Lys-257 and Pro-256 of the respective Toc proteins. The cDNA for Toc159G (both atToc159G and psToc159G), encoding the central GTPase domain, was inserted into pET21d (Novagen, Madison, WI) such that it expressed residues 727-1092 fused to a C-terminal His tag. The plasmids containing atToc33 and atToc34 were each transformed into *Escherichia coli* TG1 cells (Amersham Biosciences), and the plasmids containing psToc34 and atToc159G and psToc159G were transformed into *E. coli* BL21(DE3) cells. These cells were grown in

LB media to an A_{600} of 0.4 and induced with 1 mM Isopropyl 1-thio-β-D-galactopyranoside for 4 hours at 37°C. The E. coli cells were lysed by three passages through a French press (Thermo Electron Corp., Waltham, MA) at 20,000 psi in the presence of lysis buffer (20 mM $NaPO_4$ (pH 8.0), 0.5 M NaCl, 1 mM $MgCl_2$, 0.1% Triton X-100, 1 mM β-Me). The soluble protein was separated from inclusion bodies and cell debris by centrifugation at ~45,000 xg for 30 min. The His-tagged proteins were purified under nondenaturning conditions using Talon Co^{2+} IMAC (BD Biosciences, San Jose, CA). The bound proteins were washed with 15 mM imidazole and eluted with 250 mM imidazole. Eluent was immediately diluted with 2.5X GBS and 50% glycerol yielding a storage condition of 1X GBS (20 mM Tricine-KOH (pH 7.65) 1 mM $MgCl_2$, 50 mM NaCl, and 1 mM βMe) with 20% glycerol and frozen at -80°C until used. The concentrations of the purified recombinant proteins were determined using the Bradford assay (Bio-Rad, Hercules, CA). The purity of the proteins was estimated by scanning densitometry of a Coomassie Brilliant Blue-stained SDS-polyacrylamide gel to be greater than 95%.

2.3.2 Phosphate Release Assay for GTP Hydrolysis

GTP hydrolysis of psToc34, atToc33, atToc34, atToc159G and psToc159G were all performed in the same manner using a novel activated charcoal, phosphate-release assay. In a flat-bottom 96-well microplate, reactions were carried out in GBS, 10 nM [γ-^{32}P]GTP (MP Biomedicals, Solon, OH), and varying amounts of cold GTP (and any additional substrate) in a final volume of 100 μl. The addition of Toc protein started the reaction, and at various times, as indicated in the figures, a 12.5 μl aliquot was removed

and added to 200 μl of 10% w/v activated charcoal in 50 mM HCl, 5 mM H_3PO_4. Vigorous pipetting with a multichannel pipette mixed the charcoal/aliquot mixture. At the completion of the reaction, the charcoal suspension was transferred to a 96-well 0.2 μm filter plate (Pall Corporation, Ann Arbor, MI) and vacuum filtered into a receiving 96-well microplate. An 8 μl aliquot was taken of the filtrate and added to 150 μl of MicroScint40 scintillation fluid (PerkinElmer Life Sciences, Waltham, MA). Again, vigorous pipetting was performed to ensure even distribution in the scintillation fluid. Counting was performed on a 96-well microplate scintillation counter (TopCount NXT Microplate Scintillation Counter, PerkinElmer Life Sciences). In all cases, minimums of three independent experiments were performed, counted in duplicate for each data point, and cross talk filteres applied. Counts/min data were graphed as counts/min versus time using the Prism software (Prism 5, GraphPad Software, San Diego).

2.3.3 Determination of Enzyme Velocity and Substrate Affinity

The conditions were designed to ensure that the reaction rate was linear over the 30-minute time course of the assay. By using multiple time points, cpm/min values were calculated from the slope of the line generated by counts/min versus time. The activity equation (Equation 1) will aid in the elucidation of these kinetic values and completion of

$$\text{Activity} = \frac{C_m I_m R_{GTP} S_f}{D_m M_{Toc} C_{dil} C_{eff} P_f} \qquad \text{Eq. 1}$$

this equation is detailed below. The slope of this line will represent CPM/min, or C_m. The isotope per time point, I_m, must be determined; it is simply the isotope concentration in the reaction multiplied by the volume of each time point aliquot. Determine the ratio of

your stock cold GTP to the volume of cold GTP in each reaction. The hot ratio is also determined in the same manner by taking the ratio of the [γ-^{32}P]GTP stock (MP Biomedical) to the actual volume of hot GTP in each reaction. The cold:hot ratio (R_{GTP}) is simply the ratio of these two ratios. Next, S_f is the scintillation fraction factor, or the reciprocal of the scintillation sample volume divided by the sum of the HCl-charcoal volume and the time point volume. Since CPM is not directly related to a scintillation event, only DPM, or disintegrations per min, one must convert CPM to DPM. This is accomplished by multiplying the Ci per time point (which is determined by multiplying the Ci concentration in the reaction by the time point volume) by 1 Ci (expressed as 2.22×10^{12} dpm) to give D_m. The number of Toc molecules, M_{Toc}, is determined by dividing the product of the volume of enzyme in each reaction and the stock mg/ml of enzyme by the molecular weight of the enzyme. The HCl-charcoal dilution factor, or C_{dil}, is determined by dividing the time point volume by the sum of the time point and the HCl/charcoal volume. The counting efficiency, C_{eff}, and isotope purity factor, P_f, are determined empirically and by contacting the manufacturer of the radionucleotide,

$$v = \frac{V_{max}[S]}{K_M + [S]} \qquad \text{Eq. 2}$$

respectively. Once all of these parameters have been determined and placed into a spreadsheet, the assay is very simple and highly reproducible, save pipetting errors by the experimenter. With each concentration of substrate, this spreadsheet will generate a single data point, expressed as μmol GTP hydrolyzed per unit time per pmol enzyme. In this case, we have chosen to express it as nmol GTP hydrolyzed per min per μmol Toc protein. Since each substrate concentration has an associated rate, one can create a graph

such that substrate concentration is on the X-axis and rate is on the Y-axis; this is also known as a Michaelis-Menten plot, Equation 2. By applying the Michaelis-Menten equation, a nonlinear fit can be made and V_{max} and K_M can be determined.

2.3.4 Optimization of Buffer and Storage Conditions

Buffers used to determine optimal storage conditions for the Toc GTPases were as follows: GBS (20 mM Tricine-KOH (pH 7.65), 1 mM $MgCl_2$, 50 mM NaCl, 1 mM β-Me), HMK (50 mM HEPES-KOH (pH 7.5), 2 mM $MgCl_2$, 40 mM KOAc, 12.5 mM imidazole, 10% glycerol, 1 mM β-Me), KSS (50 mM Tris-HCl (pH 8.0), 100 mM NaCl, 1 mM $MgCl_2$, 10 mM imidazole, 10% glycerol, 1 mM β-Me) and TTP (25 mM Tris-HCl (pH 7.3), 200 mM NaCl, 1 mM $MgCl_2$, 5 mM Imidazole, 1 mM β-Me). In addition, psToc34 was subjected to the following freezing conditions: -80°C slow, -80°C fast, -20°C and storage in liquid nitrogen; 'fast' and 'slow' refer to the relative speed at which the samples reached -80°C. Fast treated samples were snap frozen in liquid nitrogen for 30 seconds prior to being placed in a -80°C freezer in a foam insulated container. Furthermore, psToc34 was incubated in GBS titrated through a pH range that extended from 6.1 to 11.9. GBS was made with the following buffering agents for a given pH range: MES (pH 6.1-6.7), HEPES (pH 6.8-7.5), Tricine (pH 7.6-8.4), Tris (pH 8.5-9.1) and CAPS (pH 9.2-11.9). At each pH titration step, psToc34 was assayed for maximal velocity as described earlier.

2.3.5 Effect of Cation Replacement on psToc34 Activity

psToc34 was incubated in 1X GBS buffer in the presence of 5 mM (saturating conditions) selected metal salts as follows: $MgCl_2$, $CaCl_2$, $CdCl_2$, $CoCl_2$, $CuSO_4$, $MnCl_2$, $NiSO_4$ and $ZnCl_2$ for 10 minutes at 25°C to allow for cation replacement. A mixture of both [γ-^{32}P]GTP (10 nM) and variable amounts of cold GTP was added to start the reactions. The hydrolysis activity of psToc34 was measured as described earlier and graphed as a percentage of psToc34 activity in GBS buffer.

2.3.6 Creation of psToc34 Mutants

Mutations of the putative Arg-finger Arg-133 as well as the glutamic acid E210 responsible for orienting the guanosine ring of GTP were performed with QuickChange PCR mutagenesis (Stratagene) using the primers below.

R133A forward and reverse:

5'-GATGCCTACGCGGTGGACAACCTGGAC-3'

5'-GGTTGTCCACCGCGTAGGCATCCAGC-3'

E210A forward and reverse:

5'-CCCTGTGGTGCTGATTGCGAACTCTGGCCGGTGC-3'

5'-GCACCGGCCAGAGTTCGCAATCAGCACCACAGGG-3'

E210Q forward and reverse:

5'-CCCTGTGGTGCTGATTCAGAACTC-TGGCCGGTGC-3'

5'-GCACCGGCCAGAGTTCTGAATCAGCACCACAGGG-3'

2.3.7 Circular Dichroism Spectroscopic Analysis of psToc34(R133A)

Circular dichroism spectroscopy was performed on an Aviv Series 202 circular dichroism spectrometer (Aviv Instruments, Lakewood, NJ). After dialyzing extensively into 50 mM NaH_2PO_4 pH 7.8, 10 mM NaF, the final concentration of the psToc34(R133A) mutant protein was determined to be 7.58 μM using the Bradford Assay. Circular dichroism spectra were collected at 25°C as 2 s averages at 1 nm intervals from 185 to 285 nm. Five spectra were averaged, corrected for buffer contributions, smoothed, and converted to molar ellipticity using the Aviv software, version 2.71. Deconvolution was performed using the CDPro software with IBase3, a reference set of 37 soluble proteins (111). From these data, the secondary structural features of psToc34(R133A) were determined. The STRIDE program was employed to calculate the percent secondary structural elements of crystallized wild type psToc34, chain B, PDB code 1H65.

2.3.8 Activation Energies of the Toc GTPases

Reactions were performed ranging in temperature from 4°C (277K) to 45°C (318K) in 0.6 ml microcentrifuge tubes. Prior to initiation of reaction by addition of Toc protein, the temperature of the reaction buffer and nucleotide was allowed to equilibrate

$$\ln k = -\frac{E_a}{RT} \qquad \text{Eq. 3}$$

for 10 min. Rates were determined as above in hydrolysis assays and graphed as the natural log of the rate (lnk) versus the inverse of the absolute temperature, expressed in Kelvin (10^3/T, K^{-1}). E_a value was determined using the Arrhenius equation (Equation 3), where k is the rate in nanomoles of GTP hydrolyzed per min per μmol Toc protein; R is

the universal gas constant; T is the temperature in Kelvin; and E_a is the energy of activation as expressed in kcal/mol.

2.3.9 Nucleotide Binding Studies Using NTA-Magnetic Absorption

Using iron-incorporated agarose beads with Ni-NTA chemistry (Qiagen Inc., Valencia, CA), various Toc proteins are recaptured via their C-terminal hexahistidinyl tags in a 200 µl reaction volume. This approach affords us the ability to selectively immobilize and extensively wash each protein in the presence of a 96-well hybrid plate magnet. Competition assays for nucleotide binding were performed in GBS buffer with each purified Toc GTPase. The assay contained 20 nM of the GTPase, [α-^{32}P]GTP (MP Biomedicals) with a specific activity of 3000 Ci/mmol, an excess of Ni-NTA agarose magnetic particles and increasing concentrations of competing, unlabeled nucleotide as indicated in the figure 2-10 legend. The conditions were optimized to cover >3 orders of magnitude of the competitor with sufficient data points to permit an accurate nonlinear fit. The reaction was carried out in a 96 well microplate in a total volume of 100 µl. First, a serial dilution of unlabeled competitor was carried out in a separate plate leading to a concentration 4-fold greater than indicated on the x axis. Then, 25 µl of the resulting solution was transferred with a 12-well multichannel pipette into each row of wells in the reaction plate. The [α-^{32}P]GTP was diluted and added to each well of the reaction plate, also in a 25 µl volume. Finally, the Ni-NTA agarose magnetic particles and enzyme were added to start the reaction in a volume of 50 µl. The reaction proceeded for 30 minutes on ice before the plate was transferred to a novel high performance hybrid plate magnet. We used a new class of magnet plates recently developed at the Department of Energy Joint

Genome Institute at Lawrence Berkeley National Laboratory for biological and industrial applications. They utilize hybrid technology that combines linear permanent magnetic and ferromagnetic material to produce significantly higher fields and gradients than currently available on commercial magnetic plates. This hybrid structure exhibited maximum fields in excess of 9000 G, which allowed for greater holding forces on magnetized targets that are being processed, as well as permitting faster draw down. Following immobilization in high field strength, the reaction mixture could be easily removed by aspiration and replaced with 300 µl of GBS. Each well could then be washed continuously with GBS for 2-3 min with a microtiter plate washer (Skatron Microwash II, Norway) to remove all nonspecific background. The wash buffer was then aspirated and replaced with 100 µl of elution buffer (GBS with 500 mM imidazole) and removed from the magnet for 5 min with periodic agitation. After replacement on the magnet for 5 min to ensure immobilization of the beads, 20 µl of the elution was removed for scintillation counting. These 20 µl samples were removed from each well in triplicate and each competition reaction was performed in duplicate. In addition, to avoid the ambiguous results associated with homologous binding competitions performed at a single concentration of labeled nucleotide, at least two concentrations of [α-^{32}P]GTP were used in each case. Thus, the entire competition experiment was repeated using a 3-fold higher concentration of the labeled nucleotide. The samples were counted in a 96-well format using the Toc Count scintillation counter (PerkinElmer Life Sciences) with Microscint fluid, and cross-talk filters were applied before the data were analyzed.

2.3.10 Global Fit Analysis of Nucleotide Binding Data

Using the experimental procedure described above, there were a total of 12 data sets per global fit analysis (i.e. two replicates, each counted in triplicate at two different nucleotide concentrations). These values were fit to Equation 4 using GraphPad Prism 4.0c with the log K_d values shared for global fitting and the amount of hot and cold

$$\text{Total Binding} = \frac{B_{\max}[Hot]}{[Hot]+[Cold]+K_d} + NS \qquad \text{Eq. 4}$$

nucleotide constrained according to the experimental design. The remaining variables were given best-fit values by nonlinear regression. For heterologous binding competitions, the experiments were performed in the same manner, but Equation 5 fit the analysis. In this case, the K_d value measured in the previous experiment was substituted

$$\text{Total Binding} = \frac{B_{\max}[Hot]}{[Hot]+K_d\left(1+\frac{[Cold]}{K_i}\right)} \qquad \text{Eq. 5}$$

into the equation, and the log K_i value was shared for all data sets for global fitting. The amount of labeled and nonlabeled GTP was held constant, and the remaining variables were given best-fit values by nonlinear regression. For data analysis, a confidence of 95% was used.

2.4 Results

2.4.1 Expression and Purification of Toc Proteins and Transit Peptide

We overexpressed atToc34ΔTM and atToc33ΔTM (*E. coli* TG1) (where 'at' refers to *Arabidopsis thaliana*) and psToc34ΔTM and atToc159G (*E. coli* BL21[DE3]) (where 'ps' refers to *Pisum sativum*) as soluble protein and purified via IMAC using the

Figure 2-1. Overexpression and purification of Toc GTPases and transit peptides. Panel A, atToc33 and atToc34 were overexpressed in E. coli strain TG1, atToc159G, and psToc34 in E. coli strain BL21(DE3). Proteins were purified under nondenaturing conditions using Co^{2+} IMAC and eluted with a step gradient from 15 mM (wash 3) to 250 mM imidazole (elution 1–3). Total protein, pellet, flow-through (lanes 1–3), washes (lanes 4–6), elutions (lanes 7–9), and marker (lane 10) were separated by SDS-PAGE followed by Coomassie Blue staining. Panel B, lanes 1–5 are marker, psToc34, atToc33, atToc34, and atToc159G, respectively. Toc proteins were loaded under equal mass conditions (100 ng), separated by SDS-PAGE, and followed by Coomassie Blue staining. Panel C, transit peptide was purified using chitin affinity chromatography. Total protein, pellet, soluble fraction, flow-through, wash and elution (lanes 1–6) were separated by SDS-PAGE and visualized by Coomassie Blue staining. Panel D, MALDI-TOF of SStpNt was performed on a Bruker Daltonics MicroflexTM mass spectrometer, with apomyoglobin used as an internal standard for calibration. The +2 and +3 charge states of apomyoglobin species can be seen at 8477 m/z (average molecular weight of apomyoglobin is 16,952) and 5651.7m/z, respectively. The +1 and +2 charged SStpNt species are found at 6125.9 and 3062.6m/z. The species at 4152.6 m/z is a fragment resulting from proteolysis during isolation.

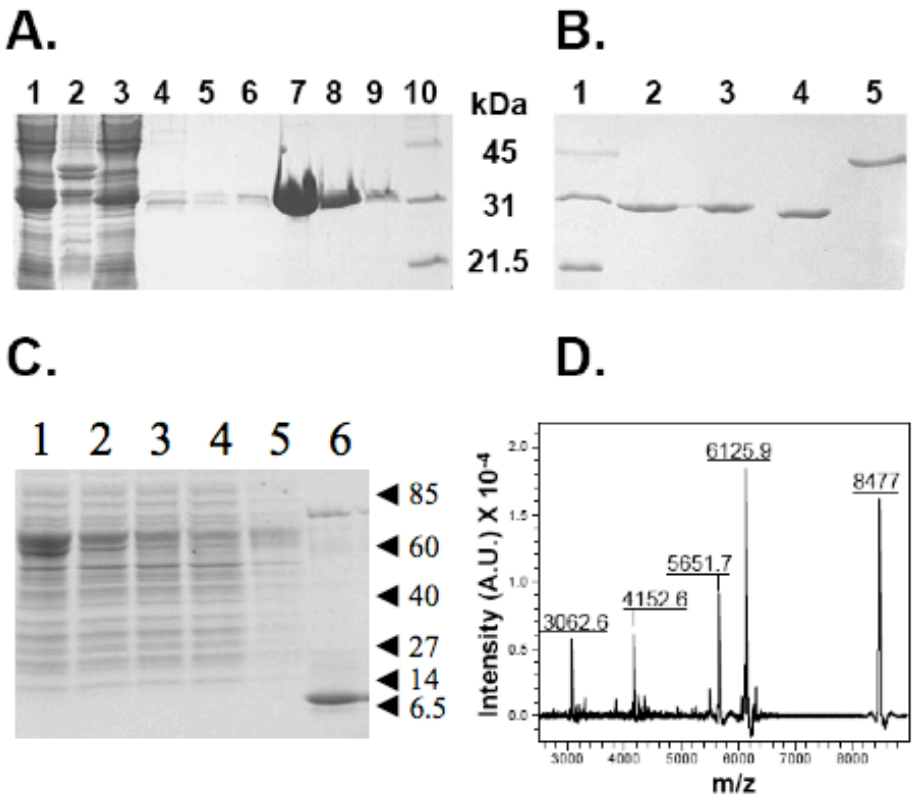

A.
1 2 3 4 5 6 7 8 9 10
kDa
45
31
21.5
B.
1 2 3 4 5
C.
1 2 3 4 5 6
85
60
40
27
14
6.5
D.
6125.9
8477
5651.7
4152.6
3062.6
Intensity (A.U.) X 10-4
m/z

Figure 2-1

C-terminal hexahistidinyl tag, Figure 2-1A. As a matter of convention, all Toc proteins used in this study represent the soluble, GTPase domain free of transmembrane domain as denoted by ΔTM. *E. coli* supernatant, pellet and flow through are shown in lanes 1-3 of Figure 2-1A whereas three consecutive column washes are visualized in Figure 2-1A lanes 4-6, respectively. Three elutions of protein are shown in Figure 2-1A lanes 7-9 and molecular weight markers are in lane 10. To verify purity, 100 ng of each protein was run on 15% acrylamide SDS-PAGE and concluded to be greater than 95% pure, Figure 2-1B where lanes 1-5 correspond to marker, psToc34, atToc33, atToc34 and atToc159G, respectively. The transit peptide construct with a C-terminal intein and chitin-binding domain was overexpressed in *E. coli* ER2566 cells as soluble protein. One-step purification was accomplished using a chitin affinity column with intein-mediated selfcleavage, and elution was induced by addition of β-Me, Figure 2-1C. Supernatant, flow through and three column washed are visualized in Figure 2-1C lanes 1-5, respectively. Cleaved protein was purified to homogeneity, as confirmed by gel electrophoresis, Figure 2-1C, lane 6, and MALDI-TOF mass spectrometry Figure 2-1D. MALDI-TOF MS of transit peptides was performed with apomyoglobin used as an internal standard on a Bruker-Daltonics MicroflexTM mass spectrometer shown in Figure 2-1D. The +2 and +3 charged apomyoglobin species can be seen at 8477 m/z and 5651.7 m/z, respectively; the average molecular weight of apomyoglobin is 16,952 Da. The +1 and +2 charged SStpNt transit peptide species are found at 6125.9 and 3062.6 m/z, respectively. The FindPept tool (http://ca.expasy.org/) was used to identify the peptides that correspond to the main peaks. The largest peak at 6125.9 m/z corresponds to the full-length transit peptide, whereas the minor peak at 4152.6 m/z represents either an

alternative translation initiation at Met-22 or alternatively a degradation product where short N- and C-terminal regions were proteolytically removed during expression and purification, Figure 2-1C. Similarly, MALDI-TOF analysis of the purified *Pisum sativum* transit peptide (SStpPs) indicated that the full-length peptide had the expected mass of 6182.2 (data not shown).

2.4.2 Generation of Glycerol Stabilized IMAC-Toc34 Columns

The requirement to have a generous amount of protein stabilized and ready for elution led to the development of stabilized psToc34 columns. TALON resin (BD Biosciences) was used to immobilize psToc34 via the C-terminal hexahistidinyl tag. TALON relies on Co^{2+} as the divalent metal cation and resulted in considerably more stability when stored for long periods of time as compared to Ni^{2+} (data not shown). TALON purified psTo34 (bound and washed with 5 mM imidazole to prevent non-specific protein binding and thus contamination) was placed into a 5 cm BioRad mini centrifuge column with glass frit. GBS buffer with 20% glycerol was added and allowed to drain. GBS with 20% glycerol was again added, and the top and bottom of the mini-column was capped and sealed with Parafilm. The columns were then allowed to slow freeze at -20°C and remained stable for up to a year. Upon slow thawing on ice, GBS buffer was passed through the column using centrifugation not in excess of 700 g. Generally 3 ml (or 2 column volumes) of GBS buffer was sufficient to remove glycerol. 250 mM imidazole in TALON buffer (50 mM $NaPO_4$ pH 7.0) was used to elute the column in five 500 µl elutions. The two most concentrated fractions were pooled and quantified.

2.4.3 Effects of Buffers, Storage Conditions, Enzyme Concentrations and Metal Ions

One possible explanation for the variation in reported activities observed for the Toc GTPases is their sensitivity to various buffers, storage conditions, and metal ion contaminants. As such, it was important to test how different buffer systems affected the hydrolysis activity measurements. We tested four buffers for their effect on the GTPase activities of psToc34. A comparison of the enzymatic activity of psToc34 in these four buffers is shown in Figure 2-1A. Despite the differences in their composition, all of these buffers yielded relatively similar activities of psToc34; however, GBS appeared to have slightly higher levels of GTPase activity after background subtraction.

Upon determining the best buffer for enzymatic activity, an additional variable is how the protein is stored prior to use; therefore, we also tested several freezing and storage conditions as follows: -80°C slow, -80°C fast, liquid nitrogen storage (or -196°C), and -20°C as shown in Figure 2-2A. We found that -80 °C slow freeze afforded the greatest maintenance of activity, and under optimal storage conditions, we were able to freeze and thaw the protein approximately 3 times before activity became impaired (data not shown). Furthermore, GBS buffer was able to maintain the GTPase activity of the Toc proteins at -80°C in 20% glycerol for up to 4 weeks, after which the activity began to diminish (data not shown). The activity of psToc34 was assayed as a function of the pH in Figure 2-2B. We varied several buffers (each buffering agent at 20 mM) from pH 6.0 to 12.0 and tested the maximal velocity as described above. Consistent with previous publications reporting the activity of psToc34 in GBS buffer, pH 7.6 was

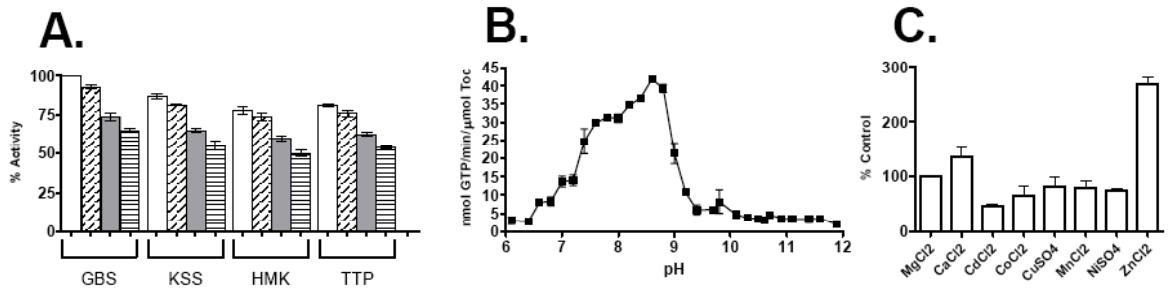


Figure 2-2. Buffer, storage condition, pH titration and metal ion exchange. Panel A, four buffers were chosen to assay the kinetic parameters of the Toc GTPases: GBS, KSS, HMK and TTP (see Materials and Methods). psToc34 was assayed for maximal activity in each buffer and at four different storage conditions: -80°C slow, -80°C fast (liquid nitrogen first, then -80°C), - 20°C and liquid nitrogen, depicted as white, diagonal lined, grey and horizontal lines, respectively. *B*, the pH of GBS was altered using different buffering agents to obtain buffer pH between 6.1 and 11.9. *C*, psToc34 was incubated with 5 mM of the following cations: $MgCl_2$, $CaCl_2$, $CdCl_2$, $CoCl_2$, $CuSO_4$, $MnCl_2$, $NiSO_4$ and $ZnCl_2$. After sufficient time for metal ion exchange, GTP hydrolysis was measured in GBS supplemented with the appropriate metal cation. Rates are plotted as % control.

chosen (59). According to Figure 2-2B, the pH optimum for psToc34 is between 7.5 and 8.2, and we therefore maintained the pH at 7.6 in accordance with the published GBS buffer.

Because it has been reported previously that Ras and other small GTPases are affected by the metal cofactor in the nucleotide-binding site (112), we attempted to remove Mg^{2+} from the active site of the Toc proteins by dialysis with EDTA in Mg^{2+} free GBS. This treatment consistently resulted in protein precipitation (data not shown). Alternatively, we were able to add various metal salts at a large molar excess to determine whether these metal ions could possibly exchange with the Mg^{2+} ion in the active site. The results of how $MgCl_2$, $CaCl_2$, $CdCl_2$, $CoCl_2$, $CuSO_4$, $MnCl_2$, $NiSO_4$, and $ZnCl_2$ affect activity is shown in Figure 2-2 C. Suppression of activity was seen with all metals but two, CaCl2 and ZnCl2, of which the ZnCl2 stimulated the hydrolysis activity nearly 2.7-fold. As a control, each metal salt was incubated with nucleotide (in the absence of enzyme) showing no effect on the spontaneous rates of GTP hydrolysis (data not shown).

2.4.4 Hydrolysis Activity of the Toc GTPases

The enzymatic parameters K_M and V_{max} have been reported in the past with substantial variation using a polyethyleneimine-cellulose TLC technique and image analysis. To provide a more robust method, we used an activated charcoal, pulldown assay using radioactive [γ-^{32}P]GTP. This assay employs liquid scintillation counting to quantitate the amount of P_i released by GTP hydrolysis. In this assay, we incubated the ΔTM Toc proteins with [γ-^{32}P]GTP at 25 °C. Aliquots of the reaction were added to 10%

(w/v) activated charcoal where only the hydrolysis product $^{32}PO_4^{-3}$ along with H_2O, HCl, and H_3PO_4 remain in the filtrate after a 0.2 μm vacuum filtration step. Aliquots of this filtrate were counted in a scintillation counter. A bovine serum albumin control yielded counts analogous to spontaneous hydrolysis (data not shown). Counts/min data from at least three independent experiments were obtained and graphed as nanomoles of GTP hydrolyzed per min per μmol of Toc protein, Figure 2-3, A-D. This analysis indicates that atToc33, atToc34, and psToc34 share very similar K_M and V_{max} values, whereas atToc159G does not. Values from 3.5 to 6.3 μM for the Michaelis-Menten constant, K_M, and 35–37 nmol of GTP hydrolyzed per min per μmol Toc protein for the maximal velocity, or V_{max}, were obtained for the smaller GTPases, Table 2-1. The G domain of atToc159 had a K_M and a V_{max} of 21.16 μM and 10.13 nmol GTP hydrolyzed per min per μmol Toc protein, respectively, Table 2-1. In the case of the Toc34 subfamily of proteins, all three displayed a sharp substrate-velocity curve, whereas atToc159G did not, representative of its relatively low maximal velocity and decreased affinity for substrate.

2.4.5 Hydroysis Rates of the Toc GTPases are not Influenced by Concentration-Dependent Dimerization

The psToc34 protein has been shown to undergo concentration dependent dimerization as assayed by size exclusion chromatography, analytical ultracentrifucation and crosslinking and/or gel shift assays (53). Since the crystal structure indicates the involvement of multiple residues of one monomer interacting with the bound nucleotide of the other monomer, it could be inferred that dimerization may play a role in the kinetics of GTP hydrolysis. To that end, we tested whether dimerization modulated the

	V_{max}	K_M	E_a	k_{cat}
	nmol/min/μmol	*μM*	*kcal/mol*	min^{-1}
psToc34	37.4 ± 1.0	3.7 ± 1.0	13.5 ± 0.6	0.037 ± 0.001
atToc33	35.4 ± 1.2	5.7 ± 0.9	15.6 ± 0.3	0.035 ± 0.001
atToc34	35.1 ± 1.0	6.3 ± 0.8	15.7 ± 0.7	0.035 ± 0.001
atToc159G	10.13 ± 0.5	21.2 ± 3.0	10.1 ± 0.4	0.010 ± 0.0005

Table 2-1. Kinetic parameters of the chloroplast Toc GTPases. Maximal Velocity, or V_{max}, is reported as nmol GTP hydrolyzed per minute per μmol Toc protein. The affinity for substrate, or K_M, is reported in μM. The energy of activation, or E_a, is reported in kcal mol^{-1}. Finally, the turnover rate, or k_{cat}, is reported in GTP hydrolytic events per minute, or min^{-1}.

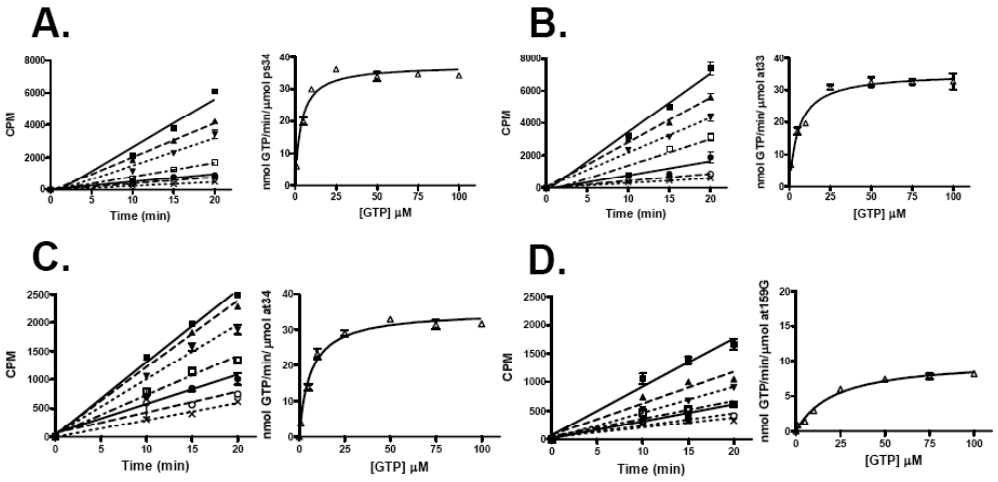


Figure 2-3. Determination of K_M and V_{max} values of Toc GTPases. A–D, represent counts/min versus time (left) and rate versus substrate concentration (right) of the four Toc proteins psToc34, atToc33, atToc34, and atToc159G, respectively. In the left panel of A–D, the indicated concentration of total GTP (μM) is 1, ■; 5, ▲; 10, ▼; 25, □; 50, ●; 75, ○; and 100, ×, respectively. The [γ-32P]GTP in all experiments was held constant at 10 nM. Linear regression of counts per min yielded a slope that was then mathematically transformed into a rate expressed as nanomoles of GTP hydrolyzed per min per μmol of Toc protein, see "Experimental Procedures." The rate at each GTP concentration was then graphed to yield the Michaelis-Menten substrate velocity plot. The data were fit to the Michaelis-Menten equation to determine the V_{max} and K_M values of each protein.

V_{max} or K_M of the proteins. Interestingly, the GTP hydrolysis rate of the four Toc GTPases, when corrected for protein concentration, do not increase in rate as a function of protein concentration, Figure 2-4. The vertical *dashed* and *dotted lines* in Figure 2-4 represent Toc protein concentrations of 1.7 and 16.9 μM, respectively. These concentrations correspond to values at which homobifunctional crosslinking revealed psToc34 to be monomeric and mostly dimeric, respectively. Therefore, the maximal rate of the psToc34 protein is not affected by protein dimerization *in vitro*. This does not preclude the possibility that dimerization *in vivo* may affect the hydrolytic rate and thus protein import.

2.4.6 The Mutant Protein psToc34(R133A) is Monomeric and Lacks GTPase Activity

The crystal structure of the psToc34 homodimer reveals the side chain of Arginine 133 of one monomer extending deeply into the GTP-binding pocket of its dimeric partner (Figure 1-4) suggestive of an arginine finger, a moiety common to many GTPase/GAP crystal structures. An 'arginine finger' presents a local positive charge in order to compensate for the negative charges on the oxygen atoms of the γ-phosphate during the transition state of GTP to GDP. Although there are two closely positioned arginines in the dimeric interface of psToc34, Sun *et al.* hypothesized that Arg-133 functioned as the arginine finger (61). Equivalently positioned arginine fingers have been observed in the GAPs co-crystallized with other small GTPases such as H-Ras (113), CDC42 (114), and RhoA (115).

By testing the homobifunctional crosslinkers listed in Figure 2-5, it was shown

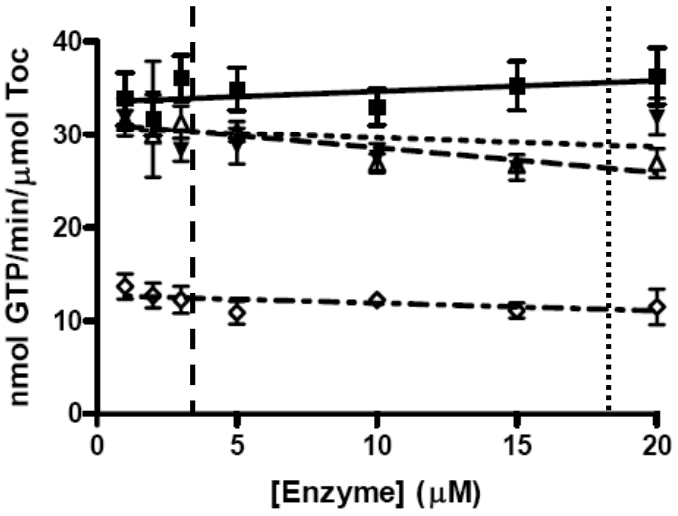


Figure 2-4. Hydrolysis rate of psToc34 is not influenced by protein concentration. Hydrolysis data of psToc34 (solid line, ■), atToc33 (dashed line, △), atToc34 (dotted line, ▼) and atToc159G (dot-dash-dot line, ◇) were assayed at 1, 2, 3, 5, 15 and 20 μM Toc protein. Resultant data were normalized for protein concentration. Dashed and dotted lines indicate protein concentrations where the Toc protein was shown to be monomeric and dimeric, respectively.

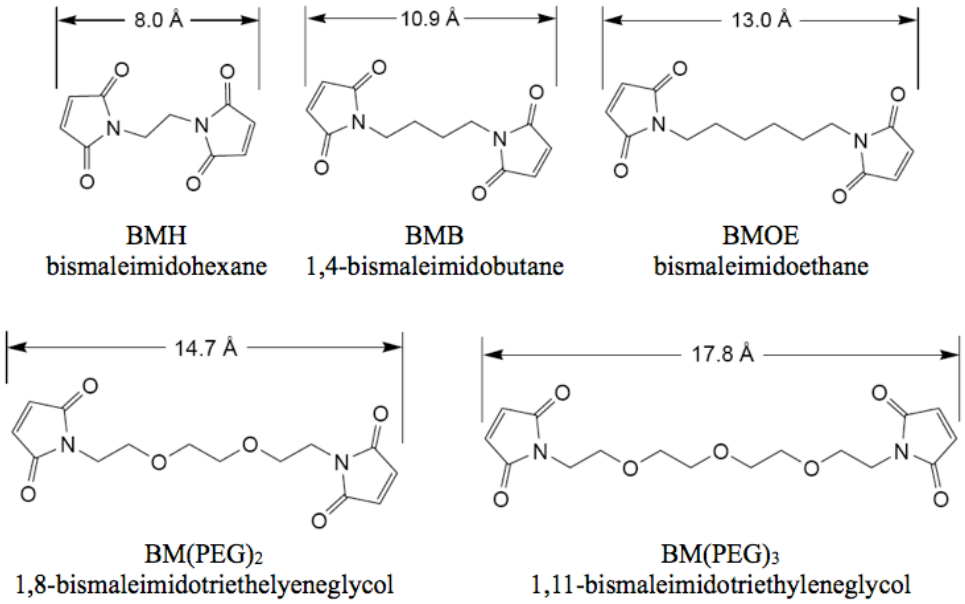


Figure 2-5. Chemical Structures used for Homobifunctional Crosslinking. Maleimido crosslinkers are used to crosslink –SH groups in proteins or thiols in other molecules. This study used five crosslinkers, as indicated in the figure. Each is capable of linking two cysteine amino acids as long as those residues are close in proximity and between pH 6.5-7.5. The length, in Angstroms, of the crosslinker spacer arm is indicated.

that all crosslinkers were able to trap a portion of the dimeric psToc34 (data not shown). The crosslinker bismaleimidohexane (here on out referred to as BMH) was chosen for all further experiments. Wild-type psToc34, as shown in Figure 2-6 lanes 1 and 2, has a defined profile under conditions of homobifunctional crosslinking with BMH; in the absence of crosslinker, psToc34 is observed as a monomer whereas in the presence of crosslinker, a second species at 58 kDa is observed. The shift in size indicates that two psToc34 molecules were been trapped by linking their respective cysteine residues (located at position 215, located in the large loop at the top of the molecule in Figure 1-4). Evidence suggests the psToc34 monomers are joined covalently since the DTT present in the sample-loading buffer does not alter their gel mobility. As indicated in figure 2-5 lane 3, the R133A mutant protein remains primarily monomeric indicating that this mutation has disrupted the psToc34 homodimeric interface.

In addition to eliminating concentration-dependent dimerization, the mutation R133A also abolishes the *in vitro* GTP hydrolytic activity (Figure 2-7). The low level of hydrolysis is essentially indistinguishable from the rates of spontaneous GTP hydrolysis, whereas wild-type psToc34 exhibits a sharp substrate-velocity curve, also shown for comparison. This very low activity precludes determination of the V_{max} or K_M values with any statistical certainty. These two observations taken together indicate that the R133A mutation disrupts both GTP hydrolysis in the monomer and prevents homodimerization.

To rule out the possibility that the R133A mutant resulted in misfolding or some global structural change, circular dichroism spectroscopy was performed on purified psToc34(R133A) shown in Figure 2-8. Comparison of the data to the published CD

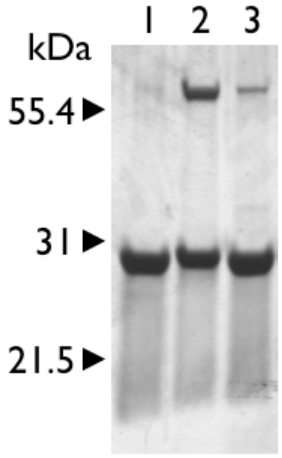


Figure 2-6. Homobifunctional crosslinking of *wt* and mutant psToc34. Wild type psToc34, upon DTT mediated reduction, runs on SDS-PAGE as a monomer of 29 kDa, lane 1. Incorporation of BMH (see chapter 3) facilitates the maleimido-crosslinking and thus the observed species at 58 kDa, lane 2. The mutation R133A renders the psToc34 protein unable to form homodimers and thus unable to be trapped to a significant degree by the crosslinking agent BMH, lane 3.

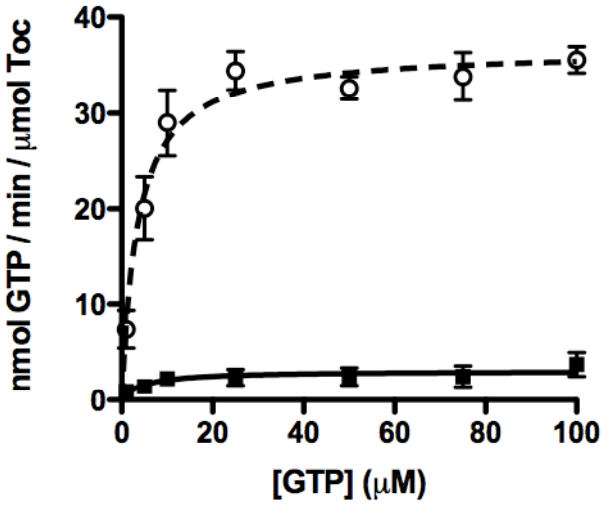


Figure 2-7. The mutant form of psToc34 lacks GTPase hydrolytic activity. psToc34(R133A) mutant protein, solid line, ■, is severely reduced in its GTP hydrolytic activity as compared with wild-type psToc34, dashed line, ○.

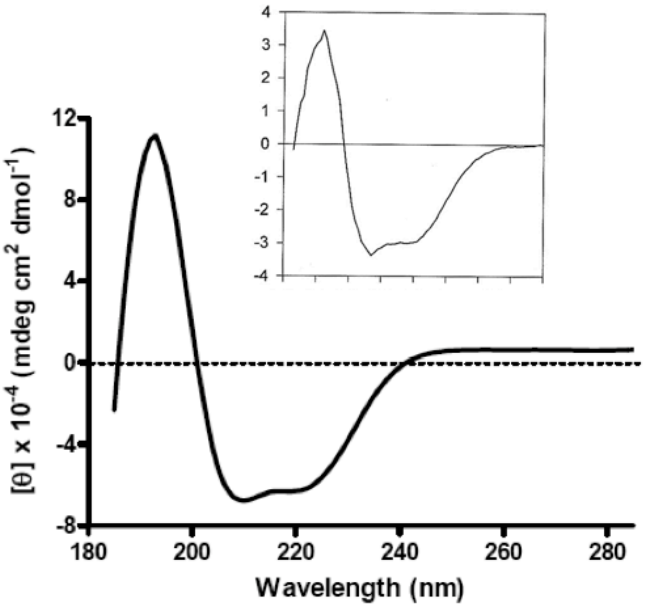


Figure 2-8. Far UV circular dichroism spectrum of psToc34(R133A). psToc34R133A was diluted to 7.5 μM in 50 mM NaH_2PO_4, pH 7.8, 10 mM NaF; data was collected at 25°C. [θ] represents mean residue ellipticity with the units of millidegrees cm^2 $dmol^{-1}$. The inset figure, CD of wild type psToc34) is for comparison and is from Schleiff, *et al.*, 2002.

spectra of wild-type psToc34 (inset in Figure 2-8) reveals high spectral similarity (108). Deconvolution was performed on the CD spectra using the CDPRO program (http://lamar.colostate.edu/~sreeram/CDPro/main.html). The secondary structural content predicted by this program is shown in Table 2-2.

2.4.7 Activation Energies of the Toc GTPases

To determine the energy of activation for the various Toc proteins, Toc protein was incubated in GBS buffer, at different temperatures ranging from 4 to 45°C (the proteins were not stable above 55°C; data not shown). The hydrolysis assay was performed as described above and the rate of hydrolysis was calculated as before. An Arrhenius plot was created from the natural log of the rate and the inverse of temperature expressed as $10^3/T$ (K^{-1}) shown in Figure 2-9. The energies of activation, E_a, expressed in kcal/mol for psToc34, atToc33, atToc34, and atToc159G are shown in Table 2-1.

2.4.8 Nucleotide Binding Activity of the Toc GTPases

A novel approach was used to determine the equilibrium dissociation constants of the various Toc proteins for GTP, GDP, and other nucleotides. The particular Toc protein was incubated with a known concentration of radiolabeled [α-^{32}P]GTP as well as increasing concentrations of unlabeled GTP in the case of homologous competition. Homologous and heterologous competition assays were carried out on the Toc GTPases using a variety of substrates to determine affinities and to gain insight into the significance of the interacting moieties, as shown in Figure 2-10, A-F. Panel A-D in Figure 2-10 represent the binding of GTP (squares), GDP (circles) and XTP (triangles)

	α-helix	3/10 helix	β-sheet	Turn	Unstructured
psToc34(wt)[a]	0.360	0.055	0.190	0.170	0.225
psToc34(R133A)[b]	0.346	0.000[c]	0.182	0.220	0.252

Table 2-2. CD Secondary Structural Analysis of *wt*psToc34 and psToc34(R133A). [a]Secondary structure content of wt protein was determined using STRIDE program with Chain B coordinates (pdb id 1H65, Sun *et al*.). [b]Secondary structure estimation of R133A was based on CD data deconvoluted with CDPRO as described in experimental procedures. [c]Due to our instrument's lamp properties we are unable to collect data below 185 nm which is required to assign 3/10 helix content by employed deconvolution software (see Materials and Methods).

	GTP[c]	GDP[d]	XTP[d]	GMP-PNP[d]	GTP-γ-S[d]	UTP[d]
psToc34	50 (42-61)	151 (135-170)	41 (36-47)	288	70	$2.15x10^5$
atToc33	29 (21-39)	78 (63-91)	63 (54-68)	-	-	-
atToc34	1219 (807-1426)	2735 (1667-4375)	853 (710-1028)	-	-	-
atToc159G	406 (270-611)	3365 (2535-4467)	-[e]	-	-	-

Table 2-3. Binding of nucleotide substrates to the Toc GTPases. Values in nM, values in parentheses represent 95% confidence interval, [c]K_d, [d]K_i, [e]not determined. Data presented here are from global fits of multiple nucleotide concentrations, therefore, the data presented in Fig. 2-10 approximates the obtained values.

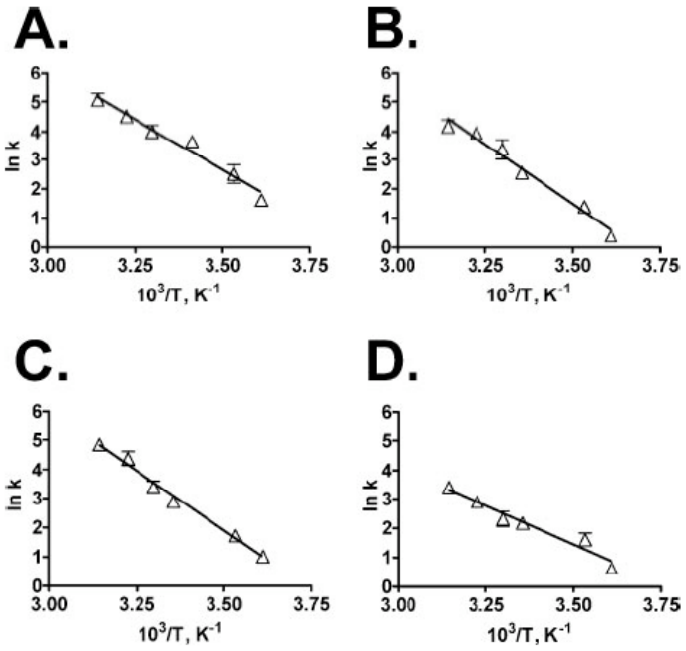


Figure 2-9. Energy of activation of the Toc GTPases. A–D, represent the dependence of the rate of psToc34, atToc33, atToc34, and atToc159G on temperature, respectively. The maximal rate of GTP hydrolysis was determined for each protein at various temperatures. The natural log of the rates of GTP hydrolysis of the Toc GTPases are plotted as a function of the inverse of temperature 10^3/T in Kelvin.

Figure 2-10. Nucleotide binding activity of the Toc GTPases. A–D, represent the outcome of homologous and heterologous nucleotide binding competition assays for psToc34, atToc33, atToc34, and atToc159G, respectively. K_d and K_i values were determined for GTP, □; GDP, ●; and XTP, △,. Note that the atToc159G-XTP heterologous competition data were not of sufficient quality to allow a confident fitting of K_i; however, a trend line is included for visual clarity. E, is the result of a heterologous competition of [α-^{32}P]GTP with the nonhydrolysable analogues GTP-γ-S, ▲, and GMP-PNP, ◇. Various other nucleotides were used as competitors (F), 8-bromo-cGMP, ■; 2',3'-cGMP, ▲; 3',5'-cGMP, ▼; ATP, ◆; CTP, ●; TTP, □; UTP, ▽; and CDP, △, most of which did not compete for binding. Both E and F were performed with psToc34.

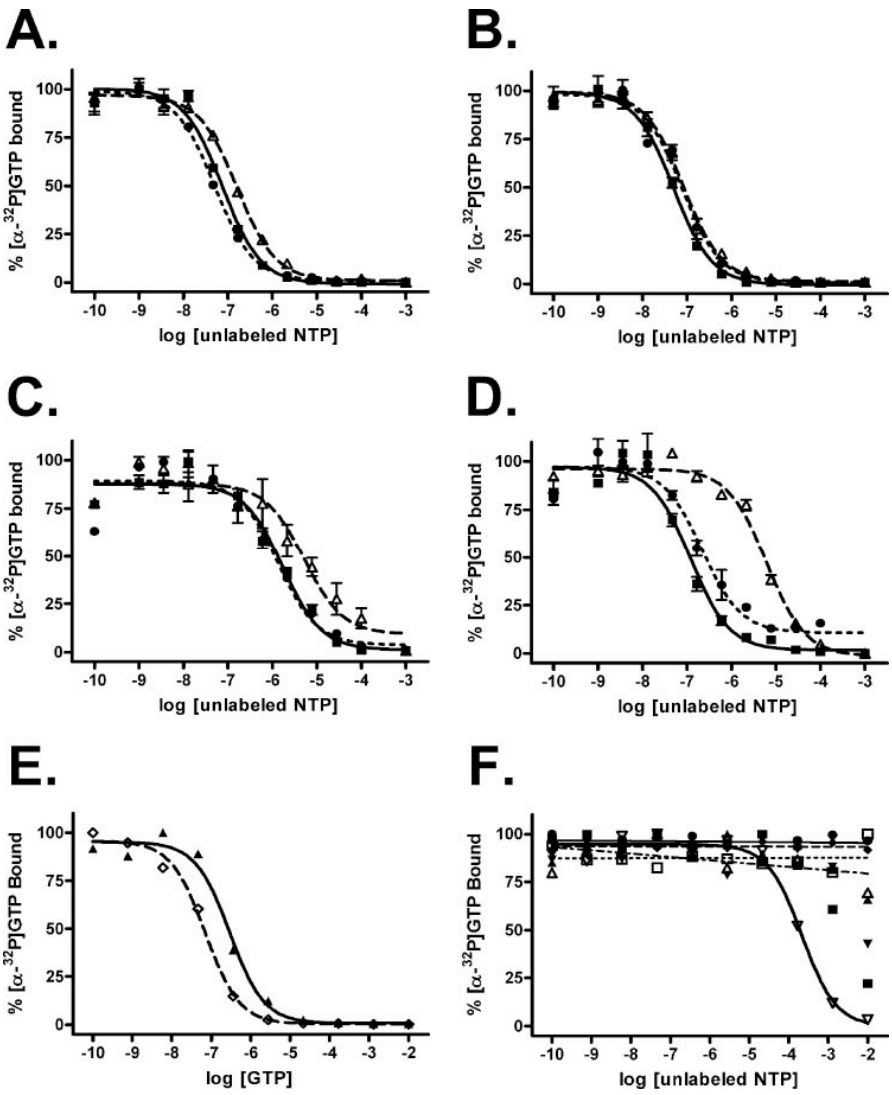

A.
B.
C.
D.
E.
F.
% [α-32P]GTP bound
% [α-32P]GTP Bound
log [unlabeled NTP]
log [GTP]
100
75
50
25
0
-10
-9
-8
-7
-6
-5
-4
-3
-2

Figure 2-10

All of the Toc GTPases in this investigation bound GTP but with varying degrees of affinity, ranging from 29 nM to 1.2 μM (Table 2-3). Although these enzymes have already been implicated as GTPases, no systematic enzymatic comparison has been made. Unlike the hydrolysis data, psToc34 and atToc33 both bind GTP quite strongly with K_d values of 50 and 29 nM, respectively, whereas atToc34 and atToc159G have considerably lower affinities. The difference in affinity of the psToc34 family for GTP and GDP was not great, showing only a 2- to 3-fold difference. In contrast, whereas atToc159G does not bind GTP as tightly as the small Tocs, it appears to be the most effective discriminator of GTP and GDP with nearly a 10-fold difference (Table 2-3).

Heterologous competitions also demonstrated that these GTPases have nearly identical affinities for GTP and XTP. Various other substrates were tested with psToc34, and strong affinity was also shown for GTP-γ-S and GMP-PNP (Figure 2-10 E). These results show that, although they fail to be hydrolyzed, the GTP-like properties of GTP-γ-S and GMP-PNP both compete for binding; however, GTP-γ-S with its lower K_i value suggests it is the more appropriate nonhydrolyzable GTP analogue for psToc34. In this assay, psToc34 did not have any significant affinity for the cGMP analogues, the purine ATP, nor the pyrimidine TTP, Figure 2-10, F. However, most interestingly, it was able to slightly bind the pyrimidine UTP, which shares an analogous placement of a carbonyl oxygen with the purine GTP, suggesting that this oxygen is critical for recognition by psToc34. This may also explain the ability of psToc34 to bind XTP.

2.4.9 Nucleotide Exchange of psToc34 is Not Stimulated by Transit Peptide

To determine whether transit peptides affect the rate of GDP/GTP exchange,

psToc34 was preincubated with [α-^{32}P]GTP, and the dissociation of labeled nucleotide was monitored by scintillation counting as a loss of counts as a function of time under several conditions. Figure 2-11, dashed line with closed squares, represents the basal rate of GDP loss with psToc34 alone in GBS. The remaining data indicate that there is no significant difference between the rate of GDP for GTP exchange without SStpNt (open triangles) relative to the rate of GDP for GTP exchange at any amount of SStpNt, as indicated in Figure 2-11 legend.

2.4.10 Creation of a Toc XTPase

Both Toc34 and Toc159 are present in the Toc Core Complex (Figure 1-3) and evidence exists suggesting these two proteins may form a heterodimer (68,109). Since the contribution of each of their GTPase activities to the overall process of protein import is unknown, the ability to distinguish catalytic events at one GTPase protein over the other (*e.g.* Toc34 GTP hydrolysis versus Toc159 GTP hydrolysis) may aid in elucidating the precursor protein import mechanism. To this end, we designed a mutation in psToc34 changing glutamate 210 to glutamine resulting in the psToc34(E210Q) mutant protein. This mutation should allow psToc34 to recognize xanthosine rather than guanosine such that the protein is an XTPase instead of a GTPase (116). As a negative control, we created psToc34E210A. Figure 2-12 A reveals that wild type protein hydrolyzes GTP at a maximal velocity of ~35 nmol per min per μmol Toc protein with a K_M of 3.3 μM. The proteins psToc34(E210Q) and psToc34(E210A) hydrolyze at ~16 and ~37 nmol per min per μmol Toc protein, respectively, with K_M's of 23.9 and 54.2 μM, respectively. Alternatively, figure 2-12 B shows that wild type psToc34 is unable to hydrolyze XTP at

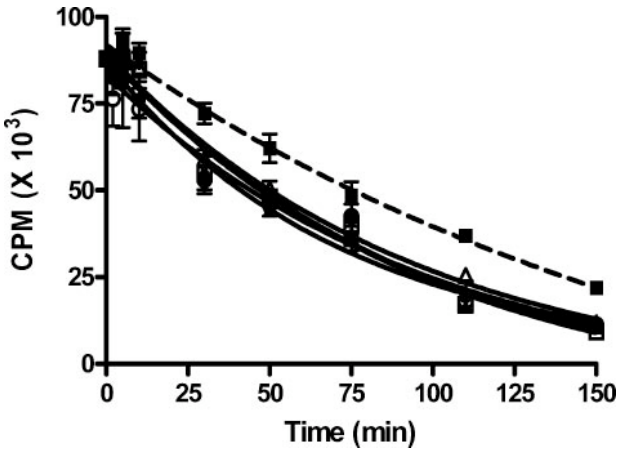
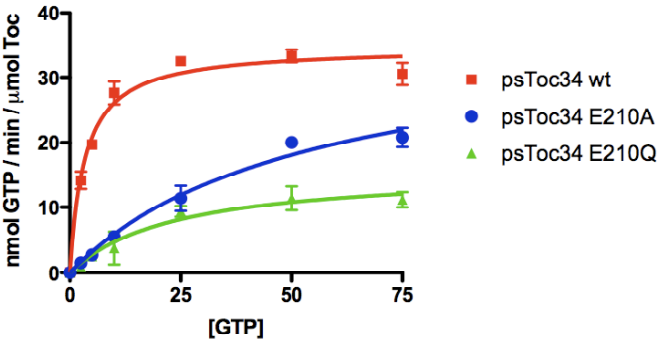
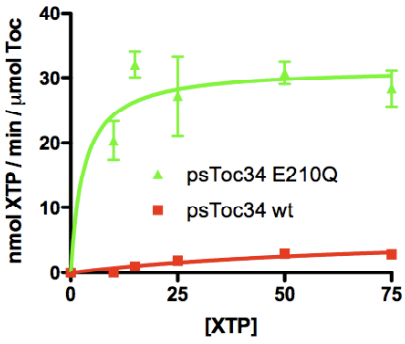


Figure 2-11. Effect of transit peptide on GDP/GTP exchange rate. psToc34 was preloaded with [α-32P]GTP and then incubated with the following: GBS, dashed line, ■; 100-fold GTP, solid line, △; and the following represented by dotted lines, 100-fold GTP with 0.3-fold SStpNt, □; 100-fold GTP with 1.5-fold SStpNt, ●; 100-fold GTP with 7.5-fold SStpNt, ▲; or 100-fold GTP with 37.5-fold SStpNt, ○. No significant difference in the rate of GDP loss was observed between 100-fold GTP and any amount of SStpNt in the presence of 100-fold GTP.



	psToc34 wt	psToc34 E210Q	psToc34 E210A
Vmax	34.78	15.94	37.77
Km	3.351	23.94	54.19



	psToc34 E210Q	psToc34 wt
Vmax	31.53	6.230
Km	3.000	75.33

Figure 2-12. Creation of a psToc34 XTPase. The psToc34 protein was mutated at a critical residue involved in the orientation of the guanosine group of GTP. Panel A shows that the mutants E210A and E210Q have significantly reduced GTPase activity, blue and green, respectively. However, panel B indicates that the psToc34 E210Q mutant can successfully distinguish XTP from GTP in a γ^{32}P[XTP] experiment; note that the V_{max} and K_M for XTP are similar to that of GTP for wt psToc34.

an appreciable rate, reaching a V_{max} of 6.2 nmol XTP per min per μmol Toc and K_M 75.3 μM. The psToc34(E210Q) protein hydrolyzes XTP with a V_{max} of 31.5 nmol XTP per min per μmol Toc and a K_M of 3 μM. This shows, for the first time, substrate specificity alteration in a Toc GTPase and indicates clearly the E210Q mutation has shifted the substrate specificity of psToc34 for XTP instead of GTP.

2.5 Discussion

Key elements of the translocation complex of the outer membrane of the chloroplast had been identified and the functions of these individual components had been probed to some degree, but the mechanistic details of the Toc complex remain unclear. To better understand the function of the Toc complex, the behavior of the individual Toc components must be investigated in vitro, and more specifically, their basal enzymatic activities must be explored. Several groups had reported basal GTP hydrolysis rates for recombinant, ΔTM forms of psToc34, atToc33, atToc34, and atToc159G. Although it would not be surprising for these rates to vary between the different homologues, the substantial variation in the reported kinetic properties between different research groups, and on occasion even within a given research group for the same protein, is troubling. For example, with psToc34, careful analysis of the published data reveals hydrolysis rates within the same article that vary from 0.588 to 26.5, when expressed as nanomoles of GTP per min per μmol Toc protein (61). Moreover, substantial variability is seen when comparing the hydrolytic rates (in nmol per min per μmol) of homologous proteins between pea and *Arabidopsis*, where values range from 0.588 for psToc34 (61) to ~300 for atToc33 and atToc34 (59). Upon comparing the

reported values for rates of hydrolysis in the literature, a lack of standardization becomes apparent. Also, there were experimental design problems, including reporting rates of GTP hydrolysis that are nonlinear with time (55,67,106), kinetic analyses performed with subsaturating levels of GTP (106,109), and application of nonlinear fits to poor or limited data with no error analysis (77).

To help reconcile these conflicting reports, we determined the enzymatic properties of these four Toc GTPases in parallel, thus enabling a direct comparison of their GTPase properties. One possible explanation of the observed variations in the literature is that different conditions were used by different laboratories to test their GTPase activities. By systematically testing several buffer systems and storage conditions, it was clear that psToc34 was fairly robust and tolerant of different buffer and storage means. In light of the optimized buffer, pH, and storage conditions, which are quite similar to those reported by others, the variations in reported rates cannot be because of variable conditions. All together, the buffers, storage conditions, and pH could at most only account for ~30% change in activity; those reported for the Toc GTPases vary in some cases by 100-fold (59).

It has been shown for other small GTPases that require Mg^{2+} for their activity (21,31,35,106) that very few other cations can substitute for Mg^{2+} in the catalytic site. The Mg^{2+} ion in the active site of psToc34 was replaced with several different cations and it was found that only Zn^{2+} could support hydrolysis activity of psToc34 at or above the Mg^{2+} level. Although zinc has a smaller radius than magnesium (1.34 versus 1.60 Å) it may still be able to fit into the metal-binding site of psToc34, thereby stabilizing GTP. Indeed, other divalent metal cations have been shown to bind to other GTPases, for

example the replacement of the Mg^{2+} by Mn^{2+} in p21 Ras results in a higher GTPase activity (112). This stimulation has been suggested to involve an increase of the pKa of the γ-phosphate of GTP resulting in an increase of reaction rate at neutral pH. Schweins, *et al.* determined that this relationship between pKa of nucleotide and hydrogen ion abstraction potential indicated that the GTP itself acts as a general base in the reaction. This divalent metal cation-mediated rate increase was also shown to be the case with two other GTPases: Rap1A and Ran (112). The lack of elevated GTP hydrolysis by psToc34 with Mn^{2+} is puzzling; however, the non-Ras-like G2 motif and its interactions with the γ-phosphate of bound nucleotide may account for these observations.

As a result of the systematic comparison, we observed a number of differences between the enzymatic properties of atToc159G and the small Toc GTPases; atToc159G demonstrated a lower V_{max}, a higher K_M, a lower E_a, a higher k_{cat}, and a relatively lower affinity for GDP and GTP. One possibility that may account for these enzymatic differences are the residues coordinating the Mg^{2+} ion.

Although the enzymatic characterization of psToc34 clearly shows that the rate of GTP hydrolysis is insensitive to enzyme concentration, analysis by homobifunctional crosslinking reveals that the oligomeric properties of psToc34 over a similar concentration range leads to an increased population of the dimer. Whereas dimerization as a function of protein concentration is not a novel idea (117,118), the dimeric form of psToc34 is no more active than its monomeric form. Interestingly, a mutation, psToc34(R133A), results in a primarily monomeric species at all protein concentrations tested, including those that were shown to be primarily dimeric for the wild type protein. Furthermore, the R133A mutant was unable to hydrolyze GTP at any appreciable rate. In

light of evidence suggesting that psToc34(R133A) is correctly folded, the structural basis for why this mutant is unable to undergo dimerization or perform GTP hydrolysis is unknown. Nonetheless, the causal relationship between loss of dimerization and GTP hydrolytic activity was not resolved by the current experimentation. Although the precise relationship between oligomerization and GTPase activity is complex, one possible explanation of these results is that when psToc34(R133A) is expressed in *E. coli*, it is loaded with Mg^{2+} GTP during expression and folding. However, because this mutation is catalytically inactive, there is no opportunity to hydrolyze this GTP to GDP+P_i, thus trapping this protein in the GTP-bound form. This is unlike the wild type protein which, when isolated and crystallized, was found to be exclusively in the GDP-bound form (61); there is no GTP-bound crystal structure to date. My data support the proposal that Arg-133 functions as the arginine finger that contributes to the stabilization of the dimeric form of psToc34. Further binding studies could potentially confirm the nucleotide binding status of the mutant protein.

Because this work has been limited to the soluble forms of the Toc GTPases, how their transmembrane domains may influence either their oligomeric behavior or their catalytic activity remains unclear. However, using the soluble form of psToc34, our laboratory has clearly demonstrated the ability of this domain to form homodimers, yet we failed to see any evidence of its ability form homotetramers (53,100). This observation is consistent with the crystal structure, which also reported a dimeric structure with a 2-fold axis of symmetry (61). The ability of psToc34 to oligomerize into only dimers is especially intriguing in light of the recent low resolution structure of the pea Toc translocon that contains four Toc34 subunits with a single Toc159 subunit (25).

This may suggest that the native Toc complex contains a pair of Toc34 dimers. Although speculative, the homodimerization that is observed *in vitro* may also exist *in vivo* and may become disrupted by either precursor binding or, alternatively, through interaction with Toc159, to yield a transient heterodimer. Future work will be required to dissect the interplay by which both nucleotides and transit peptides modulate the oligomeric properties of the Toc GTPases.

The comparison of activation energies for GTP hydrolysis between the Toc proteins shows values of ~10–15 kcal mol^{-1} (Figure 2-9). This is similar to the activation energy of another small GTPase, EF2, of ~20 kcal mol^{-1} (119). It was, however, interesting to observe that although atToc159G has a lower V_{max} and a higher K_M value, it appeared to have a significantly lower activation energy (10.1 versus ~15). This would suggest that although atToc159G has a lower affinity for productive binding of GTP, upon binding, the orientation of the nucleotide was in some ways more favorable for hydrolysis, thus a lower energy transition state. The lower nucleotide affinity reflected in the K_M could be the result of some steric constraints imparted by the additional N- and C-termini residues found in atToc159G (42 kDa) as compared to psToc34 (29 kDa). It is also possible that the addition of these flanking sequences may somehow contribute to its distinct kinetic and thermodynamic parameters. Unfortunately, there is no structural insight into these regions because they were not present in psToc34. How the acidic N-terminal and membrane-associated C-terminal residues influence the enzymatic properties as well as homo/heterodimerization of atToc159 will be difficult to ascertain because the full size protein is insoluble when expressed in a heterologous system.

Heterodimerization and reciprocal activation of GTP hydrolysis is not a novel

idea; in fact, Sun *et al.* has proposed homodimerization between psToc34 monomers and possible heterodimerization between atToc33 and atToc34. This has been well studied in another protein transport system that involves GTPases, the SRP54 and Ffh from *E. coli*. In this system, it has been shown that heterodimerization elicits a reciprocal GAP activity from each monomer, thus coordinating GTP hydrolysis, completing the GTPase cycle, and thereby facilitating protein transport. Although the interactions between the Toc GTPases may mechanistically be different from the SRP54 and Ffh GTPases, the possibility exists that homodimerization and/or heterodimerization may modulate the activities of the Toc GTPases and influence the functionalities of these proteins *in vivo*.

Investigations into the ability of preproteins and/or transit peptide-derived synthetic peptides to stimulate the GTP hydrolysis rates of the Toc homologues is another area of some conflict and confusion in the literature. For instance, one group reported that there is an ~30-fold stimulation of hydrolysis by Toc34 when in the presence of preprotein (78); however, this same group subsequently reported no effect upon the addition of synthetic peptides comprising the N- and C- termini of a bipartite form of the prSSU transit peptide (55). Furthermore, an N-terminal peptide from prSSU had the equivalent stimulatory activity as the full-length preprotein with atToc159G alone and with the reconstituted complex (25). However, in this more recent paper, they reported only ~4-fold stimulation and not the previously reported ~30-fold effect. Although the enzymatic properties of the native or reconstituted Toc complex may certainly be different from the individual components, our results (Figure 2-4) indicate that the oligomeric state of psToc34 and the other Toc homologues do not stimulate the hydrolysis rates *in vitro*. A further concern when comparing synthetic peptides to the full-

length preproteins is that *E. coli* expressed preproteins are insoluble and require chemical denaturation for solubilization. This may interfere with the GTPase assay because of indirect effects of the denaturant. Additionally, the use of short synthetic peptides could have unintentionally split a contiguous recognition element present in the full-length transit peptide. Finally, short synthetic peptides would abrogate any structural contributions from the mature domain as has been clearly demonstrated for prSSU (96).

2.6 Summary

In this chapter, the basal kinetic characterization of the soluble domains of the Toc GTPases has been carried out and values of V_{max}, K_M, E_a, k_{cat}, K_d and K_i were reported. A storage buffer and conditions that maintain enzymatic activity were identified. It was also evidenced that although the Toc GTPases undergo concentration dependent dimerization, this did not result in an acceleration of hydrolytic activity. The crystal structure of dimeric psToc34 suggested that residues from one monomer interact deeply within the GTP-binding pocket of the other monomer and led to the speculation that residue 133 was a putative 'arginine finger'. To further explore this possibility, we created the psToc34(R133A) mutant and determined that it was correctly folded yet lacked GTPase activity and was primarily monomeric at a concentration which was shown to be dimeric for the wild type protein.

The function of the transit peptide in the GTPase cycle of the Toc GTPases has been debated. Research has suggested that transit peptide could act as the Guanine nucleotide Exchange Factor, or GEF, for either psToc34 or psToc159. Here, we devised a nucleotide exchange assay to test if this was the case. Our data suggests that transit

peptide does not act as a GEF for psToc34. Finally, since both Toc34 and Toc159 are present in the Toc Core Complex, the ability to enzymatically distinguish these two proteins has led to the creation of a psToc34 XTPase.

Chapter III

Toc Protein Interactions

3.1 ABSTRACT

The Toc GTPases (Translocon of the Outer Chloroplast membrane) function as receptors and/or gatekeepers to recognize and facilitate transit peptide-mediated precursor protein import. This complex process occurs at the outer membrane of the chloroplast. Our studies of the Toc GTPases utilize soluble constructs devoid of a transmembrane domain, therefore, any contributions from lipids have not been explored in detail. Here, we present evidence that outer membrane-like liposomes increase the GTPase activity of psToc34 whereas control liposomes and detergent micelles do not. Furthermore, by using a novel photoactivatable lipid crosslinker, we attempt to crosslink psToc34 interacting with the lipid bilayer. The crystal structure of psToc34 revealed the ability to form a homodimer and sequence similarity suggest the possible formation of a heterodimeric species between Toc34 and Toc159 proteins. Interactions between homo- and heterodimers may both be involved in the Toc mediated import process. Here, we present data that suggest the psToc34 homodimer is regulated by transit peptides and the transition state analogue GDP:AlF_4. Finally, we show that psToc34 and psToc159G form a nucleotide and transit peptide regulated heterodimer.

3.2 INTRODUCTION

In higher plants, most chloroplast proteins are nuclear encoded, translated on free ribosomes in the cytosol and require post-translational targeting and translocation into the chloroplast (120) and (Figure 1-5). This occurs via the general import pathway mediated

by the transit peptide (tp), a cleavable extension of 30-100 amino acids present at the N-terminus of preproteins (17). Translocation of precursor proteins across the double membranes of the chloroplast occurs simultaneously at contact sites formed by the protein complexes Toc and Tic (Translocon of the outer/inner chloroplast membrane) (107).Upon import of preprotein into the organelle, the transit peptide is cleaved, producing the mature protein (46).

While the stoichiometry is still debated, the minimal Toc translocon complex consists of the β-barrel translocation channel Toc75 associated with two receptor GTPases, the small Toc34 and the large, acidic Toc159 in either a 4:4:1 or a 6:6:2 stoichiometry (25,100). Despite the size difference, the GTPases exhibit both high sequence similarity in the central GTP-binding domain and similar membrane topology, inserting into the chloroplast outer membrane via a C-terminal transmembrane domain (53,121). Several recent studies using Blue Native PolyAcrylamide Gel Electrophoresis (BN-PAGE) analysis have isolated Toc core complexes approximately twice the size of those previously observed, suggesting that further assembly occurs (51,100,122). Higher order oligomers with stoichiometries of 6:6:2 and 8:8:2 have been proposed and observed (100,122). These discrepancies may be due to the transient nature of Toc complex assembly under varying conditions including the presence or absence of inner membrane interactions, nucleotide effects, as well as lipid contributions and/or interactions.

According to homodimeric crystal structures of Toc34 from *P. sativum* (psToc34), residues from each monomer participate deeply in the nucleotide-binding pocket of the other monomer (Figure 1-4). Therefore, in order for nucleotide exchange to occur, the protein may require large conformational changes or even monomerization

(61,63). Additionally, the sequence similarity between GTP-binding domains of the different Toc GTPases suggest that heterodimers may form in the native Toc complex (25,53,59,61,77,123). This raises the possibility that the nucleotide binding status and Toc protein oligomerization may play an important role in preprotein import into chloroplasts.

In order to probe interactions of the Toc GTPases with lipids and/or membranes, peptides and nucleotides, we have analyzed the purified cytosolic domains of psToc34 (transmembrane domain-free 29 kDa domain from *Pisum sativum*) and psToc159G (the central 42 kDa GTPase domain of Toc159 from *Pisum sativum*). We report that the GTPase activity of psToc34 is modulated by chloroplast outer membrane-like liposomes and is either not stimulated or inhibited by some detergents. Furthermore, we present evidence that both proteins undergo concentration and nucleotide/peptide dependent homo- and heterodimerization. We have explored the effect of nucleotide and transit peptide substrates on psToc34 indicating they influence the monomer-dimer equilibrium. Additionally, psToc34 with bound transition state analogue, GDP:AlF_4, is shown to be primarily dimeric and has extremely low affinity for transit peptide. This is may suggest that GTP hydrolysis occurs in the dimeric state and is requisite for transit peptide release and subsequent translocation. These results provide new insights on the dynamics of the oligomeric organization of the Toc GTPases and the function of homo- and heterodimerization is discussed.

3.3 MATERIALS AND METHODS

3.3.1 Generation of Liposomes and Detergent Micelles

Liposomes were generated by the sonication method. Briefly, solid lipids or lipids dissolved in chloroform were purchased from Avanti Polar Lipids and stored at -20°C until used. Lipids dispersed in chloroform were dried under anhydrous nitrogen gas resulting in a dried lipid film in glass reaction tubes. In the case of heterogenous lipid mixtures, various lipids were mixed in the appropriate molar ratio by vigorous vortexing prior to being dried under nitrogen stream. Following chloroform evaporation, phospholipids were rehydrated in 0.1 x PBS buffer (17 mM KH_2PO_4, 50 mM Na_2HPO_4, 13.6 mM NaCl at pH 7.4) to a concentration of 3 mg/ml total lipid and vortexed vigorously to generate MLVs or multilamellar vesicles. MLVs were then frozen in liquid nitrogen for approximately 10 s and thawed in 25°C water for five freeze-thaw cycles. Liposomes were then held at 70°C for approximately 1 h to ensure that phospholipids were above their gel-liquid crystalline phase transition temperature (TM) followed by sonication for 20 min, or until the solution became clear, in a bath sonicator (Fisher Scientific, Pittsburg, PA).

Through a collaboration with a chemistry department Ph.D. student, Matthew Smith and his advisor Dr. Michael Best, we were provided with dried Benzophenone diacylglycerol (bDAG). This is a diacyl glycerol lipid with a benzophenone head group, which when excited with 532 nm light, acts as a zero-length croslinker. The bDAG lipid was included at 10 mole percent and liposomes were prepared as above.

Detergent micelles were generated by weighing out solid detergents and bringing them up in 100 µl ddH_2O prior to dilution into the GTPase assay. Detergents were

utilized at 25% above and below their critical micellar concentration (CMC). The CMC for n-Octyl-β-D-glucoside (octylglucoside, or OG) is 25 mM therefore was used at 31.25 mM and 18.75 mM (124); the CMC for dodecyl-β-D-maltoside (dodecylmaltoside, dM) is 170 μM and was therefore used at 212 μM and 127.5 μM (125); the CMC for Triton-X100 (TX-100) is 320 μM as was therefore used at 400 μM and 240 μM (126).

3.3.2 Homobifunctional Chemical Crosslinking

Both psToc34 and psToc159G have a cysteine present in the 'largest loop', which is solvent accessible (61). However, psToc159G has three additional cysteines, which upon incubation with a Cys-reactive crosslinker, result in concatenation and thus smearing on a SDS-PAGE gel. This routinely resulted in the inability to distill information from its interactions either with itself or its heterodimeric partner. Therefore, primers were designed to mutate the other cysteines to either phenylalanine or serine. All mutagenesis was carried out with QuickChange PCR mutagenesis (Stratagene). Figure 3-1 reports the location of the cysteines on psToc159G and compares them to homologous positions on psToc34. The primers used to mutate Cys 1008, Cys 1067 and Cys 1088 are as follows:

C1008F forward and reverse:

5'-GTTTGTAGCGCAGTTCTCACATATTGTGCAACAGTC-3'

5'-GTTGCACAATATGTGAGAACTGCGCTACAAACAC-3'

C1067S forward and reverse:

5'-CAAAACCTTCAGGGAGTAAAACAATAGCAACAGC-3'

5'-GCTGTTGCTATTGTTTTACTCCCTGAAGGTTTTG-3'

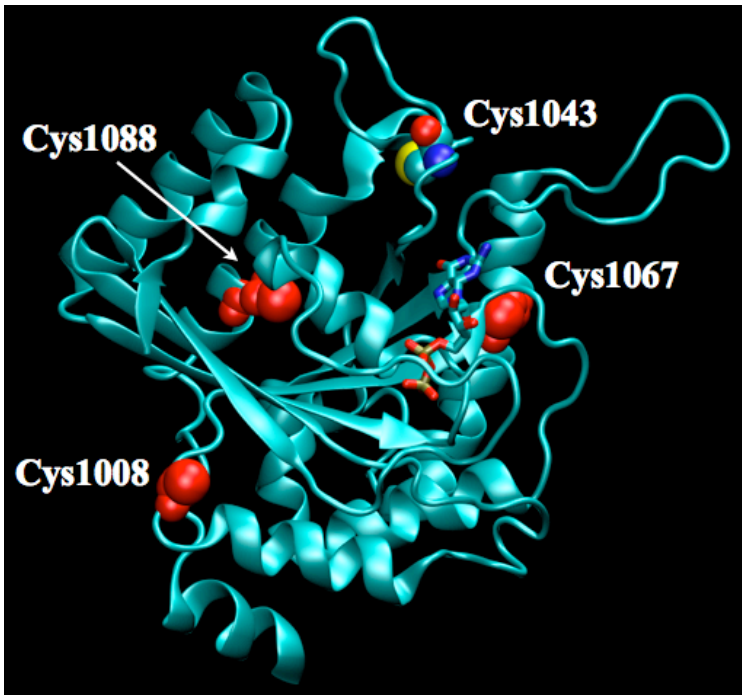


Figure 3-1. Mutagenesis of psToc159G. The structure of psToc159 was created by structural alignment superposition analysis of the crystal structure of psToc34 (1H65) and was reported in Reddick *et al*, 2007. The psToc159G protein has a cysteine in position 1043, analogous to the invariant C215 from psToc34. However psToc159G also possesses three other surface exposed cysteines. These have been mutated to Serine for all subsequent experiments involving cysteine-reactive probes; these cysteines are shown in red while Cys1043 is shown in CPK colors. The bound GDP molecule is shown in licorice and CPK colors.

C1088S forward and reverse:

5’- GAATCACCCCTTGTTTAGGAAGAACCG-3’

5’- CGGTTCTTCCTAAACAAGGGGTGATTC-3’

Toc proteins (psToc34 and psToc159G) harboring only one cysteine residue were allowed to interact in 1X GBS buffer containing 25-molar fold excess of TCEP reductant and were crosslinked by the dropwise addition of 10-fold molar excess of the homobifunctional crosslinker, BMH (Figure 2-5). TCEP and crosslinkers were purchased from Pierce Chemicals and were stored desiccated at 4°C until use. Protein was reduced with TCEP for 15 minutes at room temperature. TCEP was used because it is devoid of sulfhydryl groups, which compete for the maleimide reaction between the cysteine and the homobifunctional crosslinker. Crosslinker was added dropwise while gently vortexing the sample in a 0.6 ml Eppendorf tube. The crosslinking reaction was allowed to proceed at room temperature, in the dark for 2 hours (or times listed in subsequent Figures). The crosslinking reaction was quenched by the addition of 50-molar fold excess of β-Me and samples were treated for SDS-PAGE and/or Western analysis. Monomer-dimer ratio was determined by SDS-PAGE separation of proteins followed by Coomassie Brilliant Blue (CBB) staining and scanning densitometry using Quantity One software (Bio Rad, Hercules, CA).

3.3.3 SDS-PAGE and Western Analysis of Crosslinked Proteins

All proteins were added to SDS-PAGE 4X sample buffer, vortexed vigorously and boiled for 3 minutes. SDS-PAGE was carried out on either a 15% gel (Tris-glycine), a Tris-Tricine multi-phase gel (for separation of small species) (127), and/or separation

on a precast (Pierce, Rockford, IL) 12-20% Tris-HEPES gel. 15% gels were run at a constant 25 mA, Tris-Tricine gels were run at a constant 100 V, and Tris-HEPES were run at a constant 150 V. For CBB visualization, gels were stained in CBB for approximately 1 h and subsequently destained for approximately 1 hr and visualized on a visible light transilluminator (LabWare). For Western blot analysis, the gel (with prestained markers) was transferred to a Western transfer apparatus, assembled, and transfer was performed using a commercial battery charger set to 24 V for 2 h in a cold room (4°C) in the presence of ice cold transfer buffer (25 mM Tris, 193 mM glycine, 20% methanol). The PVDF membrane (Millipore, Billerica, MA) was marked with a number 2 pencil. The blot was blocked in Tris Buffered Saline with 0.1 % Tween-20 with the addition of 3% Kroger brand non-fat milk (TBST+NFM) for approximately 1 h at room temperature with constant rocking or nutation (optionally, blocking can be performed over night at 4°C). After blocking is complete, primary antibodies (anti-SStpNt at 1:50,000; anti-psToc34 at 1:75,000; and anti-psToc159G at 1:60,000) in TBST+NFM were incubated with the blot at room temperature with constant rocking or nutation for 1 h. Washing was performed four times with TBST+NFM with care. Secondary antibody used was goat-anti-rabbit HRP conjugated (Columbia Biosciences, Columbia, MD) and was incubated at 1:50,000 for 1 h at room temperature with constant rocking or nutation. Final washing was performed with TBST four times to ensure no free secondary antibody remains. The blots were exposed by the incubation of a 1:1 mixture of HRP substrate and Luminol (Millipore) for approximately 10 minutes. Chemiluminescent analysis was carried out on a BioRad imager set to chemiluminescent mode for 60 minutes and between 5 and 20 photographs were taken at even intervals.

Quantitation of the Western was performed using the QuantityOne software (BioRad) volume counting toolbar.

3.3.4 Transit Peptide Crosslinking and Detection

Toc protein (psToc34 and/or psToc159G) was incubated with 5-fold molar excess transit peptide (SStpPs and/or SStpNt) for approximately 10 minutes (with and without the addition of 200 μM GTP and/or GMP-PNP or other nucleotides). Homobifunctional crosslinker (BMH) was added at 10-fold molar excess (relative to Toc protein) dropwise with gentle agitation and was incubated at room temperature for 2 h in the dark. Subsequent detections (CBB and/or Western Analysis) were performed as described above. Free transit peptide is not visualized when running a 15% Tris-glycine or a 12-20% Tris-HEPES gel due to the inability to resolve proteins/peptides below 10 kDa. Therefore, a Tris-Tricine gel was run in order to visualize free transit peptide, however this resulted in too little difference in apparent molecular mass between crosslinked species of psToc34 and/or psToc159G. Therefore, visualizations of free transit peptide were abandoned in order to gain separation between monomeric, dimeric, adduct (Toc protein crosslinked to transit peptide) and heterodimeric interactions.

3.3.5 Nucleotides and Transition-State Analogue Modulation of psToc34

The transition state analogue GDP:AlF_4 was incubated with psToc34 at approximately 1000:1 molar fold concentration relative to psToc34 for 1 hour at room temperature; nucleotides were incubated at 5 mM with psToc34 protein for the same time period. Toc protein was rapidly separated from free transition state analogue and/or

nucleotides by size exchange on a PD-10 column (GE Healthcare, Piscataway, NJ) pre-equilibrated with 1X GBS buffer. psToc34 protein with bound transition state analogue was then re-reduced with the addition of 5-molar fold excess TCEP (Pierce, Rockford, IL) and incubated at room temperature for 15 min in the dark. Crosslinking was performed with the addition of 10-molar fold excess relative to psToc34 of BMH drop-wise with gentle agitation and incubation at room temperature in the dark for 1 h. The sample was quenched with the addition of 50-molar fold excess of β-Me, and incubation for 5 minutes at room temperature. Sample was added to 4x SSB, vortexed vigorously and boiled for 3 minutes prior to being run on a 15% SDS-PAGE gel, stained with CBB and visualized. Monomer and dimer species were quantitated with scanning densitometry using the Quantity One software (BioRad) and compared to non-crosslinked monomer Toc protein.

3.4 RESULTS

3.4.1 Liposomes and Detergent Micelle Modulation of psToc34 Activity

In the plant cell, the psToc34 protein is anchored to the chloroplast outer membrane via a C-terminal α-helix, however, all *in vitro* work with psToc34 presented in this dissertation is performed with a transmembrane domain deletion mutant, referred to as psToc34ΔTM2, here on out referred to as psToc34 (Figure 1-4) and (108). The chloroplast outer membrane is composed of 32% phosphatidylcholine (PC), 17% monogalactosyldiacylglycerol (MGDG), 29% digalactosyldiacylglycerol (DGDG), and 10% phosphatidylglycerol (PG) (92). Previous work has shown that recombinant psToc34 lacking a transmembrane domain interacts with liposome membranes (128).

Therefore, we approximated the chloroplast outer membrane by creating 'OM Mimetic' liposomes comprised of 30 mol% dipalmitylphosphatidylcholine (DPPC), 25 mol% dilinoeoylphosphatidylglycerol (DLPG), 25 mol% DGDG and 20 mol% MGDG. Control liposomes were comprised of 100 mol% DPPC, 100 mol% DLPG or 50 mol% DPPC and 50 mol% DLPG. Liposomes were generated via sonication according to Materials and Methods. Confirmation of proper liposomal formation was assayed by the reduction of turbidity and emergence of a clear solution suggesting that the diameter of the liposomes had become smaller than 300 nm and thus no longer absorbed visible light (data not shown). By incorporating 5 mM and 25 mM of the liposomes in various GTPase assays, we tested to see if the hydrolysis activity of psToc34 could be modulated by a membrane environment that more closely resembled that of the chloroplast outer membrane. The addition of either DPPC, DLPC or a 50/50 mixture of the two lipids did not stimulate the GTPase activity of psToc34 (Figure 3-2). However, upon the incorporation of OM Mimetic liposomes there was an observed increase in the maximal GTPase activity of psToc34. Changing the lipid concentration from 5 mM to 25 mM did not result in any greater stimulation (Figure 3-2).

In order to determine if the effects seen with liposomes were due to the lipids themselves or simply a change in dielectric constant of the medium, detergents, in powder form, were brought up in 100 μl and subsequently diluted to their final concentrations (25% above and 25% below their CMC) in the reaction (Figure 3-3). In all cases, detergent micelles either reduced the activity of psToc34 or maintained it at 'unstimulated' levels. Both octylglucoside (OG) and dodecylmaltoside (dM) both severely reduced GTPase activity of psToc34 (Figure 3-3). The lower concentration (25% below the CMC) of

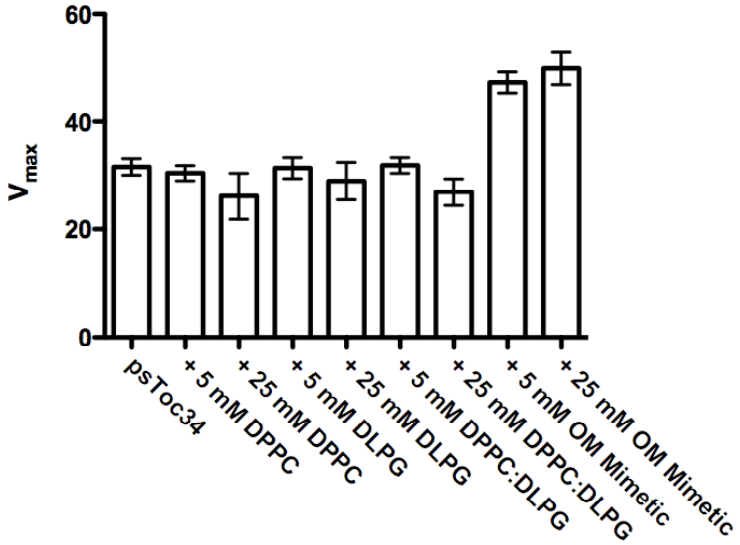


Figure 3-2. GTPase Activity is Modulated by Liposomes of Varying Character. OM Mimetic liposomes which contain DPPG, DLPG, DGDG and MGDG were created to mimic the galactolipid containing chloroplast outer membrane.. Control liposomes were comprised of DPPG, DLPG or equimolar amounts of DPPG/DLPG. The GTPase activity of psToc34 was measured in the absence of liposomes (psToc34) or in the presence of 5 mM and 25 mM liposomes, noted in the figure.

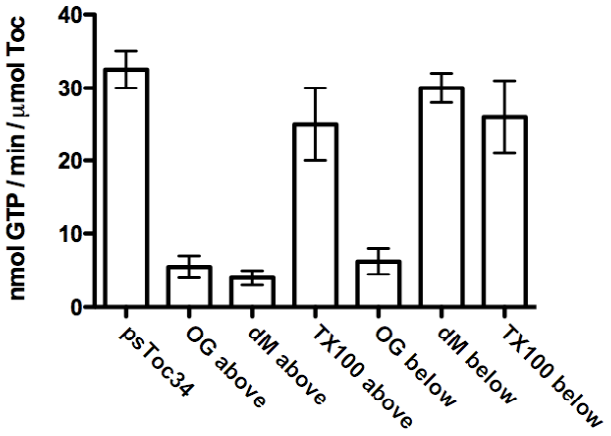


Figure 3-3. Effect of detergent micelles on the GTP activity of psToc34. The hydrolysis rate of psToc34 was measured alone, or in the presence of two different concentrations of three common detergents, octylglucoside (OG), dodecylmaltoside (dM) and Triton X-100 (TX100). The denotation 'above' and 'below' represent 25% above the CMC and 25% below the CMC, respectively.

of octylglucoside still diminished psToc34 GTPase activity. Both concentrations of Triton X-100 permitted GTPase activity by psToc34 while only the lower concentration of dM allowed for activity (Figure 3-3).

3.4.2 Trapping psToc34 on Lipid Membranes

The full-length psToc34 protein is insoluble in heterologous expression systems and we therefore used a truncated version devoid of the C-terminal transmembrane domain for our work on this protein. Due to the removal of several C-terminal residues, including the removal of a putatively flexible linker between the GTPase domain of the protein and the transmembrane domain (61), the actual orientation of psToc34 on the lipid membrane is unknown. Since psToc34 acts as a precursor protein receptor, the orientation of the protein on the membrane could be of importance for the protein import cycle. In order to probe the orientation of psToc34, we engaged in a collaboration with the laboratory of Dr. Michael Best in the Chemistry Department at the University of Tennessee. Dr. Best's laboratory synthesized bDAG, or diacyl glycerol with a benzophenone group attached to the lipid headgroup thus creating a lipid-attached photoactivatable crosslinker exposure of bDAG to 532 nm laser light resulted in the benzophenone group acting as a zero-length crosslinker. By incorporating bDAG at 10 mol % into both control liposomes and OM-mimetic liposomes the orientation of psToc34 on the lipid surface might be determined. Upon illumination with a neodymium laser at 532 nm, we attempted to crosslink psToc34 to the bDAG. The arrow indicates that very little psToc34 was effectively crosslinked (Figure 3-4, arrow).

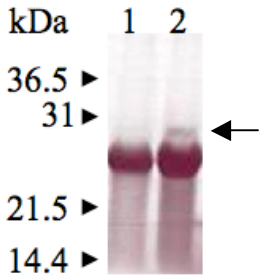


Figure 3-4. Lipid Crosslinking to psToc34. Purified psToc34 was incubated with control and OM-mimetic liposomes containing 10 mol % bDAG (see Materials and Methods). Lane 1 represents 10 mol % bDAG in control liposomes (45/45 DPPC/DLPC). Lane 2 represents 10 mol % bDAG in OM Mimetic liposomes. There is no crosslinked species present in lane 1, however a small crosslinked species of approximately 30 kDa (indicated by an arrow) is believed to be the addition of several bDAG lipids and can be visualized in lane 2.

3.4.3 Heterodimerization of psToc34 and psToc159G is Revealed by Homobifunctional Crosslinking

As was suggested by the crystal structure of psToc34, as well as revealed by our laboratory and others, both psToc34 and psToc159G undergo concentration dependent homodimerization *in vitro* and most likely exist as homodimers *in vivo* (53,122,129,130). The homodimerization of the Toc proteins gives rise to the speculation that this monomer/dimer transition is a potential regulation point for GTPase activity (or is regulated by GTPase activity) and/or translocation. Therefore, we utilized the crosslinker BMH to trap dimeric species of psToc34 and psToc159G and visualized them via SDS-PAGE (Figure 3-5). The psToc34 species are indicated by ▲ and ▲▲ representing monomeric psToc34 (29 kDa) and dimeric psToc34 (58 kDa), respectively (Figure 3-5 lane 1). This confirmed earlier reports using analytical ultracentrifugation and gel filtration chromatography that psToc34 was involved in a monomer-dimer equilibrium (53,130). The monomeric (42 kDa) and dimeric (84 kDa) species of psToc159G were visualized and are indicated by ■ and ■■, respectively (Figure 3-5 lane 2). Finally, when psToc34 and psToc159G were present in a 1:1 ratio, the 71 kDa heterodimeric species, represented by ▲■, can be observed (Figure 3-5 lane 3).

3.4.4 The Dimer of psToc34 is Modulated by Nucleotides and a Transition State Analogue

The crystal structure of psToc34 revealed a homodimer, and subsequent experimentation has shown psToc34 to undergo concentration dependent dimerization (53), however, the function of this monomer-dimer equilibrium is still

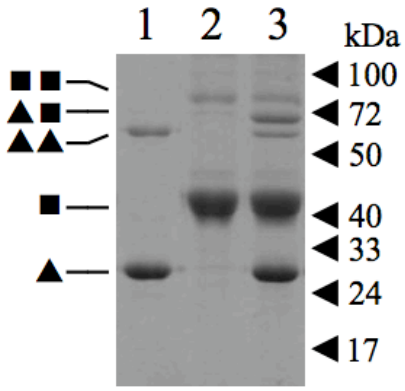


Figure 3-5. psToc34 and psToc159G undergo homo- and heterodimerization. Lanes 1, 2 and 3 represent equal loading of psToc34, psToc159G and an mixture of psToc34 and psToc159G, respectively. Molecular weight markers are indicated on the right while shapes on the left indicate the following: triangle, psToc34 monomer; square, psToc159G monomer; double triangle, psToc34 homodimer; triangle and square, psToc34-psToc159G heterodimer; double square, psToc159G homodimer. Notice that the heterodimer is preferred over either of the homodimers, as revealed by a reduction in density in both homodimeric species and a concomitant intensity increase in density in the heterodimer. psToc159G, although loaded at the same concentration as psToc34, runs as a more diffuse band.

debated (53,61,130). Homodimerization and heterodimerization of the Ffh and FtsY GTPases involved in the bacterial translocon have been shown to be functionally important for protein translocation (131,132). Analogously, homo- and heterodimerization may play a functional role in chloroplast protein import. Therefore, it is important to understand how the Toc monomer/dimer equilibrium is regulated by transit peptides and nucleotides.

Using psToc34 as the model protein, we tested the ability of psToc34 to form homodimers in the presence of wild type transit peptide and a mutant form that lacks Proline 26, Glycine 28 and Proline 35, termed SStpNtΔPGP (for location of residues, see Figure 4-2). This transit peptide mutant was identified by our laboratory and shown to be unable to compete against wild type transit peptide during a chloroplast import assay (133). All transit peptides used in this experiment lack the cysteine at position 58, which was replaced with tyrosine. The removal of the cysteine was necessary in order to only probe Toc protein dimerization using the cysteine active crosslinker BMH. In the absence of crosslinker, psToc34 (when run on a reducing SDS-PAGE gel) runs at its monomeric size of 29 kDa, but when BMH is added, the 58 kDa dimeric form is trapped (Figure 3-6 lanes 1 and 2). Scanning densitometry was used to quantitate the amount of dimer present on the gel and arbitrarily set the dimer present to a value of 1.0 (Figure 3-6, lane 2). The incorporation of 5-fold molar excess transit peptide disrupted the dimeric form of psToc34 resulting in the vast majority of the protein observed as the monomer (Figure 3-6 lane 3). The observation that little dimeric species was apparent indicated that the transit peptide was effective at disrupting the dimeric form. SStpNtΔPGP was incubated with psToc34 (Figure 3-6, lane 8). This mutant peptide did not effectively stimulate the

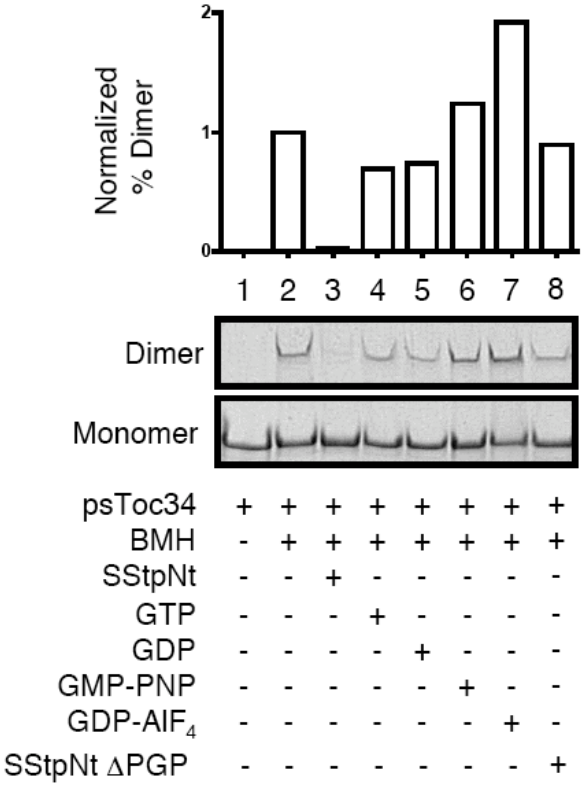


Figure 3-6. The psToc34 Dimer is Modulated by Nucleotides and Transition State Analogues. The psToc34 protein was incubated alone (lane 1) or crosslinked by BMH (lane 2), in the presence of SStpNt transit peptide (lane 3), GTP (lane 4), GDP (lane 5), GMP-PNP (lane 6), GDP-AlF_4 (lane 7) or SStpNtΔPGP (lane 8). The transit peptides were present at 5-fold molar excess over psToc34 and the nucleotides and transition state analogue were present at 5 mM.

dimer to monomer transition as was observed for the wild type peptide (Figure 3-6, compare lanes 3 and 8).

When psToc34 was soaked in 5 mM GTP and/or GDP prior to crosslinking, the addition of nucleotide resulted in a loss of dimer by 20% (Figure 3-6, lanes 4 and 5). Furthermore, the addition of 5 mM GMP-PNP increased the dimeric form by 20% (Figure 3-6 lane 6). Although the bar graph does not contain error bars, this experiment was repeated and resulted in similar results. It is not known why the GDP and GTP treatments resulted in slightly less dimer while the GMP-PNP treatment resulted in more dimer. The incorporation of the transition state analogue GDP:AlF_4 significantly stabilized the dimeric form of psToc34 by 2-fold (Figure 3-6 lane 7).

3.4.5 Transit Peptide Modulates Heterodimerization of psToc34 and psToc159G

According to the crystal structure of psToc34, the nucleotide-binding site is also the dimerization interface (61) and therefore, homodimerization and heterodimerization may rely on the bound nucleotide. In order to test for nucleotide effects on homo- and heterodimerization, we utilized homobifunctional crosslinking. Detection was performed by Western analysis, which allowed for greater sensitivity over SDS-PAGE. For example, the incorporation of transit peptide in the psToc34 homodimeric crosslinking reaction (section 3.4.4 above) reduced the amount of dimeric psToc34 to the point that it was no longer visible as analyzed by SDS-PAGE followed by CBB staining (Figure 3-6 lane 3). However, with the aid of chemiluminescent Western analysis, the remaining psToc34 dimer (when transit peptide was present) could be visualized (Figure 3-7, A lane 5, ▲▲).

Figure 3-7. Transit Peptide Binding and Heterodimerization. Panel A, Four crosslinking reactions were performed and SDS-PAGE followed by western analysis. This was performed such that psToc34 was incubated with transit peptide and BMH (lanes 1, 5 and 9); psToc159G was incubated with transit peptide and BMH (lanes 2, 6 and 10); both psToc34 and psToc159G were incubated with transit peptide and BMH (lanes 3, 7 and 11); and finally both psToc34 and psToc159G were incubated with transit peptide, GMP-PNP and BMH (lanes 4, 8 and 12). Lanes 1-4 were probed with anti-SStpPs (α-tp), lanes 5-8 were probed with anti-psToc34 (α-psToc34) and lanes 9-12 were probed with anti-psToc159G (α-psToc159G). The symbols '+' and '-' are used to indicate the presence or absence of proteins, transit peptides, crosslinker and/or nucleotide in the reaction. The shapes are as follows: ▲, psToc34; ■, psToc159G; ▲▲, psToc34 homodimer; ■■, psToc159G homodimer, ▲■, psToc34-psToc159G heterodimer. A ▲★ represents the psToc34-SStpPs adduct and the ■★represents the psToc159G-SStpPs adduct. Panel B, the heterodimeric species (▲■) was quantified in lanes 7 and 8 and in lanes 11 and 12. Values in lanes 7 and 8 were normalized to lane 7 while values in lanes 11 and 12 were normalized to lane 11.

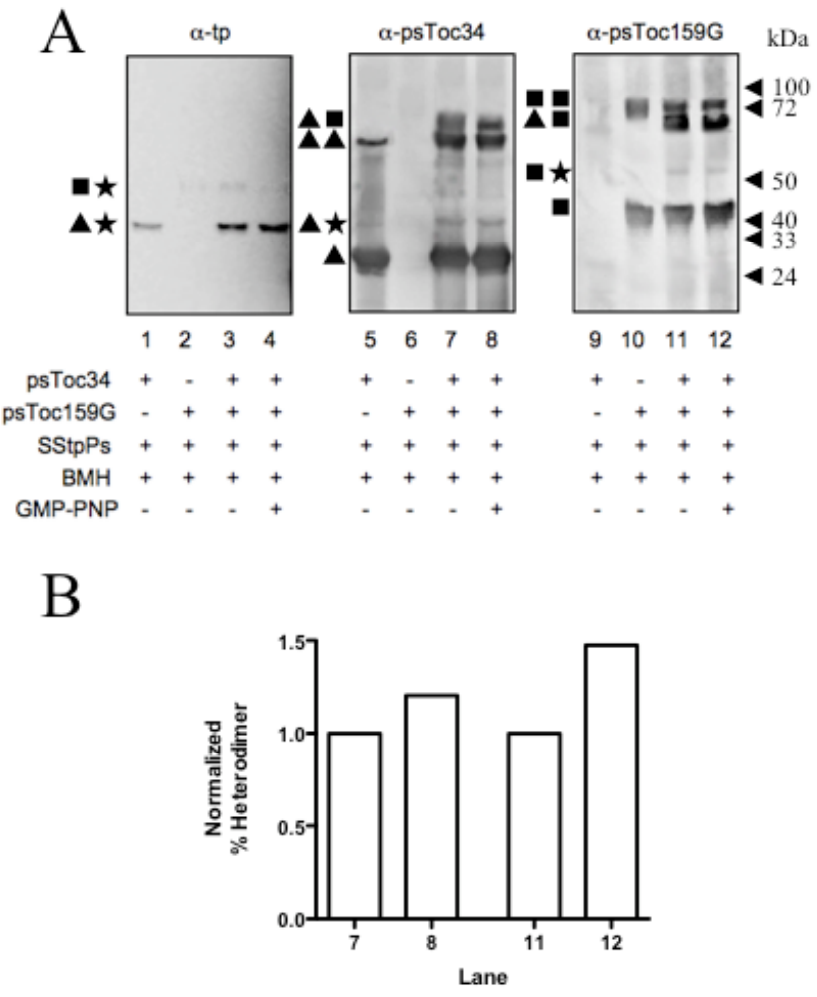

A
α-tp
α-psToc34
α-psToc159G
kDa
100
72
50
40
33
24
1 2 3 4 5 6 7 8 9 10 11 12
psToc34 + - + + + - + + + - + +
psToc159G - + + + - + + + - + + +
SStpPs + + + + + + + + + + + +
BMH + + + + + + + + + + + +
GMP-PNP - - - + - - - + - - - +
B
Normalized % Heterodimer
1.5
1.0
0.5
0.0
7 8 11 12
Lane

Figure 3-7

Comparisons of the 35 kDa psToc34-transit peptide adduct species (▲★) in lanes 1 and 3 in Figure 3-7, A, suggest transit peptide crosslinks preferentially with psToc34 when psToc159G is included in the reaction. The incorporation of GMP-PNP further increases the affinity of psToc34 for transit peptide (Figure 3-7, A lane 4 ▲★). There is a faint band at approximately 48 kDa in lanes 2-4 (■★) that indicates transit peptide binding to psToc159G was rare.

As stated earlier, the psToc34 homodimer (▲▲) was not completely abolished through interaction with transit peptide, however it was significantly reduced (Figure 3-7, A lane 5). No noticeable change was detected in the homo- and heterodimerization of psToc34 in response to GMP-PNP however the inclusion of psToc159G resulted in the increased abundance of dimeric psToc34 (Figure 3-7, A lanes 7 and 8). Lane 10 represents the monomer/dimer equilibrium of psToc159G in the presence of transit peptide. Comparison of the monomeric (■) and dimeric (■■) species in Figure 3-7, A lane 10 with those of Figure 3-5 lane 2 suggests that transit peptide stimulated the homodimerization of psToc159G. Lanes 11 and 12 in Figure 3-7, A show the presence of a heterodimer of psToc34 and psToc159G (▲■) and another species, the psToc159G-transit peptide adduct (■★). This adduct band was undetectable in lane 10, and therefore the presence of psToc34 may have stimulated the association of transit peptide with psToc159G making it evident in lanes 11 and 12. Scanning densitometry indicated that the heterodimeric species (▲■) in lanes 7 and 11 became more intense (lanes 8 and 12) with the addition of GMP-PNP (Figure 3-7, B).

3.5 Discussion

The proteins psToc34 and psToc159 exist in the galactolipid rich outer leaflet of the chloroplast outer membrane and identify transit peptides, bind to them and import them through the outer membrane in a guanosine nucleotide dependent manner. We hypothesized that the basal hydrolytic rate of psToc34 may be increased and/or modulated by incubating the protein in a more chloroplast outer membrane-like environment. Therefore, we performed GTPase measurements of psToc34 alone, and in the presence of control and OM Mimetic liposomes, Figure 3-2. This experimentation revealed that control liposomes comprised of DPPC and/or DLPC did not modulate the GTPase activity of psToc34 (Figure 3-2). In contrast, OM Mimetic liposomes (containing galactolipids) increased GTPase activity, which suggested the lipid environment might influence Toc GTPase activity and play a role in chloroplast protein import. The addition of transit peptide would presumably magnify the results obtained (for the OM Mimetic liposomes) however it was not included in these experiments. Incorporation of transit peptide resulted in the rupture of liposomes (data not shown and (33)). This liposomal lysis may be due to curvature stress derived from the interaction of transit peptide amphipathic helices with the lipid envelope. How this *in vitro* observed phenomenon is abrogated (or potentially taken advantage of) by the chloroplast *in vivo* is not understood and in need of further study.

When psToc34 was incubated with detergents 25% above and 25% below their respective CMC values, only Triton X-100 (at both concentrations) and dodecylmaltoside (25% below CMC) retained psToc34 wild type GTPase levels (Figure 3-3). The detergent octylglucoside (at both concentrations tested) and dodecylmaltoside (at 25% above CMC)

reduced GTPase activity to less than ~10 nmol GTP per min per μmol Toc. The reduction in activity possibly resulted from the denaturing effects of the detergents themselves and is seen with the higher concentration of detergent, and in one case, the lower concentration (OG below, Figure 3-3). Octylglucoside is used in the laboratory routinely for extracting integral membrane proteins, and it was surprising to find that both concentrations used resulted in reduced psToc34 activity.

Since psToc34 was shown to have increased GTPase activity in the presence of OM Mimetic liposomes, we wanted to learn the orientation of psToc34 on the lipid membrane. Therefore, we performed a liposomal crosslinking experiment through collaboration with the Chemistry Department here at the University of Tennessee. The photoactivatable crosslinker lipid benzophenone diacylglycerol (bDAG) was incorporated into OM Mimetic liposomes at 10 mol %. After allowing psToc34 to interact with these liposomes, the crosslinked product could be visualized by SDS-PAGE (Figure 3-4). This is a preliminary result and in need of further experimentation. It is tempting to speculate that Figure 3-4 reveals psToc34 interaction with lipid membranes as captured by bDAG incorporated liposomes. However, a greater amount of protein loaded in lane 2 suggests that this may be an artifact. Nevertheless, photoactivatable lipid crosslinking can still be a potent tool for the future. Perhaps in further experimentation, psToc34 can be crosslinked to ^{14}C labeled bDAG affording a more robust method of detection. This may allow us to determine if psToc34 alters its lipid interface upon differential nucleotide loading states and/or transit peptide binding. By performing lipid crosslinking under various conditions and coupling in-gel digestion with MALDI-TOF

mass spectrometry, the comparison of control and lipid-crosslinked psToc34 MALDI spectra may reveal the location of the psToc34 lipid interface.

The crystal structure of psToc34 revealed that this protein exists as a homodimer with residues of one monomer participating deeply within the nucleotide-binding pocket of the other monomer (61). Our observations that the transit peptide significantly disrupts the homodimer and that the transition state analogue GDP:AlF_4 stimulates dimerization suggests substrate and nucleotide may govern the monomer/dimer equilibrium which in turn may have biological relevance. Disruption of GTPase dimers is common with the SRP GTPases where each monomer acts to stimulate the other in trans (134). Furthermore, since the transit peptide proline/glycine mutant was unable to stimulate monomerization of psToc34, this suggests that these residues could be involved in binding psToc34, potentially interacting at the dimeric interface or even contacting the bound nucleotide.

A heterodimeric species composed of psToc34 and psToc159G has been suggested (135). The observation of a heterodimeric species in Figure 3-5 lane 3 indicates its existence *in vitro*, however further work will be needed to confirm that this species exists *in vivo*. Nonetheless, the psToc34 and psToc159G proteins could be visualized as both homodimers as well as heterodimers (Figure 3-5). When both proteins were incubated together in a 1:1 ratio, chemiluminescent quantitation (Figure 3-7, B) suggested that formation of the heterodimeric species was preferred in the presence of the GTP analogue GMP-PNP. Due to the specificity of the crosslinking reaction, the heterodimeric species represents one molecule of psToc34 and one molecule of psToc159G, therefore, lanes 7 and 11 and 8 and 12 in Figure 3-7 should be visually

identical. However, two different primary antibodies were used for detection (as noted in Figure 3-7). The anti-psToc34 and anti-psToc159G antibodies may recognize differentially presented epitopes, which may account for the observed variation in chemiluminesence signal. Nevertheless, formation of a psToc34-psToc159G heterodimer could be important for the overall import process. Our work indicates a dynamic interplay between homo- and heterodimerization along with transit peptide recognition/binding.

Previous results have implicated psToc159G as the primary transit peptide receptor, and GTP hydrolysis by psToc34 was the only GTP hydrolytic event required for import (70). However, our results suggest psToc34 binds transit peptide to a greater degree than psToc159G *in vitro* and the psToc34-transit peptide interaction was strengthened when the non-hydrolyzable GTP analogue GMP-PNP was included. Since the psToc34 and psToc159G proteins are present at equimolar amounts and free in solution, we cannot infer an order of binding events from this data. The presence of psToc159G in the assay may in some way position transit peptide to become more efficiently crosslinked to psToc34. Alternatively, the heterodimerization of psToc34 and psToc159G may allosterically modulate psToc34 and increase its affinity for transit peptide.

3.6 Summary

In this chapter, we sought to understand how membranes, membrane mimetics, transit peptides and nucleotides modulate the GTPase activity and dimeric equilibrium of psToc34. By generating liposomes with defined composition, we showed that membranes with galactolipid character are able to stimulate the GTPase hydrolysis activity of

psToc34 whereas predominantly phosphatidyl choline membranes do not. Through a collaboration, we provided a photoactivatable crosslinking tool to trap psToc34 on membranes that may provide informative results in the future. We showed that psToc34 and psToc159G undergo both homo- and heterodimerization and this dimeric activity is modulated through interactions with transit peptides and a transition state analogue. It is tempting to speculate as to the biological significance of transit peptide interaction and its importance for chloroplast protein import. This will be the subject of Chapter IV.

Chapter IV

Toc - Transit Peptide Interactions

4.1 Abstract

The result of Toc-mediated precursor protein recognition is the rapid and robust import of chloroplast destined precursors from the cytosolic compartment to the stroma. This process has been observed to be capable of importing between 9,500 and 40,000 precursor molecules/chloroplast/min (96,136). Facilitating this recognition/import process are the transit peptide and the Toc receptor GTPases, however the mechanism by which this occurs is still a mystery (135). Transit peptide interaction, Toc protein affinity for peptide, and Toc protein homo- and heterodimeric propensities are variables and in need of careful dissection. In this chapter we reveal two mutants discovered by our laboratory (133), termed ΔPGP and ΔFPVSR, that directly impact both the rate of hydrolysis and the monomer/dimer equilibrium of psToc34. Furthermore, by fluorescently labeling the transit peptide at various positions, we provide evidence that psToc34 binds to the C-terminus while psToc159G binds the entire peptide. This result was supported through homobifunctional crosslinking. Finally, it was reported by our laboratory that the transit peptide acts as the GAP for psToc34 (53), but to date, no GEF has been discovered for these receptor GTPases (129). Here, we present evidence that the psToc159G-tp adduct acts as the GEF for psToc34. Taken together, nucleotide modulation of peptide affinity, propensity to form heterodimers and the data from the mutants of SStpPs, a mechanism of transit peptide recognition followed by GAP/GEF cycles is revealed that leads to a model of chloroplast protein import, which will be the subject of Chapter V.

4.2 Introduction

Central to chloroplast protein import is the transit peptide. The DNA encoding the majority of chloroplastic proteins is nuclear encoded (2). Subsequent to transcription, RNA exits the nucleus and is translated on free cytosolic ribosomes generating the precursor protein which has an N-terminal amino acid extension known as the transit peptide (9). The transit peptide facilitates the recognition and import of the precursor proteins into the chloroplast via interactions with the Toc proteins at the outer membrane of the chloroplast. Transit peptides for different proteins and from various organisms are highly heterologous in length, composition and organization which makes it difficult to decipher the information they contain (102). Ranging in length from 25 to 150 amino acids, the primary sequence of transit peptides is highly variable and little sequence similarity is observed (137). Despite this apparent randomness, there are several shared features: all transit peptides have an uncharged N-terminus and most have a basic central and/or C-terminus (138). Transit peptides are rich in small non-polar residues such as glycine and alanine and hydroxylated residues, giving rise to speculation that they may harbor sites for phosphorylation (102).

Despite the existence of both mitochondria and chloroplasts in the plant cell, very little to no mis-sorting occurs *in vivo* (17,139,140). Mitochondrial presequences needed for proper mitochrondrial targeting and import exhibit amphipathic α-helices that have been shown to be required for correct targeting and import (141). In contrast, chloroplast transit peptides are largely unstructured in solution until exposed to a medium with lower dielectric constant such as detergent micelles or lipid membranes (17,34,94). NMR and

circular dichroism spectroscopy have revealed that chloroplast transit peptides remained unstructured in solution only until they were exposed to membranes, membrane-mimetic detergents and/or liposomes at which time they tended to form helices (11,94). Although the primary sequences of transit peptides show significant variability, transit peptides that share little homology compete for import (91). Therefore, it was suggested that the information contained within them was of a structural nature rather than that of primary sequence (11,98). Unfortunately, due to their propensity to be unstructured, crystallization of transit peptides has not been achieved and only limited NMR characterization has been performed (17). It is hypothesized that the transit peptide secondary structure induced by membranes or membrane mimetics is recognized by the Toc GTPases (11,17,18,55).

The variability in sequence and peptide composition has led to the proposal that transit peptides may contain domains with different and/or possibly overlapping function(s) that are required for successful targeting to the chloroplast import machinery (34,53,94,101,137). These functions include, but are not limited to, cytosolic guidance complex interaction (hsp and 14-3-3 protein interactions), chloroplast outer membrane lipid interaction, and interaction with the various Toc proteins. It is been generally accepted that transit peptides contain three distinct regions: 1) an uncharged N-terminus, 2) a central domain rich in hydrolylated amino acids, and 3) a C-terminal domain abundant in positively charged residues (17,18). Furthermore, loosely conserved motifs have been identified as 'FGLK motifs' (94), an example of which is present in the C-terminal domain of the Ferredoxin transit peptide of the organism *Silene pratensis* (103) and have been shown recently to be relatively prevalent (133,142). This motif, which can

also exist as FPVSR (103), is characterized by an aromatic, a 'turn residue', followed by aliphatic and a positively charged residue and is more evident when one reduces the stringency of the absolute position of the amino acids (6,142).

Transit peptides have been shown to interact with the Toc proteins in order to gain entry into the chloroplast and this interaction involves the nucleotide GTP (9,53,97,100,122). Early crosslinking studies implicated Toc159, Toc34 and Toc75 as transit peptide-interacting partners (24,143), however, more recent data has refined the timing of the interactions that lead to translocation (144). Exactly how, where and to what extent peptide binding occurs via the Toc GTPases is a matter of debate and is the central focus of this chapter. Since the transit peptide is unstructured in aqueous environments (similar to the cytosol) but gains secondary structure, and possibly proto-tertiary structure upon lipid and Toc protein interaction, it is mechanistically interesting and deserving of close attention. Therefore, in order to characterize the binding of transit peptides to the Toc GTPases, we used both wild type and mutant transit peptides and performed kinetic, affinity and dimerization assays in order to probe the functional interaction between psToc34, psToc159G and the transit peptide.

4.3 Materials and Methods

4.3.1 Transit Peptide Mutagenesis

Point mutations were made to the SStpPs transit peptide using the QuickChange PCR kit (La Jolla, CA). The SStpNt was mutated such that three point mutations were introduced at positions P26A, P28A, P36A; this mutant is referred to as SStpNtΔPGP. Mutagenic primers to create the deletion mutant SStpNtΔFPVSR (Figure 4-2) are not

listed and the reader is directed to (133). Table 4-1 lists the mutagenic primers used for SStpPs point mutations and primers for SStpNtΔPGP. All mutant forms of transit peptide were purified as stated below.

4.3.2 Protein Purification

Both psToc34 and psToc159G were purified as detailed in Chapter II and Chapter III; for all experiments involving psToc159G in this chapter, the single cysteine mutant (see section 3.3.2 and Figure 3-1) was used in order to better quantify the crosslinking and protein-protein interactions. Transit peptide, whether it was SStpPs or SStpNt or any mutants thereof, was cloned into the pTYB2 vector and expressed in ER2566 *E. coli* cells under IPTG induction at 20°C overnight. Transit peptide protein was purified as per Chapter II using the chitin bead system. The purification of transit peptide takes advantage of the IMPACT system, or Inteine Mediated Purification with and Affinity Chitin-binding Tag (Figure 4-2, A). Briefly, cells grown to an OD_{600} of 0.4 and were induced overnight with 1 mM IPTG, collected by centrifugation and were lysed with 0.5 mg/ml lysozyme and sonicated at 10 seconds on and 10 seconds off for two minutes. The lysate was clarified by centrifugation in Oak Ridge tubes in an SS-34 rotor at 40,000 g. Supernatant was gravity flowed over a 10 ml chitin bead slurry column pre-equilibrated with column buffer, subsequently washed and then incubated with 50 mM β-Me overnight at 4°C. The following morning, the column was eluted with elution buffer containing 50 mM β-Me and collected as six fractions of 6 ml each. Elutions were flash frozen and lyophilized after which they were brought up to 1 ml in ddH_2O in order to precipitate dnaK and other chaperones (which are not soluble in pure water) that may

have co-purified with the transit peptide. An SDS-PAGE gel was run in order to determine sample purity and MALDI-TOF mass spectrometry was performed to ensure the sample was the correct size (Figure 4-1). Samples were quantitated for protein concentration and aliquotted at 0.1 mg and 0.25 mg samples, flash frozen in O-ring lid tubes and lyophilized and stored at -20°C until used.

4.3.3 Circular Dichroism Spectroscopy

Circular dichroism spectroscopy was performed on an Aviv Series 202 circular dichroism spectrometer (Aviv Biomedical, Lakewood, NJ). After resuspending lyophilized peptide in 0.1 x PBS, the BCA assay was used to determine concentration. Circular dichroism spectra were collected at 25°C as 2 s averages at 1 nm intervals from 185 to 285 nm. Three spectra were averaged, corrected for buffer contributions, smoothed, and converted to molar ellipticity using the Aviv software, version 2.71. The helix promoting solvent 2,2,2-Trifluoroethanol was combined with ddH_2O and 1 x PBS in order to solubilize the lyophilized peptide in the various concentrations of TFE necessary to perform analysis (Figure 4-2). Deconvolution was performed using the CDPro software, available online at http://lamar.colostate.edu/~sreeram/CDPro/. From these data, the secondary structural features of transit peptide were determined.

4.3.4 Generation of Transit Peptide Affinity Column and Differential Binding of psToc34 with Nucleotides and Transition State Analogues

The pTYB2 transit peptide (SStpNt-Intein-CBD construct (133)) was transformed into ER2566 *E. coli* cells, grown to OD_{600} 0.4 and induced with 1 mM IPTG overnight at

25°C. Cells were lysed via pulsed sonication (Fisher Scientific 550 Sonic Dismembrator) and the incorporation of 0.5 mg/ml lysozyme. The fusion protein construct was separated from soluble *E. coli* proteins on a chitin column (New England Biolabs, Ipswich, MA). This chitin matrix, with transit peptide construct attached via high affinity interaction, was then aliquotted into BioRad spin columns for the remainder of the experiment.

Purified psToc34 was incubated in 5 mM nucleotides (GDP, GTP, GMP-PNP) and/or 1000:1 fold transition state analogue (GDP:AlF_4) for one hour at room temperature in order to replace the bound nucleotide (GDP) with the desired nucleotide and/or transition state analogue. The GDP:AlF_4 was generated by combining 30 μM $AlCl_3$ and 5 mM NaF; the 1000:1 ratio describes the effective transition state analogue concentration relative to the Toc protein concentration (145). For control, psToc34 was also soaked in 5 mM GDP to ensure the salt form of the nucleotide was not altering the observed results. Because the hydrolytic rate of psToc34 is significantly low (35 nmol/min/μmol Toc protein) it is assumed that the majority of the GTP soaked psToc34 is GTP-bound since it is used within 1 hour. The psToc34 protein was rapidly separated from bulk free nucleotide by size exchange on a PD-10 column (GE Healthcare, Piscataway, NJ) equilibrated with GBS buffer. The psToc34 protein with various nucleotides and GDP:AlF_4 was allowed to incubate in the transit peptide affinity column (presumably interacting with transit peptide). The flow through was collected, the columns were washed with 500 μl GBS and then eluted with a 200 μl addition of 8 M urea. The flow through and elutions were then run on SDS-PAGE gels followed by CBB staining to determine the relative affinities of psToc34 soaked in different nucleotides and/or transition state analogues for the bound transit peptide.

4.3.5 Hydrolysis Measurements of psToc34

GTPase measurements were performed as described in Chapter II, section 2.3.2.

4.3.6 Effect of Transit Peptide on Nucleotide Exchange

The psToc34 protein (0.5 mg) was incubated with [α-^{32}P]GTP (0.5 mCi of 800 Ci/mmol, MP Biomedicals) and EDTA in GBS for 1 h at room temperature in a 500 μl reaction volume. The unbound nucleotide, EDTA, and imidazole were removed by loading the mixture onto a PD-10 desalting column (Amersham Biosciences) and eluted in GBS; ~2% of the psToc34 was routinely labeled. The eluent was collected in 60 μl fractions; psToc34-containing fractions began after ~3.2 ml of elution, and the concentrations of these fractions were determined using the Bradford assay. The requisite amount of psToc34 was added to create a 200 nM solution, and 50 μl was aliquoted into each well of a microtiter plate. A time course of the dissociation of GTP label was started with a 50 μl addition of 100-fold GTP or 100-fold GTP and transit peptide at 0.3-, 1.5-, 7.5-, or 37.5-fold molar excess over psToc34; GBS was used as a negative control. After each of the wells had incubated for the indicated time, the plate was placed on the hybrid magnet and then washed 12 cycles in a microtiter plate washer. The remaining GBS was aspirated away and replaced by GBS with 50 μl of 500 mM imidazole. Half of the elution was transferred into 100 μl of MicroScint scintillation fluid and counted in the TopCount (Packard Instrument Co.). Data were fit using a single-phase exponential decay in Graphpad Prism 4.0c.

4.3.7 Homobifunctional Chemical Crosslinking

The purified protein psToc34 (25 μl of 20 μM) was incubated either alone or in the presence of the following: 5-fold excess SStpNtΔPGP, SStpNtΔFPVSR, *wild type* SStpNt or cysteine mutants thereof. After incubation for 10 min at room temperature in GBS buffer with 100 μM TCEP, transit peptides or mutants thereof were added the crosslinker BMH was added at 5-fold excess (over transit peptide, 25-fold excess over Toc protein) and allowed to incubate for 1 hour (30 minutes in the case of cysteine mutants) at room temperature. Crosslinking was terminated with the addition of 5 mM β-Me and 20 μl 4 X SSB. Samples were run on either a Tris-Tricine gel system in order to visualize the three species visible, free transit peptide, monomeric psToc34 and dimeric psToc34, or a 4-20% Tris-Hepes precast gel from Pierce. Due to limitations of the Tris-Tricine gel system, the adduct of psToc34 and SStpNt was unable to be resolved and therefore necessitated another gel system.

4.3.8 Analysis of Fluorescently Labeled Transit Peptides

Transit peptides each harboring a single cysteine, were reacted with the sulfhydryl reactive fluorescent molecule 2-(4'-maleimidylanilino)naphthalene-6-sulfonic acid, or MIANS. Peptides, brought up in PBS at 1 mg/ml were incubated in 5-fold excess TCEP and then 25-fold MIANS, solubilized in DMSO, for 1 hour at room temperature. The addition of 5 mM β-Me quenched the labeling reaction and the final volume was approximately 250 μl. The reaction was added to a pre-equilibrated (in PBS buffer) YM-3 (3000 Da mwco) Microcon centrifugal filtration device from Millipore and centrifuged at 13,000 x g for 45 minutes. 200 μl PBS buffer was added and centrifuged for 20 min.

This was repeated three more times. Finally, 100 μl PBS buffer was added, gently vortexed, and centrifuged at 1000 x g inverted in a 0.6 ml Eppendorf sample tube. The labeled transit peptide was then assayed to labeling efficiency. Using the MIANS extinction coefficient of 27,000 $M^{-1}cm^{-1}$ and the A_{332}, the labeling efficiency was determined by dividing the A_{332} by the ε and multiplying this number by the molecular weight of the peptide divided by the mg/ml of the peptide (determined by BCA assay). This calculation yielded a value that is the ratio of moles of dye over the moles of peptide. Labeling efficiencies greater than 0.75, or 75% were considered acceptable for further study.

4.3.9 GEF Assay

The psToc34 protein was prepared and loaded with radioactive nucleotide in a manner similar to "Effects of Transit Peptide on Nucleotide Exchange" from Chapter II with the following exception. Approximately 25 μl of 800 Ci/mmol [α-^{32}P]GTP was added to 100 μl of psToc34 at 2.2 mg/ml in GBS buffer and allowed to incubate over night at 10°C in order to facilitate both binding and subsequent hydrolysis to GDP, which in the absence of additional GTP, remains bound. With this method, routinely ~40% of the psToc34 became bound to a radioactive nucleotide. The GEF assay was set up and carried out in a similar manner as described in Chapter II. In separate experiments, both psToc159G as well as S3C transit peptide crosslinked to psToc159G were titrated from 5 nM to 5 μM. In two 96-well plates, 50 μl of a slurry of iron-incorporated agarose beads with Ni-NTA chemistry immobilizing psToc34 (with [α^{32}P]GTP bound) was uniformly distributed in columns 1-10, rows A-H and represent approximately 50 nM psToc34 per

well. Plate 1 was used as a control, and columns 1 and 2 represented the no-addition control where only buffer was present. This was done in order to determine the spontaneous exchange of bound radioactive nucleotide as a function of time and represents both natural GDP exchange as well as loss due to protein precipitation. 200 μM 'cold' unlabeled GTP was added to columns 3 and 4 and represent the natural exchange rate in the presence of saturating amounts of substrate nucleotide. To columns 5 and 6, the addition of 5 μM wild type SStpNt recapitulated data reported in Chapter II and (53) which indicated that transit peptide does not function as the GEF for psToc34. Columns 7 and 8 had 5 μM SStpNtΔPGP. This is the 'turn residue' mutant used in this chapter which is unable to stimulate GTP hydrolysis on psToc34. Finally, columns 9 and 10 have BSA added at 5 μM as an exogenous control protein.

A crosslinking reaction utilizing the homobifunctional crosslinker BMH was set up such that psToc159G was incubated with S3C SStpNt. Although the crosslinking is not complete, i.e. there is still free psToc159G as well as free transit peptide, a considerable amount, approximately half according to scanning densitometry, is captured in the covalently crosslinked adduct of psToc159G-tp. In plate 2, columns 1 and 2 were identical to plate 1 and represent the control. Columns 3 and 4, as with plate 1, represent the addition of 200 μM exogenous 'cold' GTP and represent the natural exchange rate. Columns 5-12 are the GEF experimental wells and were constructed as follows. Columns 5 and 6, 7 and 8, 9 and 10, and 11 and 12 had the addition of 5, 50, 500 and 5000 nM psToc159G-tp adduct. A third plate was set up similarly to the first and second, however instead of psToc159G-tp adduct added in the reported concentrations, only psToc159G was added at 5, 50, 500 and 5000 nM.

After the addition of either GTP, transit peptide (and mutant thereof) or psToc159G-tp adduct, the plates were placed on a hybrid plate magnet, as previously described in detail in Chapter II and (53), and 7.5 μl samples were taken and mixed with 100 μl MicroScint scintillation fluid at various time intervals ranging from 2 minutes out to 135 minutes. The scintillation plates were gently mixed and counted over night in a TopCount Perkin Elmer 96-well scintillation counter. Data were graphed as CPM as a function of time.

4.3.10 *In Organeller* Chloroplast GTPase Assay

Chloroplasts were purified from 8-day-old pea seedlings and the concentration of chlorophyll was determined (100). The GTPase assay was performed similar to the Toc GTPase hydrolysis assay described in Chapter II section 2.3.2 and (53) with the following alterations. Lanes 1-6 (A-H) of a 96-well plate were set up for an assay with lanes 7-12 (A-H) set up for a duplicate assay. Buffer alone was placed in Lane 1 A. Chloroplasts were pipetted into lane 1 B-H at 25 mg/ml chlorophyll in 50 μl aliquots. Lanes 2-6 (A-H) had 100 μl activated charcoal slurry. The assay was initiated by the addition of precursor protein to lane 1 C-H; wells 1A and 1B are reserved for spontaneous GTP hydrolysis and non-stimulated chloroplast GTP hydrolysis, respectively. At 5, 10, 15, 20 and 25 min, a 20 μl aliquot of the reaction was removed from the wells in lane 1 and placed into the corresponding wells in lane 2, 3, 4, 5 and 6, respectively. Lanes 7-12 were used as a duplicate experiment. Since the absolute contribution from the Toc GTPases to GTP hydrolysis cannot be determined, the data was reported as CPM vs Time.

4.4 Results

4.4.1 Transit Peptide Mutagenesis and Purification

The pTYB2 vector with wild type transit peptide or mutants thereof were transformed into *E. coli* ER2566 cells and induced and purified as described in Materials and Methods. The purification profile was visualized on an SDS-PAGE gel and MALDI-TOF mass spectrometry was used to confirm both intact size and purity (Figure 4-1). Mutants were confirmed by sequencing and MALDI-TOF mass spectrometry.

4.4.2 Induced Secondary Structure of the Transit Peptide

Several studies have been performed on the structure and function of the transit peptide (11,17,18,33,94,96,98,102,108,146,147). However, to date, no studies have carefully assayed the stimulatory effects of the transit peptide on the psToc34 protein. It has been reported that the transit peptide, when added exogenously to liposomes, interacts with the membrane in a chaotropic manner and causes spontaneous lysis and release of the liposomal contents (33). This has not been fully understood since transit peptides are not lytic to the chloroplast, therefore more information is needed to understand the structure and function of the transit peptide. In order to facilitate further understanding, transit peptide mutants were made such that cysteines were introduced at various positions along the length of the transit peptide (Figure 4-2, B and Table 4-1). Circular dichroism spectroscopy was employed in order to confirm that the transit peptide (and its mutants) formed α-helices similar to wild type in the helix promoting solvent TFE (94,105). A TFE titration is shown in indicating that at approximately 40% TFE, the

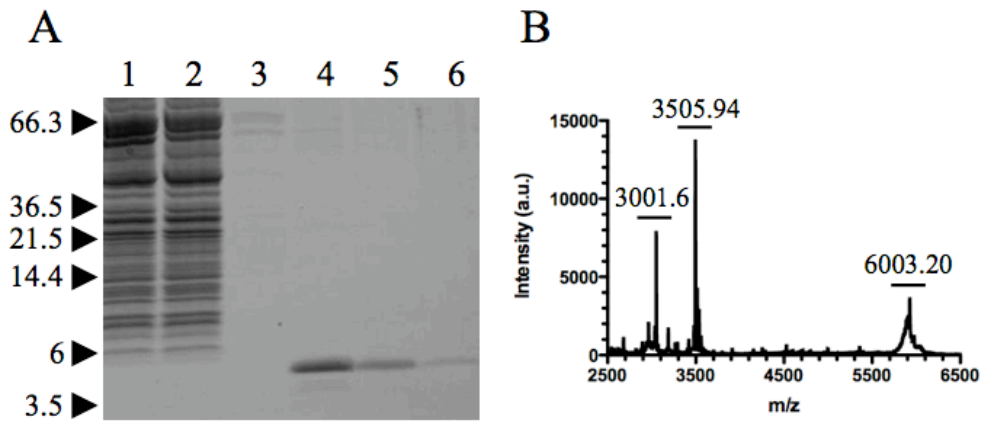


Figure 4-1. Purification of SStpPs. A, Lanes 1-6 represent a Tris-Tricine gel of lysate, flowthrough, wash and elutions 1-3, respectively. Panel B is a MALDI-TOF mass spectrometry spectrum obtained showing the +1 (6003.2 m/z) and +2 (3001.6 m/z) charge states of purified transit peptide indicating that it is the correct size and pure. Oxidized B chain of insulin from bovine was used as an internal standard (3505.94 m/z).

Primer Name	Strand	Sequence 5' to 3'
S3C	+	GGAGATATACATATGGCTTGCTCAGTTCTTTCCTC
S3C	-	GAGGAAAGAACTGAGCAAGCCATATGTATATCTCC
S8C	+	CCTCAGTTCTTTCCTGTGCAGCAGTTGCCACCC
S8C	-	GGGTGGCAACTGCTGCACAGGAAAGAACTGAGG
S15C	+	GCCACCCGCTGCAATGTTGCTCAAG
S15C	-	CTTGAGCAACATTGCAGCGGGTGGC
T27C	+	GTTGCACCTTTCTGTGGCCTTAAGTCAGC
T27C	-	GACTTAAGGCCACAGAAAGGTGCAACCATG
S34C	+	GGCCTTAAGTCAGCTGCCTGCTTCCCTGTTTCAAGG
S34C	-	CCTTGAAACAGGGAAGCAGGCAGCTGACTTAAGGCC
I45C	+	CAAAACCTTGACTGCACTTCCATTGCC
I45C	-	GGCAATGGAAGTGCAGTCAAGGTTTTG
G52C	+	CTTCCATTGCCAGCAACTGCGGAAGAGTGC
G52C	-	GCACTCTTCCGCAGTTGCTGGCAATGG
P26A	+	GCAGCTGTGGCTGCGTTCGGTGGCCTGAAGAGC
P26A	-	GCTCTTCAGGCCACCGAACGCAGCCACAGCTGC
G28A	+	GGCTCCGTTCGCTGGCCTGAAGAGCATGACC
G28A	-	GGTCATGCTCTTCAGGCCAGCGAACGGAGCC
P36A	+	GGCCTGAAGAGCATGACCGGTTTCGCTGTTAAAAAGG
P36A	-	CGGTGTTTACCTTTTTAACAGCGAAACCGGTCATGC

Table 1. Mutagenic Primers. All primers were designed using DNAStar and synthesized by IDT (Coralville, IA) and were received as lyophilized powder. Oligos were resuspended to 500 ng/μl in ddH2O which represented the 5X stock and were kept frozen at -20°C until used to make the 1X working concentration of 100 ng/μl.

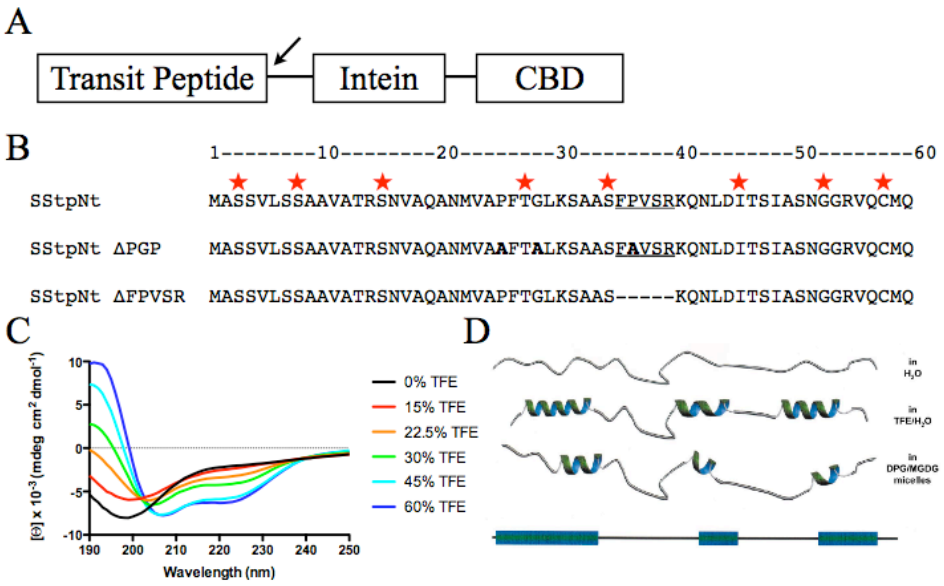


Figure 4-2. Peptide sequence and mutants. Panel A shows the construct used to purify transit peptide. The transit peptide is C-terminally fused to the self-cleaving intein protein and the chiting binding domain. Upon incubation with reducing agent, the intein protein catalyzes self cleavage and liberates the transit peptide (position of cleavage indicated with arrow). Panel B shows the sequence of SStpNt and two mutants, ΔPGP and ΔFPVSR, are such that ΔPGP replaces these residues with alanine (as indicated in **bold**) and ΔFPVSR is the ablation of these five residues. The positioning of the red stars indicates residues that have been mutated to cysteine, generating 13 unique SStpNt peptides each harboring a single cysteine residue. Panel C is the circular dichroism spectra obtained from SStpNt incubation in 0% to 60% TFE and is confirmatory of assertions made in panel D. Panel D is taken from (Bruce, 2001) and indicates that the transit peptide is a nascent chain polypeptide in solution, however, it adopts an α-helical structure upon incubation in the helical promoting solvent TFE or when it encounters detergent micelles or liposomes with galactolipid character.

transit peptide no longer gains any further α-helix (Figure 4-2, C). Figure 4-2 D, taken from (11), depicts how the transit peptide gains structure when partitioning from a fully aqueous environment into one of lower dielectric constant such as a detergent micelle or a lipid bilayer with galactolipid character. The observation that after 40% TFE no further secondary structure is gained or lost is a common feature among chloroplast transit peptides (94,105).

4.4.3 Nucleotides and Transition State Analogues Modulate Transit Peptide Affinity for psToc34

We have shown that psToc34 binds GDP, GTP, XTP, GMP-PNP, GTP-γ-S and to a small extent, UTP (Chapter II and Figure 2-10). It has been reported that the affinity of psToc34 for transit peptide is modulated by the bound GDP or GTP molecule (53,106,148,149). In fact, it was reported that in the absence of exogenous nucleotide, the dissociation rate of preprotein and psToc34 was approximately 20-fold greater and that the influence of GDP was dependent on the transit peptide used. Sveshnikova and coworkers also concluded that the dissociation of preproteins from psToc34 was reduced 3-fold when GDP was exchanged for GTP indicating that there is better binding of peptide with psToc34 in the presence of GTP. This measurement was confirmed and refined through the use of Surface Plasmon Resonance (SPR). Our laboratory reported the dissociation constant (K_d) of prSSU for Toc34 in the presence and absence of GTP was 24 nM and 310 nM, respectively (108).

The Toc proteins exhibit monomer/dimer equilibrium (Figure 3-5). The psToc34 monomer/dimer equilibrium was shifted toward the monomer by transit peptide

interaction and shifted toward the dimer by the transition state analogue GDP:AlF_4 (Figure 3-6). Since nucleotides regulate the affinity of psToc34 for the transit peptide, and the transition state analogue seems to bias the monomer/dimer equilibrium, it will therefore be important to understand these two phenomena. To this end, we have designed immobilized affinity-pull down assays to determine the relative affinity of psToc34 for transit peptide.

Chitin beads were used to immobilize the SStpNt-CBD construct where CBD is chitin-binding domain. Once SStpNt-CBD was bound and equilibrated with buffer, psToc34 in different nucleotide-loading states was incubated with it, washed with buffer and eluted from the column with 8 M urea. Beads devoid of SStpNt-CBD were used to establish a baseline that represents the total protein used, density of band set to 100 (Figure 4-3 lane 1). Lanes 2-4 represent the flow through after binding and less protein indicates a greater affinity and thus retention within the column. Similarly, lanes 5-7 represent the denatured elution where presence of protein indicates retention within the column and thus affinity. Comparison of lanes 2 and 3 and 5 and 6 suggest our results recapitulate earlier observations that psToc34-GTP exhibited higher affinity for transit peptide than psToc34-GDP. The psToc34 protein with bound transition state analogue GDP:AlF_4 showed little affinity for transit peptide (Figure 4-3 lanes 4 and 7).

4.4.4 Hydrolysis Rate and Affinity for GTP are Stimulated by Transit Peptide

Several studies have reported a stimulatory effect of transit peptide on the hydrolytic activity of the Toc GTPases (25,67,106,108). However, a thorough and quantitative analysis has not been performed. Therefore, we performed GTPase

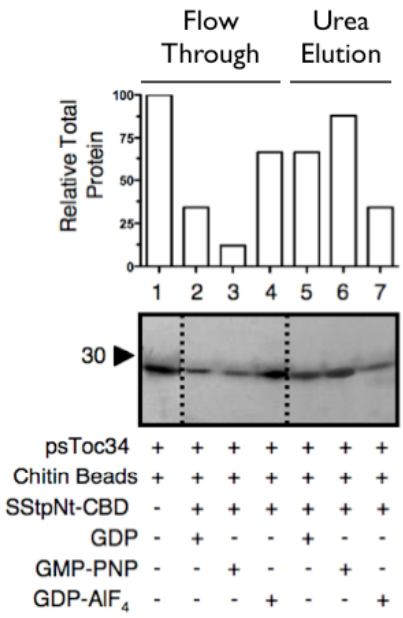


Figure 4-3. Nucleotides and transition state analogues modulate affinity of psToc34 for transit peptide. psToc34 does not show affinity for chitin beads without transit peptide-intein-CBD construct, lane 1. Chitin beads bound with transit peptide-intein-CBD construct were used to measure the affinity of psToc34 in various nucleotide loading states to transit peptide (lanes 2-7). Lanes 2-4 represent the flow through of the incubation of Toc with transit peptide and lanes 5-7 represent the urea-denatured elution of bound psToc34. Presence of protein in lanes 2-4 is representative of low affinity (and thus flow through) while presence of protein in lanes 5-7 is representative of affinity (and thus retention of protein which was released with urea denaturation). GDP or GMP-PNP loaded psToc34 had affinity for transit peptide, lanes 2, 3 and 5, 6 whereas psToc34 loaded with the transition state analog, GDP-AlF_4, does not, lanes 4 and 7. Presence of protein in lanes 2-4 is representative of low affinity (and thus flow through) while presence of protein in lanes 5-7 is representative of affinity (and thus retention of protein which was released with urea denaturation).

hydrolysis measurements with several different transit peptide concentrations in order to carefully determine the effects that transit peptide has on the activity of psToc34.

GTP is hydrolyzed at a linear rate by psToc34 (Figure 4-4, A), with a velocity of 35 nmol of GTP/min/μmol of Toc, Figure 4-4, B. When psToc34 is incubated with a 25:1 molar excess of reduced carboxymethylated lactalbumin (RCMLA), an unstructured peptide, the rate of $^{32}PO_4^{3-}$ release remains constant and is very similar to psToc34 alone (Figure 4-4, A), and the velocity reflects that of "unstimulated" psToc34 (Figure 4-4, B). Furthermore, when psToc34 is incubated in the presence of a similar molar excess of either SStpPs or SStpNt, the amount of $^{32}PO_4^{3-}$ release and the rate of GTP hydrolysis increases (Figure 4-4, A and B). Figure 4-4, C, represents a single concentration of GTP (25 μM) with SStpPs, SStpNt, and RCMLA all present at 25-fold molar excess to Toc protein. This was repeated with multiple concentrations of GTP, aliquots removed at 0, 10, 15, and 20 min, and scintillation counted yielding counts/min data that were fit to linear regression (Figure 4-4, A). Each linear regression yielded a slope that was mathematically transformed into a rate expressed in nanomoles of GTP hydrolyzed/min/μmol of psToc34, as seen in Figure 4-4, B (data shown represents psToc34 with one concentration of peptide, 25 μM, and various GTP concentrations). A substrate-velocity plot was created for each of 11 peptide concentrations ranging from 0.58- to 100-fold molar excess (data not shown). No concentration of RCMLA stimulated the velocity of psToc34 at any of the GTP concentrations assayed (Figure 4-4, B). SStpPs and SStpNt both stimulated the maximal velocity as well as reduced the K_M (Figure 4-4, B and D). Using the unstimulated velocity curve in Figure 4-4, B (solid squares, solid line), the fold-increase in rate was determined at each of the 11 peptide concentrations of

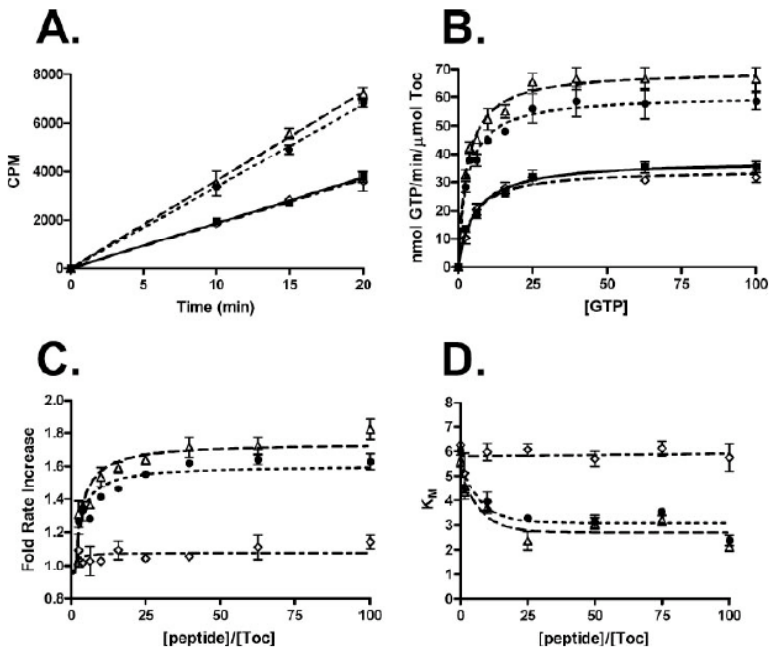


Figure 4-4. Effect of transit peptide on hydrolysis rate of psToc34. Panel A represents the increase in counts/min as a function of time for psToc34 alone, ■; in the presence of 25 molar fold SStpPs, △; SStpNt, ●; and RCMLA, ◇, respectively, with a total of 25 μM GTP. The total GTP was titrated from 1 to 100 μM; only 25 μM is shown in A, C, and D for clarity. B, multiple concentrations of GTP were used to generate the substrate velocity plot for psToc34 alone or in the presence of a molar fold excess of SStpPs, SStpNt, or RCMLA at 2.5, 4, 6.3, 10, 15.8, 25, 40, 63, and 100 over psToc34; for clarity, only 25 molar fold excess is shown. C, fold increase, over unstimulated psToc34, in rate of GTP hydrolysis, is shown as a function of the peptide to psToc34 molar ratio at each titration of peptide; rate increase data were obtained from a substrate velocity plot as in B. D, K_M values obtained from the substrate velocity plots in B are plotted indicating an increase in affinity for substrate with the titration of SStpPs and SStpNt to a minimum K_M value at 25 molar fold excess of peptide to psToc34. SStpPs, SStpNt, and RCMLA are represented as △, ●, and ◇, respectively.

SStpPs, SStpNt, and the negative control RCMLA (Figure 4-4, C). Each data point for each treatment in Figure 4-4, C represents the V_{max} value obtained from nonlinear regression for each treatment (all data points for a given treatment) divided by the V_{max} value of psToc34 with no treatment (Figure 4-4, B). Both SStpPs and SStpNt increase the rate of GTP hydrolysis by psToc34 by ~1.6-fold, whereas RCMLA did not affect the rate (Figure 4-4, C). Furthermore, the molar excess of SStpPs and SStpNt required to give half the maximal rate increase was 3.5 and 3.8 molar fold, respectively. SStpPs and SStpNt also altered the K_M value, or the affinity of psToc34 for the substrate GTP (Figure 4-4, D). Each data point in Figure 4-4, D represents the K_M value calculated from the nonlinear fit of each molar excess of SStp to psToc34. The molar excess of SStpPs and SStpNt required for half-maximal K_M reduction was 4.6 and 4.2, respectively.

4.4.5 Transit Peptide Mutants Differentially Modulate psToc34 GTPase Activity and Monomer/Dimer Equilibrium

The psToc34 protein, alone in solution, possesses a basal GTPase rate of ~35 nmol GTP hydrolyzed/minute/μmol Toc protein and that rate can be increased with the addition of either transit peptide or preprotein, Figure 4-4 and (53,100). Therefore, transit peptide mutants that lack the ability to stimulate GTP hydrolysis may provide valuable insight into the regions of the peptide responsible for acting as a GAP for psToc34. Two mutants were recently identified that had reduced chloroplast import competency (133). These were the ΔPGP and the ΔFPVSR mutants (Figure 4-2). In the case of ΔPGP, the proline, glycine and proline residues at positions 26, 28 and 36, respectively, were replaced with alanine. The ΔFPVSR mutant (representing the FGLK motif (94)) is a

truncated form of the transit peptide devoid of residues 35-39. These mutants, along with wild type SStpPs were incubated with psToc34 and their impact on GTP hydrolysis was reported (Figure 4-5, A). Wild type transit peptide stimulates the hydrolytic rate from ~35 to ~65 (compare green squares and red diamonds in Figure 4-5, A). However, incubation of the SStpPsΔPGP mutant had no effect on psToc34 hydrolytic activity (Figure 4-5, A open circles). The mutant ΔFPVSR resulted in both a reduced V_{max} (~20 nmol GTP/min/μmol Toc) and increased K_M (~18 μM) (Figure 4-5, A black triangles).

The psToc34 protein exists in a monomer/dimer equilibrium. The addition of BMH covalently trapped the dimeric species and could be visualized on an SDS-PAGE gel (Figure 4-5, B lane 1). The addition of the SStpNtΔPGP mutant did not significantly bias the equilibrium, consistent with the hydrolysis data (Figure 4-5, A open circles). Lanes 3 and 4 are quite similar, with lane 3 possessing a slightly greater amount of dimeric psToc34 (Figure 4-5, B). Lane 3 shows that interaction was occurring, however not to the degree that was apparent in lane 4 with wild type peptide. Lane 4 shows that the wild type peptide drove the monomer/dimer equilibrium strongly to the monomer as was indicated by the virtual absence of crosslinked dimer and the increase of monomeric psToc34.

4.4.6 Both psToc34 and psToc159G Bind Transit Peptide with Varying Degrees of Affinity

The knowledge that psToc34 and psToc159G act as GTPase receptors for the transit peptide has been established, however, which GTPase is the primary receptor and/or has higher affinity for the transit peptide is still a matter of debate (67,70). In order

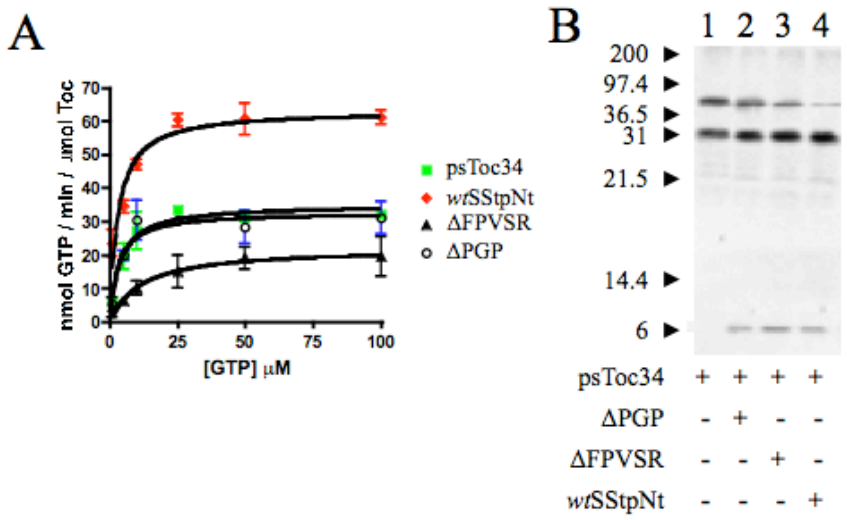


Figure 4-5. Wild type and mutant forms of the transit peptide differentially modulate psToc34. Panel A reports GTPase activity of psToc34 and depending on different effectors. The green squares represent unstimulated psToc34, the red diamonds, indicate the stimulatory effects of transit peptide, the black triangles represent the addition of the ΔFPVSR mutant SStpNt and the open circles (superimposed on unstimulated psToc34) represent the addition of ΔPGP mutant of SStpNt. Panel B reports the modulatory activities of these mutants on the monomer-dimer equilibrium of psToc34, all lanes represent protein with or without transit peptide (and mutant transit peptides) incubated in the presence of BMH crosslinker. Lane 1 is psToc34 alone, lane 2 represents the addition of the ΔPGP mutant, lane 3 represents the addition of the ΔFPVSR mutant and lane 4 represents the addition of wild type SStpNt.

to determine transit peptide binding preference, a crosslinking reaction was performed such that SStpPs was incubated alone, with psToc34, with psToc159G or with both psToc34 and psToc159G (Figure 4-6). After incubating the proteins, peptides and crosslinker for one hour at room temperature, the reaction was quenched and the samples were prepared for SDS-PAGE followed by transfer to Immobilon where they were probed with anti-SStpPs (lanes 1-4), anti-psToc34 (lanes 5-8) and anti-psToc159G (lanes 9-12) (Figure 4-6). Lanes 1-4 are run on a Tris-Tricine gel in order to visualize SStpPs whereas lanes 5-12 are run on a 15% Tris-Glycine SDS-PAGE gel, thus the discrepancy in molecular mass markers. A band at ~6 kDa represents the monomeric transit peptide (★), however a band was observed at ~12 kDa which indicated peptide dimers (★★) were formed. Lanes 2 and 3 show the peptide binding to psToc34 (▲★) and psToc159G (■★), respectively. The former showed stronger signal on the Western, and thus presumably greater amounts of bound antigen. When comparing the detected species in lane 4, there was greater transit peptide bound to psToc34 (▲★) than to psToc159G (■★). The amount of transit peptide bound to psToc159G in the presence of psToc34 (lane 4) was less than the amount binding to psToc159G alone (lane 3). Under the conditions of the experiment, psToc34 was observed to have higher affinity for transit peptide than psToc159G, however it cannot be discounted that the placement of the cysteine favors crosslinking to psToc34. Using anti-psToc34 antibodies, bands were detected in lanes 6 and 8 corresponding to monomeric psToc34 (▲), psToc34-transit peptide adduct (▲★) and psToc34 dimer (▲▲). The highest molecular weight species in lane 8 represented the psToc34-psToc159G heterodimer (▲■).

Figure 4-6. Western analysis reveals transit peptide binding preference. Panel A, SStpPs was incubated with either psToc34 alone, psToc159G alone or both psToc34 and psToc159G in a BMH mediated crosslinking reaction. Lanes 1-4 were run on a Tris-Tricine gel system while lanes 5-12 were run on a standard 15% Tris-Glycine SDS-PAGE. Lanes 2 and 3 show the α-SStpPs antibody recognizing the monomeric SStpPs (★) at approx. 6 kDa, a transit peptide dimer (★★) as well as the psToc34-transit peptide adduct (▲★, 35 kDa) and the psToc159G-transit peptide adduct psToc159G (■★, 48 kDa). Lane 4 indicates that SStpPs prefers to interact with and crosslink to psToc34 (more intense psToc34-tp adduct as compared to psToc159G-tp adduct). Lanes 5-8 and 9-12 are identical to lanes 1-4, however they were probed with α-psToc34 and α-psToc159G antibodies. Lanes 8 and 12 indicate that both proteins psToc34 and psToc159G in the presence of transit peptide tend to form the heterodimeric species (▲■). Panel B represents the quantitation of the psToc34-tp adduct (▲★) or the psToc159G-tp adduct (■★) in lanes 2 and 4, 6 and 8, 3 and 4, or 11 and 12 indicating that transit peptide binding to psToc34 increases while binding to psToc159G decreases.

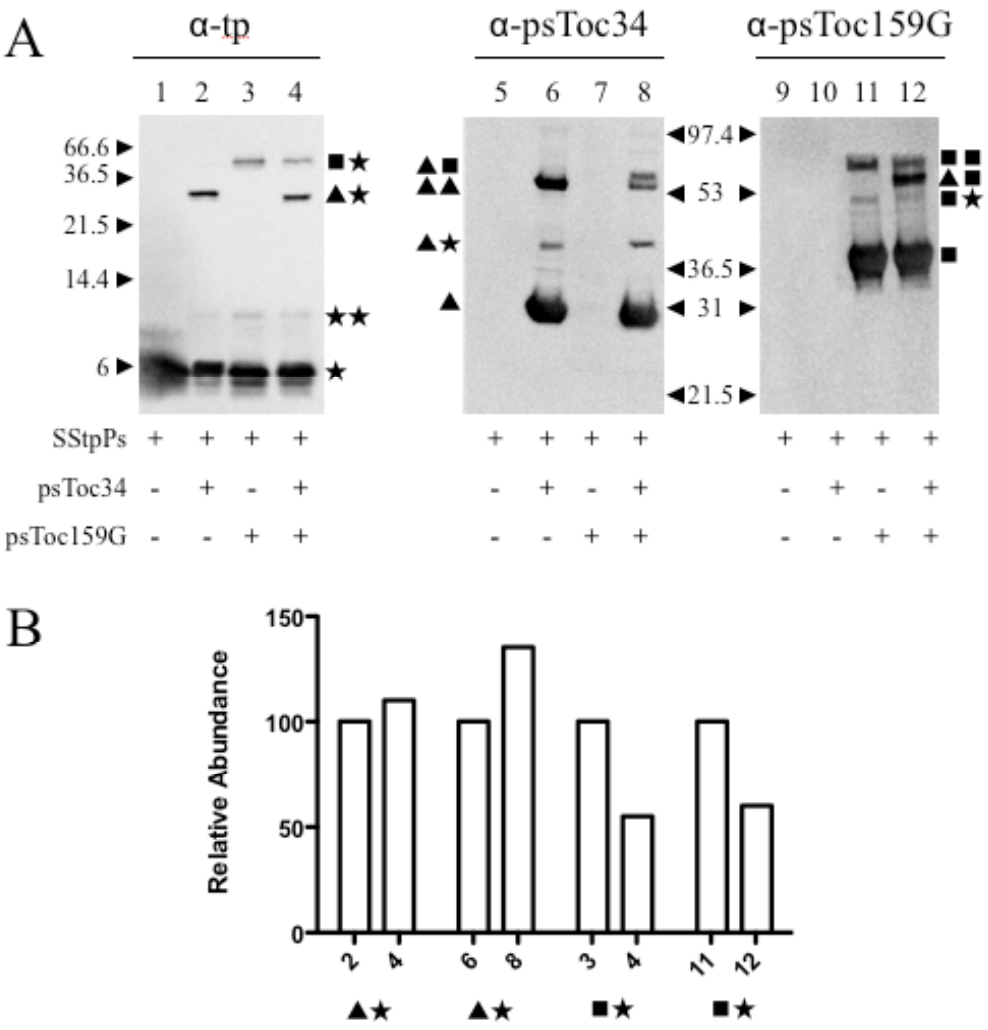

A
α-tp
α-psToc34
α-psToc159G
1 2 3 4
5 6 7 8
9 10 11 12
66.6
36.5
21.5
14.4
6
97.4
53
36.5
31
21.5
SStpPs + + + + + + + + + + + +
psToc34 - + - + - + - + - + - +
psToc159G - - + + - - + + - - + +
B
Relative Abundance
150
100
50
0
2 4 6 8 3 4 11 12

Figure 4-6

It was observed that binding of transit peptide to psToc34 (▲★) increased when psToc159G was present, lane 8. Similarly, it was observed that the psToc159G-transit peptide adduct was reduced when psToc34 was present, lane 12.

Quantitation of transit peptide-Toc protein adducts from lanes 2-4, 6, 8, 11 and 12 are shown in Figure 4-6, panel B. Using anti-transit peptide antibodies, the signal from the psToc34-transit peptide adduct (▲★) was shown to increase when psToc159G was included (Figure 4-6 B, 2 and 4). Conversely, the signal from the psToc159G-transit peptide adduct (■★) was shown to be decreased when psToc34 was included (Figure 4-6 B, 3 and 4). This trend was confirmed using using anti-psToc34 and anti-psToc159G antibodies. The signal from the psToc34-transit peptide adduct increased when psToc159G was included (Figure 4-6 B, 6 and 8) and the signal from the psToc159G-transit peptide adduct (■★) decreased when psToc34 was included (Figure 4-6 B, 11 and 12).

This experiment was designed to examine the relative affinities of the receptor GTPases for the transit peptide as well as determine qualitatively if one GTPase bound transit peptide more readily than the other. Data in Figure 4-6 suggested that psToc34 has a higher affinity for transit peptide (compare lanes 2 through 4) than psToc159G. Furthermore, it was observed that transit peptide binding to psToc34 increased in the presence of psToc159G which suggests that if a heterodimer is formed, the transit peptide predominantly bound to psToc34. More work will be necessary

4.4.7 Transit Peptide Induced Dimer to Monomer Transition is Titratable

As observed earlier by homobifunctional crosslinking, the Toc GTPases exist in a monomer/dimer equilibrium and this equilibrium is modulated through interaction with transit peptide (Figures 3-7 and 4-6). Under *in vitro* conditions presented earlier in this chapter, the transit peptide has been at a minimum of 10 molar-fold excess over Toc protein. While this may approximate the *in vivo* conditions, there are times at which little preprotein import occurs (i.e. during seedling stages or senescence). The dimer to monomer transition may be of significance in the overall import reaction and therefore we performed experiments to determine the amount of transit peptide required to elicit the Toc GTPase dimer to monomer transition.

Four ratios of Toc protein to transit peptide were assayed by chemical crosslinking followed by Western analysis (Figure 4-7). The transit peptide was incubated with psToc34 at a transit peptide:Toc ratio of 0.003, 0.03, 0.3 and 3.0 (Figure 4-7, lanes 1-4 and 9-10). Similarly, transit peptide was incubated with psToc159G at a transit peptide:Toc ratio of 0.003, 0.03, 0.3 and 3.0 (Figure 4-7, lanes 5-9 and 13-16). Lanes 1-8 were probed with anti-SStpPs antibodies while lanes 9-12 and 13-16 were probed with anti-psToc34 and anti-psToc159G antibodies, respectively. By comparing lanes 1-4 and 9-12, which were identical samples probed with two different antibodies, it was apparent that psToc34 crosslinked to transit peptide at a ratio of 0.03 peptide to protein (as observed in lane 2) and that the dimer to monomer transition began to occur at 0.3 peptide to protein ratio. This was not the case for psToc159G, which began to be crosslinked to peptide at 0.3 peptide to protein ratio and did not experience the dimer to

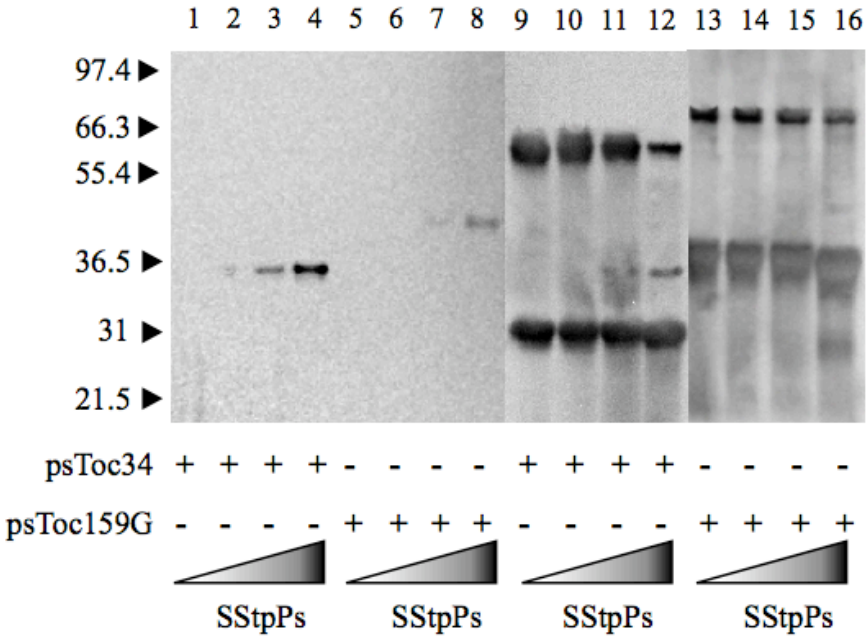


Figure 4-7. The dimer to monomer transition induced by transit peptide is titratable. Transit peptide was crosslinked with either psToc34 (lanes 1-4 and 9-12) or psToc159G (lanes 5-8 and 13-16). Lanes 1-8 were probed with anti-SStpPs antibody, lanes 9-12 with anti-psToc34 and lanes 13-16 with anti-psToc159G. The molar ratio of transit peptide to the GTPase receptor protein were as follows: lanes 1, 5, 9 and 13 had 0.003, lanes 2, 6, 10 and 14 had 0.03, lanes 3, 7, 11 and 15 had 0.3 and lanes 4, 8, 12 and 16 had 3.0. These are represented graphically at the bottom of the figure as an increase in concentration of SStpPs. Notice that only the ratio of 3.0 had a crosslinked adduct between psToc159G and transit peptide whereas a ratio of 0.03 showed signal for psToc34 indicating a more robust interaction.

monomer transition until 3.0 peptide to protein ratio (Figure 4-7, lanes 5-8 and 13-16). Higher concentrations of transit peptide were needed to bias the dimer to monomer equilibrium of psToc159G as compared to psToc34, which was more sensitive to peptide concentrations.

In order to further determine the concentration of peptide that elicited the dimer to monomer transition for psToc34 and psToc159G we performed a transit peptide titration crosslinking experiment with an expanded the ratio range (Figure 4-8). Quantitation of the dimeric Toc protein signal from a chemiluminescent Western blot was used to determine the ratio of peptide to Toc protein that elicited the dimer to monomer transition of psToc34 and psToc159G. The ratio of transit peptide to Toc protein shown in lanes 1-6 and 7-12 was 0.15, 0.5, 1.5, 4.5, 15 and 45, respectively. Using this expanded range of peptide to Toc protein ratios, we observed that the dimer of psToc34 is reduced by lower concentrations of transit peptide as compared to the dimer of psToc159G (Figure 4-8 A, compare depletion of dimeric psToc34 signal (▲▲) with the depletion of the dimeric psToc159G signal (■■). Quantitation of these bands further evidenced that a concentration of ~15 μM transit peptide (transit peptide to Toc ratio of ~1.5) disrupted 50% of the dimeric species of psToc34 whereas disruption of 50% of the dimer of psToc159G occurred at ~110 μM transit peptide (transit peptide to Toc ratio of ~11) (Figure 4-8, B).

By increasing the transit peptide to Toc protein ratio, we observed that the monomerization of psToc34 occurred more readily than that of psToc159G. We showed that psToc159G required 10-fold more transit peptide than psToc34 in order to achieve

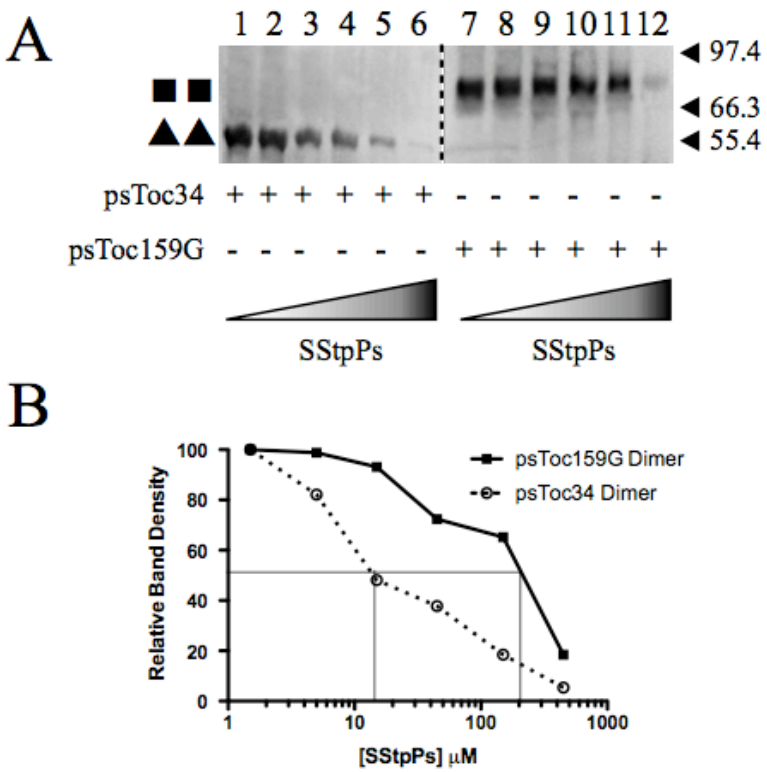


Figure 4-8. psToc34 is more sensitive to SStpPs induced monomerization than psToc159G. Panel A, lanes 1-6 and 7-12 had 10 μM psToc34 and 10 μM psToc159G, respectively. Lanes 1-6 and 7-12 had SStpPs present at 1.5, 5, 15, 45, 150 and 450 μM and were probed with anti-psToc34 and anti-psToc159G antibodies, respectively. The ratios, therefore, of peptide to Toc protein were 0.15, 0.5, 1.5, 4.5, 15 and 45. The dimeric species of psToc34 and psToc159G are designated by double triangle and double square, respectively. Panel B represents the quantitation of the dimeric species for psToc34 and psToc59G, which are shown as a dotted line and solid line, respectively. The concentration of transit peptide required to reduce the dimer to 50% intensity is shown graphically as lines in panel B.

similar levels of monomerization. The significance of this phenomenon in the role of chloroplast protein import has yet to be determined and will require further work.

4.4.8 The psToc34 Protein Interacts Primarily with the C-terminus of the Transit Peptide

The particular domain or region of the transit peptide with which psToc34 interacts has been assayed in the past (54,55). However, these measurements have met with considerable difficulty and limited success due mainly to the transient nature of this interaction (150). By understanding which part of the transit peptide the psToc34 protein interacts, we can better understand transit peptides and how their structure elicits GTPase activity on the psToc34 protein.

In order to probe the region(s) of transit peptide that may interact with psToc34, we chose to incorporate an environmentally sensitive fluorescent molecule at various positions on the transit peptide (example in Figure 4-2). The flurophore MIANS (2-(4'-maleimidylanilino)naphthalene-6-sulfonic acid, sodium salt) was used as its fluorescence wavelength maxima becomes shifted to higher wavelengths (red shifted) when in solution and a has a pronounced reduction in wavelength maxima (blue shifted) when bound by a protein, and thus shielded from bulk solvent. Therefore, cysteines were introduced into the SStpPs peptide via site directed mutagenesis at positions 3, 8, 15, 27, 34, 45, 52 and the wild type position 58. The SStpPs peptide was used instead of the SStpNt peptide due to the availability of a highly reactive antibody raised against SStpPs that has only mild reactivity toward the peptide from tobacco. These mutations were made so that the fluorescent MIANS molecule could be covalently attached. The cysteines also afford

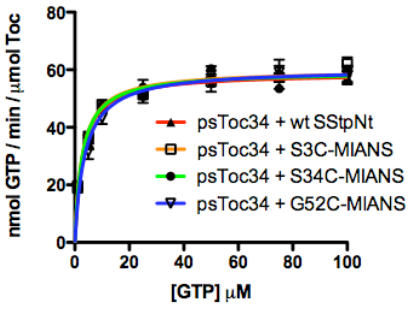
crosslinking to be performed with psToc34 to determine the region of the peptide most reactive toward the GTPase. The cysteine mutants were designed in a C58Y background so that the mutated residue represented the only cysteine present in the peptide.

Three cys-mutant transit peptides, S3C, S34C and G52C, were chosen for MIANS labeling. After the labeling reaction, fluorescently labeled peptide was purified from free MIANS and the degree of labeling was determined as described in Materials and Methods. Using a PTI fluorimeter set to 332 nm excitation wavelength and scanning emission wavelengths from 350-500 nm, spectra were recorded of the labeled peptide free in solution (Figure 4-9, B, dashed line) or in the presence of its receptor protein psToc34 (Figure 4-9, B, solid line). The peptides, free in solution, all shared a common wavelength maximum at approximately 445 nm, which suggested they were tumbling free in solution; MIANS free in solution has a wavelength maximum of 450 nm (151). Upon the addition of psToc34 protein, the spectra became blue shifted (Figure 4-9, B, solid lines). S3C-MIANS, the most N-terminal positioning of the fluorophore, showed the least amount of blue shift (from 449 nm to 430 nm, Figure 4-9, C). The positioning of MIANS at G52C or S34C, representing the C-terminal and middle part of the peptide, respectively, showed a more pronounced blue shift. S34C-MIANS experienced a shift from 442.5 nm to 412.5 nm and G52C-MIANS showed a shift from 450.5 nm to 398 nm (Figure 4-9, C). In a control GTPase experiment, all three peptides stimulated psToc34 to the same extent as wild type, which indicated they still interacted with the protein and that the placement of the MIANS group did not disrupt that interaction (Figure 4-9, A).

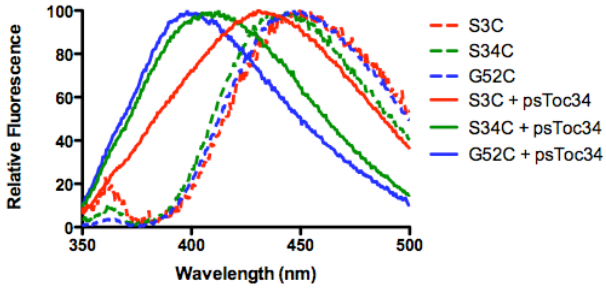
To further determine the part of the peptide that interacts with the Toc GTPase proteins, various cysteine mutant peptides were utilized in a crosslinking reaction

Figure 4-9. Fluorescently labeled peptides interact with psToc34. Three transit peptides harboring one cysteine each (S3C, S34C, G52C) were reacted with and labeled with the fluorescent molecule MIANS. Panel A, the placement of MIANS on the transit peptide did not disrupt its ability to stimulate the GTPase activity of psToc34. In Panel B, the S3C-MIANS, S34C-MIANS and G52C-MIANS peptides were incubated alone (dashed lines) or in the presence of psToc34 (solid lines) and had spectra collected by exciting at 332 nm and recording fluorescent spectra from 350 – 500 nm. The peptides S3C, S34C and G52C are represented by red, green and blue colored lines, respectively. Panel C reports the wavelength maxima of each of the line traces in panel B.

A



B



C

Constructs	psToc34	λ_{max}
S3C-MIANS	-	449.0
	+	430.5
S34C-MIANS	-	442.5
	+	412.5
G52C-MIANS	-	450.0
	+	398.0

Figure 4-9

Figure 4-10. Crosslinking of psToc34 with single Cys-SStpNt transit peptides refines location of binding. Panel A indicates graphically the position of the introduced cysteine. Panels B and C, lanes 1-8 represent the Western analysis of a 12-20% SDS-PAGE separation of the crosslinking reaction between psToc34 (B) and psToc159G (C and various transit peptide mutants. S3C, S8C, S15C, T27C, S34C, I45C, G52C and C58C SStpNt was crosslinked with psToc34 and psToc159G, lanes 1-8 in B and C, respectively. The vertical dashed lines represent data from two (or three) different westerns that are displayed and are present only to designate the fact that more than one gel transfer was utilized to obtain the displayed data. Panel D is the quantitation of band intensities in B and C.

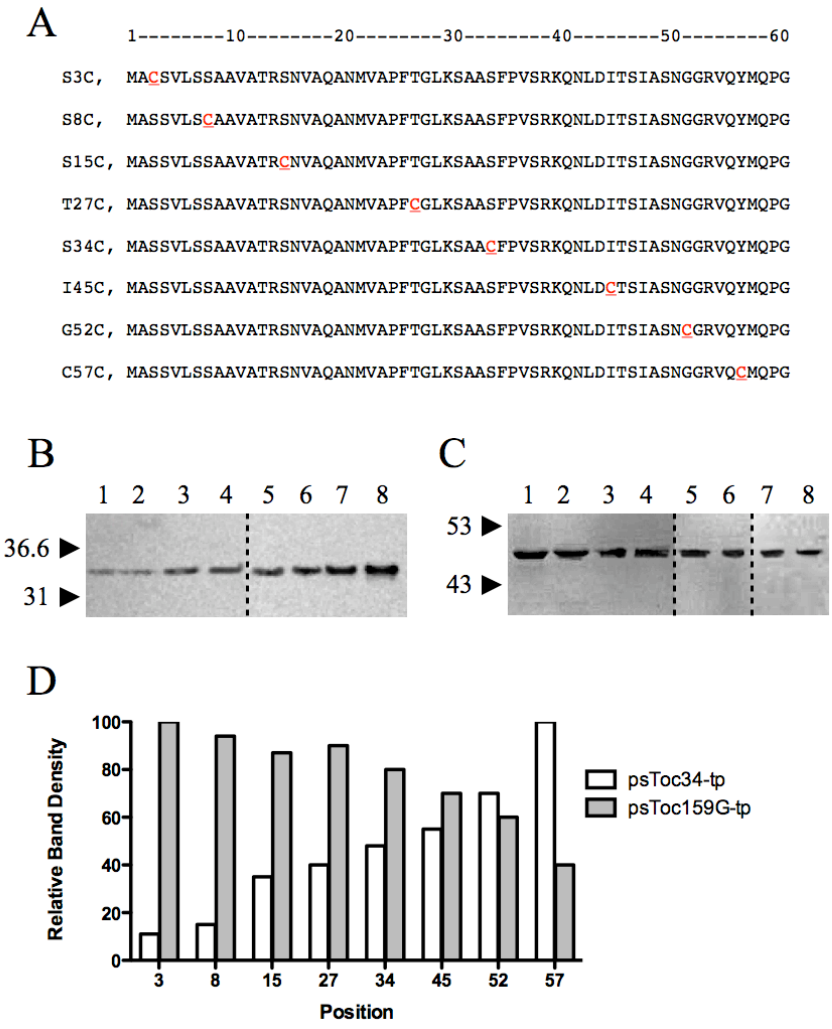

A
1--------10--------20--------30--------40--------50--------60
S3C, MACSVLSSAAVATRSNVAQANMVAPFTGLKSAASFPVSRKQNLDITSIASNGGRVQYMQPG
S8C, MASSVLSCAAVATRSNVAQANMVAPFTGLKSAASFPVSRKQNLDITSIASNGGRVQYMQPG
S15C, MASSVLSSAAVATRCNVAQANMVAPFTGLKSAASFPVSRKQNLDITSIASNGGRVQYMQPG
T27C, MASSVLSSAAVATRSNVAQANMVAPFCGLKSAASFPVSRKQNLDITSIASNGGRVQYMQPG
S34C, MASSVLSSAAVATRSNVAQANMVAPFTGLKSAACFPVSRKQNLDITSIASNGGRVQYMQPG
I45C, MASSVLSSAAVATRSNVAQANMVAPFTGLKSAASFPVSRKQNLDCTSIASNGGRVQYMQPG
G52C, MASSVLSSAAVATRSNVAQANMVAPFTGLKSAASFPVSRKQNLDITSIASNCGRVQYMQPG
C57C, MASSVLSSAAVATRSNVAQANMVAPFTGLKSAASFPVSRKQNLDITSIASNGGRVQCMQPG
B
1 2 3 4 5 6 7 8
36.6
31
C
1 2 3 4 5 6 7 8
53
43
D
Relative Band Density
100
80
60
40
20
0
3 8 15 27 34 45 52 57
Position
psToc34-tp
psToc159G-tp

Figure 4-10

(Figure 4-10). By comparing the crosslinking data obtained from the various peptides covalently linked to either psToc34 or psToc159G, it was observed that psToc34 preferred to interact with the C-terminal region of the peptide (Figure 4-10, B), while psToc159G interacted with the peptide as a whole (Figure 4-10, C). Quantitation of chemiluminescence signal was performed and is presented in Figure 4-10, D.

Here it was observed that psToc34 preferentially crosslinked to the C-terminus of the transit peptide while psToc159G preferentially crosslinked to the N-terminus. However, the ability of the two proteins to discriminate between the termini were not the same (Figure 4-10, D). This result is confirmatory of reports that suggested psToc34 and psToc159G do not share the same transit peptide binding site (152).

4.4.9 Transit Peptide Bound Toc159G Acts as GEF for psToc34

As has been reported earlier in Chapter II, the transit peptide stimulated GTP hydrolysis activity of psToc34 by acting as the GAP, or GTPase Activating Protein (53). Figure 1-5 illustrates that GTPase proteins require cofactors to complete the GTPase cycle in an efficient manner, these cofactors are GAPs or Guanine nucleotide Exchange Factors (GEFs). GTP-binding proteins such as the Ras superfamily have a nearly undetectable level of GTP hydrolysis (113). Because of the low baseline level of hydrolytic activity, GTPase proteins function as switches and are considered to be ‘on’ in the GTP-bound state and ‘off’ in the GDP-bound state (76). These proteins are cycled through their active and inactive states through the interaction with their cognate GAPs and GEFs. GAP proteins interact with the GTP-bound GTPase protein and increasing the likelihood of a hydrolytic event. By contrast, GEFs catalyze the dissociation of GDP

from the nucleotide binding pocket which is readily replaced by a GTP due to the differences in nucleotide concentrations in the cytosol (74). The mechanism of action of GAPs and GEFs differ slightly between GTPase protein subfamilies (76), however, the result of a GTPase interacting with a GAP or a GEF is nucleotide hydrolysis or nucleotide exchange, respectively.

While the transit peptide may act as the GAP for (at least) psToc34, there is no known GEF for psToc34 (100). We rationalized that the translocon could in fact be its own regulational unit, that is to say, the translocon may not need other factors in order to cycle between the GTP and GDP bound states as the GAP and GEF may be part of the translocon itself. In order to probe this possibility, we tested to see if another member of the translocon was acting as the GEF for psToc34. A nucleotide exchange assay was set up in a manner similar to Figure 2-11 such that α-^{32}P[GDP]-psToc34 was immobilized and aliquotted across a 96-well plate with various concentrations of effectors as described in Materials and Methods. The rate of GDP release was not perturbed by the addition of excess GTP, BSA, or GTP and BSA (Figure 4-11 A). The data in panel B suggested that the addition of increasing concentrations of psToc159G did not alter the overall exchange. However, the curve of exchange as a function of time was observed to be biphasic; an analysis of this is presented in the Discussion section below.

A crosslinking reaction was used to covalently attach the psToc159G protein with the transit peptide SStpNt S3C. According to earlier figures in this chapter (Figure 4-6 and Figure 4-7), approximately half of the psToc159G protein and peptide are covalently linked. This adduct was titrated in the same manner as in panel B resulting in panel C. The curve was again biphasic, which indicated there were two equilibria, however

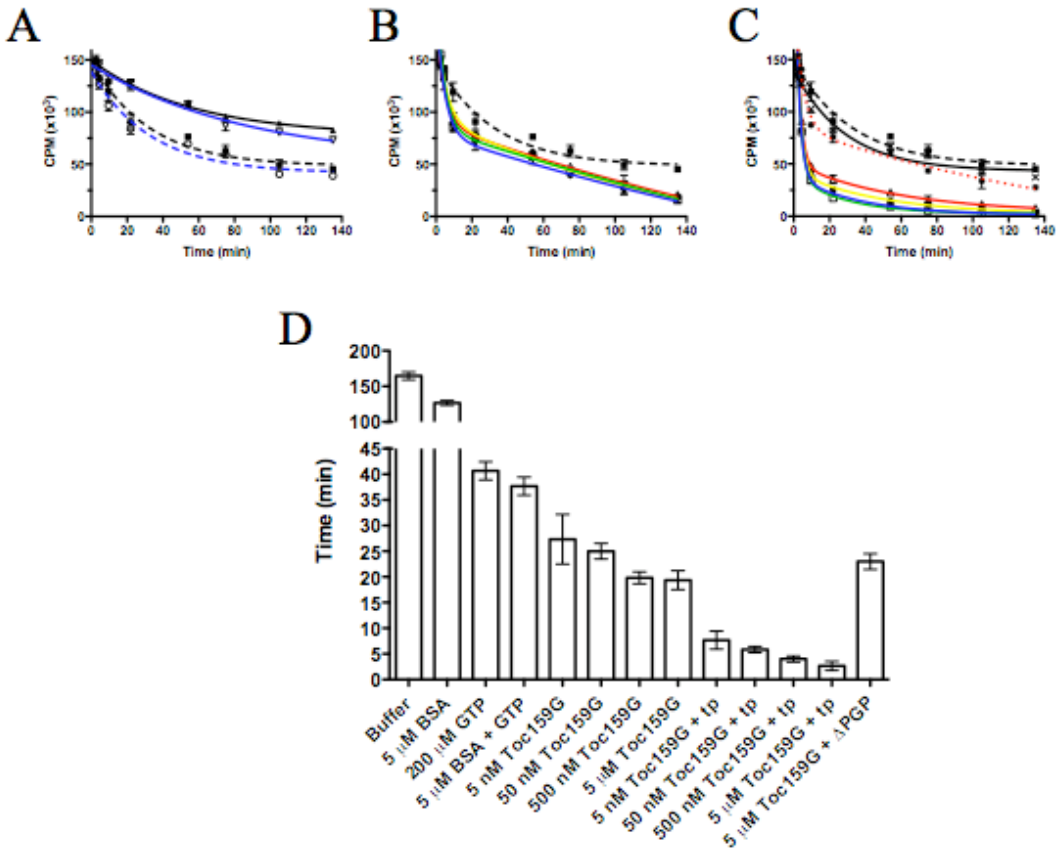


Figure 4-11. The psToc159G-transit peptide adduct acts as the GEF for psToc34. Panel A indicates that buffer and BSA controls do not contribute to the exchange of GDP reaction; excess GTP and BSA with GTP both stimulate the exchange reaction to the same basal degree. Panel B indicates that psToc159G titrated through a 1000-fold range did not stimulate the exchange reaction. Panel C shows that the psToc159G-SStpNt adduct stimulated the exchange of bound GDP for GTP for psToc34 whereas transit peptide alone and psToc159G + SStpNtΔPGP did not stimulate this exchange. Panel D is a graphical representation of the time necessary for each treatment to cause psToc34 to exchange 50% of its bound nucleotide.

α-^{32}P[GDP] was released at a greater rate. This suggested the psToc159G-tp adduct was acting as the Guanine nucleotide Exchange Factor (GEF) for psToc34. In order to validate this observation, a mutant form of the transit peptide SStpNtΔPGP was crosslinked to psToc159G and the experiment was repeated. This 'mutant adduct' was unable to stimulate the rate of nucleotide release from psToc34 any more than psToc159G alone (Figure 4-11). The amount of time necessary for the particular treatment to reduce the CPM value by 50% was measured (Figure 4-11, D). Here it was observed that psToc34 exchanged 50% of its nucleotide in approx. 150 minutes with buffer and BSA controls and the addition of 200 μM GTP reduced this time of exchange to ~40 min. A concentration of 5 μM psToc159G resulted in 50% exchange of the nucleotide bound to psToc34 in 22 minutes. However, when the transit peptide was crosslinked to psToc159G prior to incubation with psToc34, 50% exchange occurred in approximately 4 minutes.

4.4.10 *In Organellar* GTPase Assays Reveal GTP Requirement During Chloroplast Protein Import

Transit peptide interaction with the Toc GTPases results in monomerization and increased hydrolysis rates (Figure 4-5) and (53,100). While kinetic analyses have been carried out on isolated Toc GTPases either *in vitro* or as reconstituted proteoliposomes (25,53,55,67), no GTP hydrolysis studies have been conducted *in organellar* with isolated, intact chloroplasts. Therefore, intact chloroplasts were prepared from 8-day-old pea seedlings as described in Materials and Methods and (100). These organelles were assayed at 25 mg/ml chlorophyll in a 96-well microplate GTPase assay, as described in

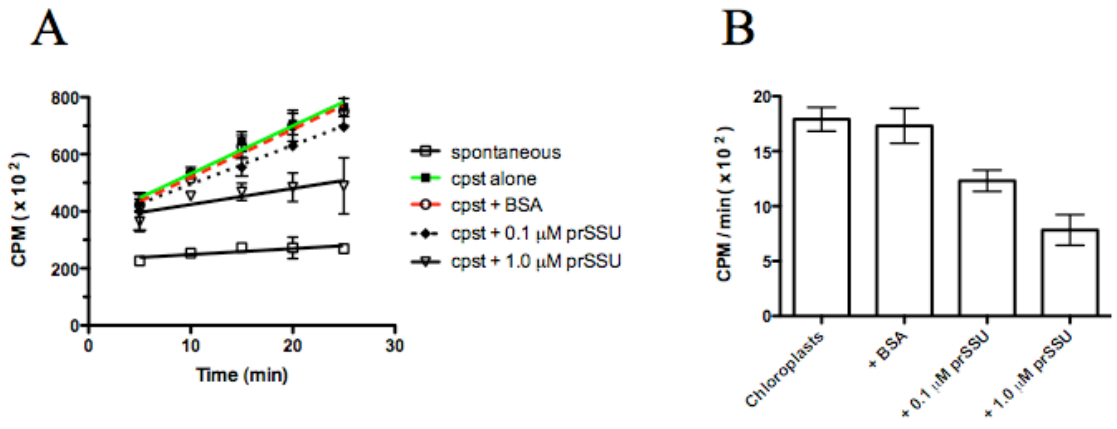


Figure 4-12. Isolated Chloroplast GTPase Assay. Panel A indicates that isolated chloroplasts hydrolyze GTP at a basal rate, solid line, black squares. The addition of 0.1 μM (open circles) and 1.0 μM (closed diamonds) prSSU causes the rate of GTP hydrolysis to drop, as shown by the dashed and dotted lines, respectively. Panel B shows the slopes for three independent experiments and indicates that BSA control does not change the GTPase rate of chloroplasts, but the addition of 1 μM prSSU decreases the observed rate of GTP hydrolysis.

Chapter 2 and (53,100). Isolated chloroplast GTP hydrolysis was determined and reported as a function of CPM *vs*. time (Figure 4-12, A, black squares). Isolated chloroplasts hydrolyzed GTP at a rate of ~1700 CPM/min and the addition of 0.1 μM and 1.0 μM prSSU resulted in hydrolysis measurements of 1500 CPM/min and 800 CPM/min, respectively (Figure 4-12). BSA controls were performed and resulted in no change in hydrolytic rate (Figure 4-12 B).

4.5 Discussion

The homo- and/or heterodimerization of the Toc GTPases is generally assumed to be a feature of the assembly of the Toc core complex (153). The notion that GTPases may dimerize is not novel, and has been documented in the bacterial SRP GTPases FtsY and Ffh (132) as well as FlhF (154) and the metal binding GTPase HypB (155). The dimerization interface is different between these various GTPases, and so is the functional significance of dimerization. The dimer to monomer transition for these GTPases are modulated by various factors including GTP hydrolysis and interaction with other proteins.

It has been reported that psToc34 exhibited differential affinity toward the transit peptide dependent on its nucleotide binding status (108). This observation fits with the accepted view that GTPases act as nucleotide dependent switches that are activated by the binding of GTP and inactivated by the hydrolysis to GDP, events that are often governed by accessory proteins called GEFs and GAPs (74,76). Our experimentation revealed that transit peptide interaction elicited greater GTPase activity by psToc34 (Figure 4-4). With Figure 2-11, we propose that transit peptide acted as the GTPase

Activating Protein for psToc34 by stimulating the rate of GTP hydrolysis without increasing the rate of GDP for GTP exchange (53). This is generally consistent with the Ras superfamily of GTPases and their associated GAPs (156). However, the fold-increase in GTPase activity observed for these GTPases upon encountering their cognate GAPs is typically much greater (52,74,114). An explanation for this discrepancy in stimulatory activity is that the Ras GTPase superfamily is generally soluble whereas the Toc GTPases are bound to the membrane via a C-terminal transmembrane α-helix. GTPase measurements of the Toc proteins are carried out with heterologously expressed soluble constructs devoid of a transmembrane domain, and this may alter their enzymatic activity. Earlier, in Chapter III, we showed that GTPase measurements of basal hydrolytic activity were elevated in chloroplast outer membrane mimetic liposomes (Figure 3-2). Furthermore, reconstituted Toc GTPase proteoliposomes showed elevated GTPase activity when encountering short synthetic peptides corresponding to the N- and C-termini of the transit peptide (55).

To better understand the affinity of psToc34 for transit peptide, we saturated psToc34 with nucleotides and the transition state analogue GDP:AlF_4 (Figure 4-3). Comparisons of analogous GTPases, namely the Ras-superfamily, suggests that nucleotide-modulated affinity for substrate is a common theme among GTP-binding proteins, however there is usually a point at which the affinity between GTPase and substrate is nearly zero (156). Figure 4-3 lanes 2 and 3 suggest psToc34-GDP affinity for transit peptide is not significantly reduced from that of psToc34-GTP. This experiment was carried out as an on-column immobilized affinity assay, whereas the report that psToc34-GTP had higher affinity than psToc34-GDP for transit peptide was measured

using highly sensitive Biosensor Surface Plasmon Resonance (108). Even though this immobilized-affinity assay is less sensitive, the affinity of psToc34 saturated with the transition state analogue GDP:AlF_4 showed less affinity for peptide (Figure 4-3 lanes 4 and 7).

It is further shown in Figure 4-4 that this GTPase stimulation increases not only the V_{max} of the enzyme but also lowers the K_M value for GTP. The >2-fold stimulation that is observed is very reproducible and is not the result of nonspecific interactions. Although this is much more activity than the synthetic peptides were capable of stimulating psToc34 as reported by Becker *et al.*, it is still significantly less than the initial activity reported value by prSSU (78). Causes for the variability between laboratories in the level of peptide and preprotein stimulation of the hydrolysis of GTP by the Toc GTPases remain unclear. All the same, the ability of the full-length transit peptide to stimulate the rate of GTP hydrolysis suggests that this sequence may somehow regulate the activity/structure of the GTPase during Toc-mediated precursor recognition. Since GTPase stimulation was not observed upon addition of the unstructured control peptide, RCMLA, this suggests that the GTPase stimulation was a result of specific interaction(s) being mediated by one or more regions of the transit peptide and is not simply the interaction of the exposed peptide backbone as has been suggested for RCMLA stimulation of ATPase activity of the chaperone hsp70 (89). These observations suggest that some region or domain of the transit peptide functions to regulate the activity/structure of the GTPase during Toc-mediated precursor recognition.

Previous data suggested that synthetic peptides corresponding to the N- and C-terminal half of the transit peptide could differentially stimulate psToc159G and psToc34

(55). However, since the peptide was presented as an N- or C-terminal truncation, a recognition domain may have been split. In order to probe possible recognition domains in the transit peptide, we assayed the ability of two mutants, SStpNtΔPGP and SStpNtΔFPVSR, to modulate psToc34 GTP hydrolysis and monomer/dimer equilibrium. These mutants were identified earlier by their inability to compete against wild type peptides for import into isolated chloroplasts (133). We showed that incubation of transit peptide with the Toc GTPases resulted in increased GTPase activity as well as a monomerization of the GTPase. The dimeric equilibrium of psToc34 was more sensitive to lower concentrations of peptide as compared to psToc159G (Figures 4-7 and 4-8). We observed that SStpNtΔPGP was unable to stimulate GTP hydrolysis and did not result in any appreciable change in the dimeric equilibrium (Figure 4-5). In contrast, psToc34 interaction with peptide devoid of a putative recognition domain, SStpNtΔFPVSR, resulted in a reduced V_{max} while concomitantly increasing the K_M and was able to elicit a modest amount of psToc34 monomerization (Figure 4-5). When incubated with this semi-conserved domain deletion mutant, psToc34 hydrolyzes GTP at a maximal rate of ~20 nmol/min/μmol Toc protein and the K_M has increased from ~3.5 to ~18 μM. It is tempting to speculate that the SStpNtΔFPVSR peptide was acting in a manner similar to an uncompetitive inhibitor. However, this presupposes that the peptide is the natural substrate for the reaction rather than GTP. Nonetheless, since the K_M was increased (less affinity for substrate) and the V_{max} was reduced, this suggested that the residues FPVSR could be involved in the reaction. Without these residues, binding may have been occurring, but perhaps release of peptide (and thus another GTP turnover) was the rate-limiting step.

The order of events as the transit peptide interacts with the Toc GTPases has been a matter of debate (55,67,70,121). Many reports have assayed the interaction between transit peptides and the Toc proteins, however, a side-by-side comparison of the relative affinities of transit peptide for psToc34 and psToc159G has not yet been reported. In this report, we showed that isolated psToc34 more robustly crosslinks to wild type transit peptide than does psToc159G (Figure 4-6). However, this raises the possibility that the position of the cysteine (C58 in transit peptide) is positioned more favorably for crosslinking to psToc34 than to psToc159G. Therefore, we mutated several transit peptide residues to cysteine (Figure 4-9 and 4-10) in order to probe whether the cysteine position would lead to better crosslinking and possibly implicate the location on the transit peptide to which psToc34 and psToc159G bind. Recently, NMR data has been put forward suggesting that psToc34 binds to the C-terminal portion of the peptide whereas psToc159G binds to the N-terminal portion (152). In order to validate these claims, we performed both fluorescence spectroscopy and chemical crosslinking with cysteins at various positions on the transit peptide (Figures 4-9 and 4-10). Our results strengthen the claim that psToc34 interacts primarily with the C-terminal portion of the transit peptide while psToc159G interacts primarily with the N-terminal region. While strongly suggestive of interaction within these regions, more experimentation will be required to confirm the absolute region of interactivity.

GTPase proteins have low basal hydrolytic rates, existing in either a GDP (off) or a GTP (on) state in order to function as molecular switches rather than molecular motors (52,74). This basal hydrolytic rate can be stimulated through the interaction of regulatory proteins such as GTPase Activating Proteins (GAP) and Guanine nucleotide Exchange

Factors (GEF) (Figure 1-5) and (76). GAPs are generally specific for their target GTPases, and act to accelerate the rate of hydrolysis effectively turning the switch 'off'. A GEF catalyzes the dissociation of bound GDP from the GTPase effectively turning it 'on'. A GEF acts through interaction either directly with the GTPase switch domains, or allosterically at an auxiliary location to lower the affinity for the bound GDP molecule such that GTP, largely through mass action, replaces GDP; the cellular concentration of GTP is several times greater than that of GDP (157). GEFs could be required for nucleotide exchange and complementation of the Toc GTPase cycle, but these effector molecules have yet to be reported (135). We showed that psToc159G alone does not act as the GEF, however psToc159G covalently crosslinked to SStpNt does, in fact, increase the rate of nucleotide exchange (Figure 4-11).

In vitro work conducted with the Toc GTPases have utilized heterologously expressed proteins, typically with affinity tags, that are soluble and devoid of their respective C-terminal transmembrane domains (158). A limited number of studies have been performed with reconstituted proteoliposomes, typically composed of Toc75, Toc34 and either Toc52 or Toc86, both fragments of Toc159 (31,55,67). The reports detailing the rate of import have used isolated intact chloroplasts and typically utilize mutated forms of prSSU (63,96,159). Therefore, we performed *in organellar* assays to validate our claims that the transit peptide increased the *in vitro* hydrolysis rates of the purified cytosolic domains of the Toc GTPases. Surprisingly, when prSSU was titrated to the chloroplasts in a chloroplast GTPase assay, the rate of GTP hydrolysis was depressed (Figure 4-12). It was hypothesized that GTP would be hydrolyzed at a higher rate when a higher concentration of prSSU was present, however this was not the observation. A

chloroplast import assay was performed with ^{35}S-labeled prSSU and indicated that the precursor protein was indeed imported and processed to the mature form, mSSU. Therefore, the hydrolytic rate depression was not due to poor import (data not shown) and represents a real phenomenon. The implications for this observation will be addressed in Chapter V.

4.6 Summary

In this chapter, we sought to understand the interactions of transit peptide with psToc34 and psToc159G by performing hydrolysis, fluorescence, crosslinking and nucleotide binding assays. By incubating psToc34 in various nucleotides and the transition state analogue GDP:AlF_4, we confirmed earlier data that psToc34 affinity for transit peptide is stimulated by GTP and the transition state of psToc34 had low affinity for transit peptide. This suggested a mechanism of transit peptide binding, induced GTP hydrolysis and concomitant transit peptide release. Through the use of two previously identified mutants, ΔPGP and ΔFPVSR, we provided evidence that these residues play a role in Toc protein binding and affect the monomer/dimer equilibrium of psToc34. More work will be needed to elucidate whether these residues are directly involved in the GTPase reaction or whether they allosterically modulate the Toc protein. Furthermore, we made several individual point mutations of the transit peptide, introducing a cysteine residue at various positions to allow the addition of a fluorescent tag or homobifunctional crosslinking. Fluorescence assays suggested that psToc34 and psToc159G do not share the same binding site on the transit peptide. In fact, our data suggests that psToc159G binds to the more N-terminal domain whereas psToc34 binds to the C-terminus.

Crosslinking helped strengthen this claim as C-terminal cysteine mutants preferentially crosslinked with psToc34. We showed that transit peptide interaction results in stimulation of the V_{max} and a concomitant reduction of the $K_{M,}$ which suggested that the transit peptide acted as the GAP for psToc34. We also determined that psToc159G crosslinked to transit peptide acted as the GEF for psToc34. Finally, we tested the GTPase activity of intact chloroplasts in an *in organellar* GTPase assay. It was determined that the rate of GTP hydrolysis was reduced with the addition of increasing concentrations of transit peptide. Further work will be needed to understand this phenomenon.

Chapter V

The Toc Clock: The Unified Model of Chloroplast Protein Translocation

5.1 Abstract

The mechanism by which the chloroplast imports proteins is not known in detail. In order to present a model of chloroplast protein import, we first provide a brief review of the evolutionary origin and stoichiometry of the Toc translocon. Next, we introduce the two currently debated models that describe events governing chloroplast protein import: the *motor hypothesis* and the *targeting hypothesis*. These models differ fundamentally as to the primary receptor of the precursor protein as well as to the function of GTP hydrolysis during the import cycle. We discuss data obtained in Chapters II, III and IV allowing us to extend our observations resulting in the creation of our unified model, "The Toc Clock".

5.2 Evolutionary Origins of the Toc Translocon

By analyzing probable events during the second endosymbiotic event which ultimately gave rise to the modern day chloroplast, the evolutionary origins of components of the chloroplast import apparatus have been postulated (8). The chloroplastic ribosomal RNA, transcription factors, DNA structure and gene organization are prokaryotic in nature (160). Comparison of the 16S RNA sequences for cyanelles, cyanobacteria and chloroplasts suggests that chloroplasts may have been derived from a cyanobacterial lineage (161). The chloroplast outer membrane used to be considered a remnant of the phagosomal membrane of the eukaryotic host (2). However, the presence of galactolipids and β-barrel proteins, features shared with membranes of the

cyanobacteria but not with eukaryotic endomembrane systems, support the prokaryotic origin of the chloroplast (162).

The once independent chloroplasts are now unable to sustain life on their own. This is due, in part, to the genomic reduction of the chloroplast, which is no longer complete for all the genes necessary for organelle functions (10). Proteins coded for by these transferred genes are synthesized on cytosolic ribosomes and are imported back into the chloroplast. However, a transfer apparatus capable of transporting chloroplastic gene products back into the organelle was most likely not in place prior to nuclear genetic transfer.

5.2.1 Cyanobacterial Origin of Toc75

Genome wide sequencing of *Synechocystis* sp. PCC 6803 revealed significant similarity between the cyanobacterial SynToc75 and the modern plant Toc75 (163). The hypothesis that *Synechocystis* SynToc75 was the ancestral progenitor of the modern day Toc75 protein conducting channel has gained support (3,10). The SynToc75 protein was shown to be related to a group of specific prokaryotic secretion channels, most of which transfer virulence factors across the outer membrane in order for the organism to establish itself (Figure 1-1) and (163). Modern day bacteria secrete such virulence factors as YopE, ExoS and SptP that target critical eukaryotic GTPase proteins responsible for intracellular signaling and cytoskeletal rearrangements (164,165). The action of these secreted virulence factors ensured the survival of the bacterium within the host phagosome (164).

5.2.2 Eukaryotic Origins of Toc34 and Toc159

The Toc34/Toc159 superfamily (including Toc33, Toc90, Toc120 and Toc132) may have been derived from a common ancestral eukaryotic GTPase (69) whereas cyanobacterial and other prokaryotic GTPases are more distantly related (4). This ancestral 35 kDa eukaryotic GTPase is most likely also the protein which gave rise to the Ras superfamily of GTPases (166). Virulence factors secreted by SynToc75 may have targeted eukaryotic GTPases related to the Ras superfamily (17). It was observed that the transit peptide acted as the GAP for the Toc GTPases (Chapter IV, Figure 4-4) and (53). Therefore, secreted virulence factors repurposed as transit peptides may provide a mechanism that led to the transit peptide targeting system for the modern day chloroplast (17). However, exactly how the Toc75 β-barrel translocation channel and the Toc34/159 GTPase proteins came together to form a functional translocon over the course of evolution is unfortunately still a mystery (135). It is thought that the multi-subunit structures of the modern Toc complex may have evolved in a series of steps, with each step providing a clear selective advantage (167).

5.3 Stoichiometry of the Toc Translocon

Several reports have analyzed the subunit organization of the isolated Toc complex (25,51,100), however the absolute stoichiometry is a matter of debate (153). Schleiff and coworkers reported the first stoichiometry of an isolated Toc complex as ~4-5:4:1 Toc34:Toc75:Toc159, respectively. While this was shown to be technically sound, the method by which the researchers used to isolate the complex may have impacted the stoichiometry (51). For example, the Toc complex was isolated from pea plants over the

course of three days, which led to the proteolytic degradation of Toc159 (comprised of A, G and M domains) to its 86 kDa fragment protein Toc86 (G and M domains) and the 54 kDa fragment Toc54 (M domain). Low-resolution cryo-electron microscopy images revealed that the complex was roughly spherical with four pores (Toc75), a central density (Toc159) and four densities at the periphery of the sphere (Toc34) (Figure 1-3). The stoichiometry of Toc proteins in the isolated core complex was confirmed through the use of a radioactive labeling (25). It was also shown that transit peptides harbouring a nano-gold particle could bind to the complex in a stoichiometric fashion such that one, two, three and four concurrently tranlocating transit peptides could be observed (25).

In response to the report that the Toc complex was composed of these three proteins at an apparent 4:4:1 stoichiometry with a mass of ~500 kDa, Kikuchi and coworkers devised a system that rapidly fractionated plants and purified the Toc translocon (51). Here, plant material was collected and the chloroplasts were fractionated in approximately 5 hours as opposed to three days. Two complexes were seen to run on BN-PAGE at approximately 1000 kDa when Toc159 was present and approximately 800 kDa when the proteolytic fragment Toc86 was present. Due to the highly labile Toc159 protein, the 800 kDa species was most prevalent (51). This suggested that the ~800 kDa complex consisted of 6 Toc34, 6 Toc75 and 2 Toc86 molecules (51). Furthermore, complexes of 400 kDa and 200 kDa were also observed, possibly corresponding to 4 Toc75 and 1 Toc54 or 2 Toc75 and 1 Toc54 molecules, respectively (51). It was speculated that species observed at or above 1200 kDa represented complexes of 8:8:2 stoichiometry, however BN-PAGE does not have significant resolution above 1000 kDa and therefore the authors could not ascribe stoichiometry to those complexes

(51,100,122). Complexes between 1000 and 1320 kDa have also been observed and suggested to have stoichiometries of either 6:6:2 or 8:8:2 (100).

5.4 Electron Microscopic Studies of the Chloroplast Outer Membrane

Electron microscopy has been employed in the past to analyze the ultrastructure of the chloroplast outer envelope (168-170). It was observed by freeze fracture microscopy that the outer and the inner chloroplast membranes come together at contact sites (Figure 5-1) and (168). A punctuate pattern of particles could be observed on the outer membrane (Figure 5-1) and (168). These particles tended to aggregate in 'valleys' of the outer membrane (Figure 5-1) and were reported to be approximately 20 to 30 nm in diameter (168). Biochemical evidence later confirmed this observation and showed that the Toc and Tic complexes interact within the intermembrane space to facilitate preprotein transport from the cytosolic compartment to the stroma (Figure 1-2) and (26,80,82). The isolated 4:4:1 Toc core complex was reported to be 13 nm wide by 10-12 nm in width (25), however Toc complexes have also been reported to possess 6:6:2 and 8:8:2 stoichiometry suggesting they may be roughly twice the size of the previously reported complexes (51,100). Although speculative, the microscopically observed 20-30 nm particles could be the 8:8:2 species that were only observed when rapidly purified from isolated chloroplasts.

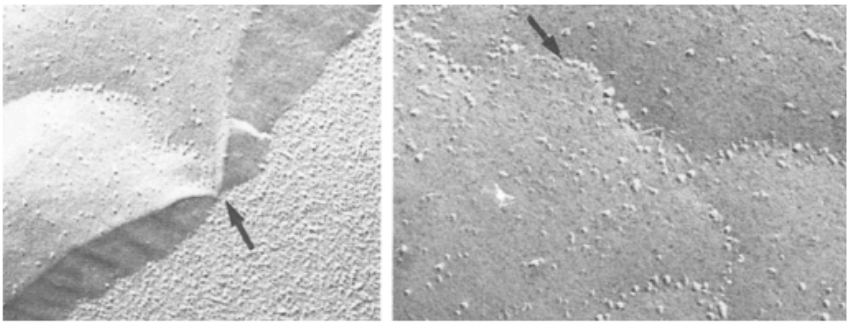


Figure 5-1. **Freeze fracture reveals punctate pattern at chloroplast outer envelope**. Cryoelectron microscopy revealed a punctate pattern on the surface of the chloroplast outer membrane (taken from Cline *et. al.*, 1985). This observed pattern was increased in frequency in the contact sites between the outer and inner membrane where protein translocation occurs. The particles (arrows) are approximately 20 nm in diameter.

5.5 Enzymology of the Toc Complex

Kinetic analyses of the Toc proteins have, for the most part, been carried out with heterologously expressed soluble (ΔTM) Toc GTPase constructs (35,53,100,106,108,153). However, since the Toc proteins are membrane bound, proteoliposomal and/or organeller data is more desirable. When the Toc core complex was reconstituted in proteoliposomes, it possessed a basal GTPase rate approximately 15-fold greater than the basal rate of isolated psToc34 (53,67). This observation suggested the addition of lipids as well as the other Toc proteins may act synergistically to stimulate the GTPase activity of Toc34 and Toc159 (171).

Similarly, the enzymatic activity of isolated psToc34 was increased by approximately 2.6-fold through interaction with the transit peptide (Chapter IV) and (53), and has been shown to exhibit more activity when in the presence of full-length preprotein (100). When the preprotein was incubated with isolated Toc core complexes in proteoliposomes, the GTPase activity of the complex was stimulated ~100-fold (67). The homodimer of psToc34 did not possess any more activity than the monomeric protein, (Chapter II) and (53). Therefore, contributions from lipids (Chapter III) and (55) and/or heterodimeric partners (Chapter IV) could account for ~40-fold difference in stimulatory activities.

5.6 Chloroplast Protein Import Models: the Motor and Targeting Hypotheses

A 6:6:2 or 8:8:2 Toc complex is present in the outer membrane of the chloroplast, however, models that diagram the order of events from targeting to import rarely include stoichiometry and are debated (135). Many models have been proposed and can be

divided into two groups referred to as the 'motor hypothesis' and the 'targeting hypothesis', reviewed in (63,91). These two models differ in the nature of the primary receptor, *i.e.* Toc34 in the motor hypothesis and Toc159 in the targeting hypothesis. Another significant defining characteristic is the function of GTP hydrolysis. The principal supposition in the motor hypothesis is that after the preprotein is received by its primary receptor, Toc34, Toc159 then actively translocates preprotein into the Toc75 β-barrel presumably utilizing energy released during GTP hydrolysis (Figure 5-2) and (67). The targeting hypothesis, on the other hand, proposes that a soluble pool of Toc159 acts as the primary receptor for the incoming preprotein. After preprotein capture in the cytosol, the Toc159-preprotein complex is targeted to the membrane where it interacts with Toc34 which facilitates translocation (Figure 5-3) (65).

5.6.1 The Motor Hypothesis

Structural analysis of the Toc core complex revealed four putative translocation channels surrounding a central finger-like domain (Figure 1-3) and (25). Based on stoichiometric data, it was proposed that these channels represented Toc75 with associated Toc34 and the central domain represented Toc159 (25,67). The motor hypothesis states that Toc34 acts as the primary receptor and passes preprotein off to Toc159 which then pushes the preprotein across the Toc75 β-barrel in a manner reminiscent of the ATP-powered protein, SecA (172). The motor function of Toc159 was based on the demonstrated ability of a minimal Toc complex comprised of Toc159 and Toc75 to translocate preproteins into a liposome and that this process was GTP-dependent (67). In support of the motor hypothesis, several studies have shown that the

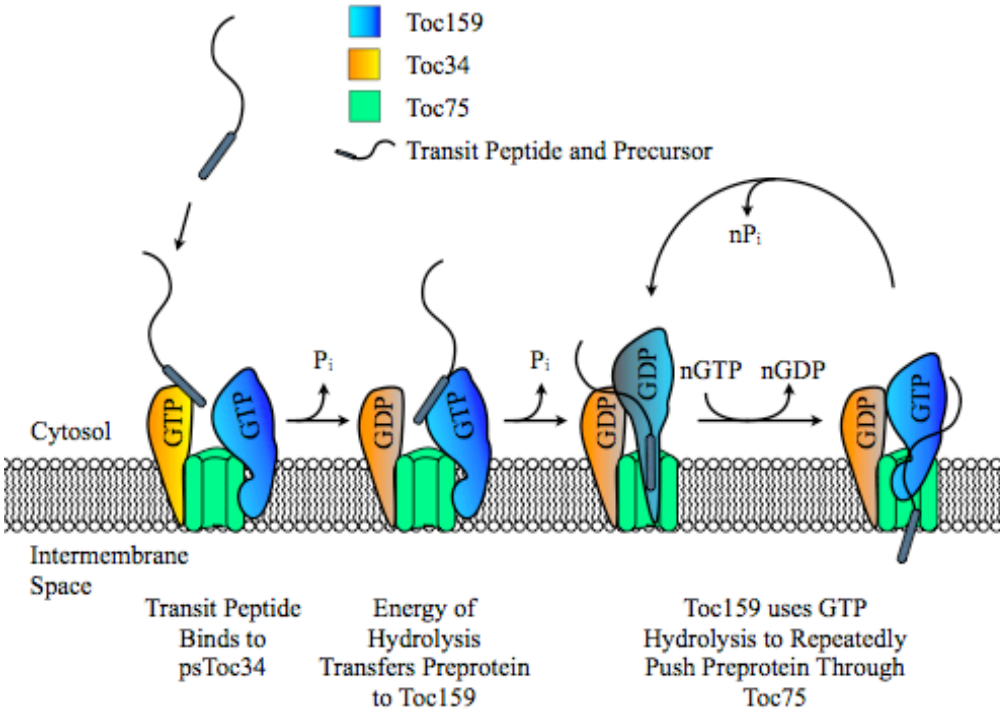


Figure 5-2. The 'motor model' of preprotein recognition by the Toc GTPases. In this model, Toc34 is the primary precursor protein receptor. Toc34 binds the transit peptide at the chloroplast outer membrane. Transit peptide binding stimulates GTP hydrolysis on Toc34 by acting as its GAP. GTP hydrolysis results in the transfer of the peptide to Toc159. GTP hydrolysis by Toc159, stimulated by transit peptide binding, causes a large conformational change in Toc159 such that the preprotein is pushed through the Toc75 translocation channel. Multiple rounds of GTP hydrolysis by Toc159 repeatedly insert and/or push the preprotein across the outer membrane and complete the translocation process. Since the stoichiometry of the isolated Toc complex was 4:4:1, Toc34:Toc75:Toc159, multiple preproteins could be recruited and bound by Toc34 and handed off to Toc159 for insertion.

Toc159 GTPase is able to bind preproteins directly and in a GTP dependent manner (53,54,108) and a knockout mutant of Toc159, termed *ppi2*, was seedling lethal (173). However, this model does not appear to be consistent with reports that GTP hydrolysis was not required by Toc159 or that the G-domain of Toc159 was not essential for protein import (64,66,70).

5.6.2 The Targeting Hypothesis

The eukaryotic SRP-dependent system of protein targeting relies on the recognition of a newly synthesized polypeptide chain prior to its targeting to the translocon by the SRP GTPases (132). In a similar manner, the targeting hypothesis states that a soluble form of Toc159 partitions into the cytosol to recognize, bind and target the newly formed precursor protein to the chloroplast translocon (65). This model is supported by cross-linking studies indicating that Toc159 is the major point of contact for preproteins during the earliest stages of protein import (21,39). Furthermore, antibodies against Toc159 inhibit the formation of a critical import intermediate *in vitro* (174). Suggestive of a cytosolic partitioning of Toc159, equal abundances of Toc159 have been found as soluble cytosolic and membrane associated forms (65). A necessary tenant of this model is the heterodimerization of Toc159 and Toc34. The crystal structure of psToc34 suggested that the Toc GTPases may undergo heterodimerization *in vivo* (61), and our laboratory recently evidenced *in vitro* heterodimerization (Figures 3-5, 3-7 and 4-6). While a soluble, recombinant form of Toc159 has been shown to bind preproteins *in vitro* (35,53), the ability of this Toc159-tp adduct to mediate productive insertion into the translocation channel has yet to be established (70,175). Furthermore, critics of the

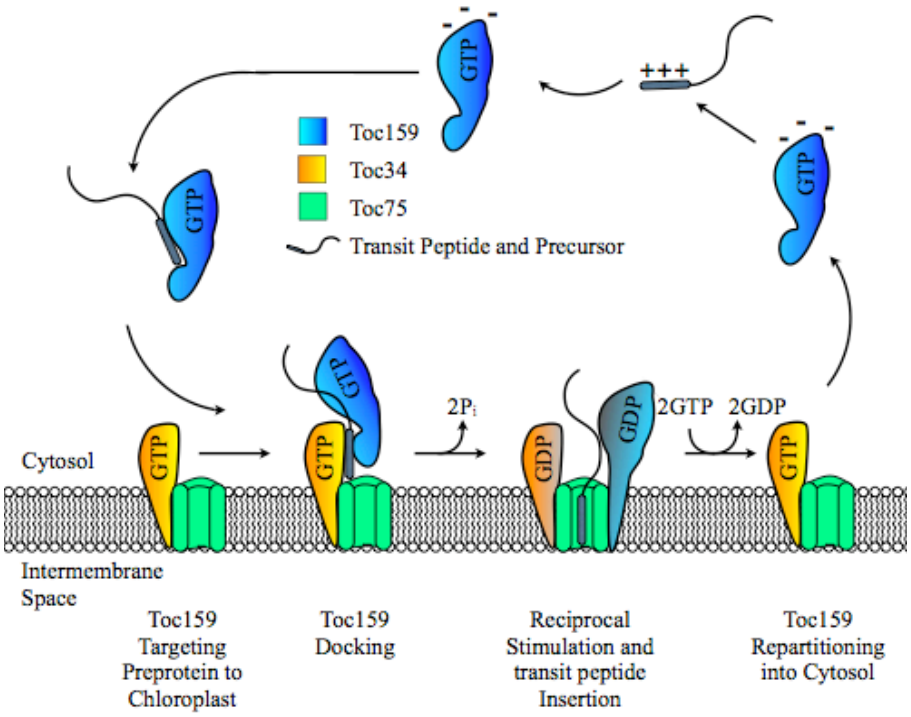


Figure 5-3. The 'targeting model' of preprotein recognition by the Toc GTPases. A newly synthesized preprotein with a positively charged transit peptide is electrostatically attracted to the central, G-domain of cytosolic Toc159 by the negatively charged amino-terminal A domain of Toc159. The preprotein-Toc159 adduct then docks at the outer membrane via heterodimerization between the Toc159 G-domain and Toc34. This G-domain interaction stimulates GTP hydrolysis by both proteins, leading to the incorporation of Toc159 into the chloroplast outer membrane and ultimately into the Toc complex. This results in the insertion of preprotein across the outer envelope membrane and into the Toc75 β-barrel. Once translocation is complete, the two GTPases undergo GDP-GTP exchange. This enables Toc159 to disengage from the Toc complex and partition into the cytosol it can attract another cargo preprotein molecule and begin the cycle again.

targeting hypothesis argue that observation of a soluble pool of Toc159 was an artifact stemming from the chloroplast purification procedure (55).

5.7 The Toc Clock

We have reported the basal enzymatic activities of the Toc GTPases (Chapter II) and shown how these activities are modulated by nucleotides (Chapter II-IV), homo- and heterodimerization (Chapters II-IV) as well as transit peptide interaction (Chapter III and IV). We showed that the Toc159G-transit peptide adduct acts as the Guanine nucleotide Exchange Factor (GEF) for psToc34 (Chapter IV). This GDP for GTP exchange causes psToc34 to gain higher affinity for transit peptide than psToc159G (Chapter III and IV). The interaction of transit peptide with psToc34 stimulates its GTPase activity by acting as its GTPase Activating Protein (GAP) (Chapter II and IV). Additionally, transit peptide interaction with psToc34 and psToc159G resulted in disruption of the dimeric species, however 10-fold less transit peptide was required for psToc34 as compared to psToc159G for dimeric disruption (Chapter IV). Furthermore, the psToc34 hydrolytic transition state takes place in the homodimer and has little affinity for transit peptide (Chapter IV). In light of our observations presented in Chapters II, III and IV, we sought to reconcile our data with previously observed phenomena and create a unified model to attempt to explain the mechanism by which the chloroplast recognizes and imports preproteins.

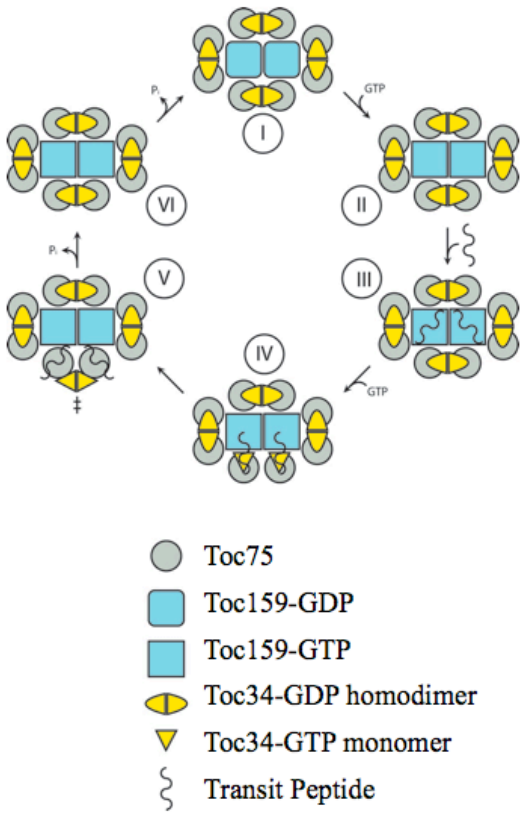


Figure 5-4. The Toc Clock. I: Both Toc159 and Toc34 are in the GDP-bound form, thus the translocon is "off". II: Toc159G binds GTP, increasing its affinity for transit peptide. III: Transit peptide binds to Toc159, increasing the it's affinity to heterodimerize with GDP-bound Toc34. IV: Heterodimerization between tp-bound Toc159 and Toc34 acts as a GEF to exchange GDP for GTP on Toc34. GTP-bound Toc34 is monomeric and has much higher affinity for transit peptide than GTP-bound Toc159. V: Transit peptide interaction with Toc34 acts as a GAP. GTP-hydrolysis occurs in the dimeric form (AlF_4 mimics transition state which is dimeric). The AlF_4 bound Toc34 has low affinity for transit peptide. This step represents the release of transit peptide (concurrent with GTP hydrolysis) to the Toc75 pore. VI: If no further transit peptides are present, Toc159 hydrolyzes GTP at a very slow basal rate, thus recapitulating the ground state, 1.

5.7.1 Step I

The ground state of the complex, with both Toc34 and Toc159 in the GDP-bound form, was shown to be inactive and thus did not bind or import preproteins (52,176). While the isolated Toc core complex possessed a stoichiometry of 4:4:1 and was 13 nm in width (25), more rapid purification techniques have isolated complexes stoichiometrically twice this size (51,100). As stated earlier, freeze fracture studies of the chloroplast outer membrane revealed particles present in the valleys of the outer membrane that were approximately 20-30 nm in diameter (168). Therefore, because stoichiometries of 8:8:2 have been reported and the particles present at the outer membrane are 20-30 nm in diameter, the Toc translocon is presented in the Toc Clock with 8:8:2 stoichiometry.

5.7.2 Step II

While it has been reported that hydrolysis of GTP by Toc159 was not necessary (70), GTP loading of Toc159 was required in order to bind preprotein (65,67). Therefore, Toc159 becomes GTP loaded prior to transit peptide interaction (Step III). The GEF for Toc159 has not been identified (135).

5.7.3 Step III

After Toc159 becomes GTP loaded, it acts as the primary receptor for the transit peptide (35,67,70).

5.7.4 Step IV

The Toc159-transit peptide-adduct was shown to act as the GEF for Toc34 (Figure 4-11) resulting in nucleotide exchange, GTP loading and thus Toc34 activation. Active Toc34 possesses higher affinity than Toc159 and presumably competes transit peptide away from Toc159 (Figures 3-7 and 4-6) and (53,56).

5.7.5 Step V

The transit peptide acts as the GAP for Toc34 (Figures 4-4 and 4-5) and (53,100), stimulating GTP to GDP hydrolysis. The transition state of Toc34 was shown to be dimeric (Figure 3-6) and (129,130) and had significantly reduced affinity for transit peptide (Figure 4-3). This could result in the release of transit peptide into the Toc75 β-barrel in order to complete translocation across the outer membrane of the chloroplast.

5.7.6 Step VI

The hydrolytic events resulting in Step I are not necessary, however are assumed to occur due to the basal hydrolytic rates of the Toc GTPases (Figure 2-3) and (53).

5.8 Summary

By reconciling data observed in our laboratory with reports regarding chloroplast protein import, we synthesized our current model (Figure 5-4). The Toc Clock has six major steps and represents a unified model of chloroplast protein targeting and translocation. The model takes into account data presented in Chapters II through IV with one exception. The GTPase activity of isolated chloroplasts was reduced by the addition

of preproteins (Figure 4-12). The chloroplasts used for kinetic analyses were isolated, thereby removing the various cytosolic GTPases. While the Toc proteins are the only GTPases present at the outer chloroplast envelope, there are stromal GTPases that could be contributing to our measurement (177-179). Measurements reporting basal chloroplast GTPase rates (Figure 4-12, green line) necessarily include all GTPases present. Whether the addition of preprotein inhibited the Toc proteins or whether it inhibited stromal GTPases is not known. More experimentation will be needed to determine whether the data presented in Figure 4-12 represents a real phenomenon related to the Toc GTPases. Therefore, data presented in Figure 4-12 is not included in our model.

Chapter VI

Conclusions and Future Directions

6.1 Conclusions

This study has detailed the *in vitro* enzymology, oligomerization and transit peptide interactions of the Toc GTPases as well as the *in organeller* GTPase activity of isolated chloroplasts allowing, for the first time, the creation of a unified model of chloroplast protein import. This study had initially sought to reconcile enzymatic data that was reported in the literature with significant discrepancies as outlined in (53). Through the adaptation of a previously published ATPase assay (89), a 96-well highly quantitative and high-throughput GTPase assay was devised which has allowed the comparative kinetics of the Toc GTPases to be fully explored. This GTPase assay has proved useful not only in determining various kinetic parameters, but has also revealed that the transit peptide functions as the GAP for psToc34 by stimulating its hydrolytic activity. Furthermore, the application of homobifunctional crosslinking to determine oligomeric status, fluorescence spectroscopy to determine binding sites and interaction domains, as well as quantitative nucleotide release assays have allowed us to develop a working model for chloroplast protein translocation, which we presented in Chapter V.

By assaying the monomer/dimer species of the Toc GTPases, we revealed that both psToc34 and psToc159G homodimerize and heterodimerize. While nucleotides can slightly alter the propensity of the Toc GTPases to dimerize, the dimeric equilibrium is dramatically shifted toward the monomeric species through interaction with transit peptide. The transit peptide acts to stimulate monomerization of both psToc34 and

psToc159, however psToc34 requires ~10-fold less peptide to elicit similar monomerization effects. The transit peptide affinity of the Toc GTPases was also influenced by the bound nucleotide. The GTP-bound form of psToc34 had higher affinity for transit peptide than psToc159G, confirming earlier reports (108). Taking advantage of a robust crosslinking reaction, it was shown that the transition state analogue GDP-AlF_4 caused the psToc34 protein to preferentially form a dimer, indicating that GTP hydrolysis occurs when psToc34 is dimeric. An immobilized affinity assay revealed that when psToc34 is saturated with this transition state analogue it had low affinity for transit peptide. This suggested that GTP hydrolysis is the switch that releases bound transit peptide, presumably into the Toc75 β-barrel protein.

The observation that psToc34 and psToc159G have affinity for transit peptide and this interaction results in an increased hydrolysis rate (at least at psToc34) has been shown in the past (53,55,59,78,100,106). However, the region of the transit peptide to which psToc34 and psToc159 bind remained elusive. By mutating residues at various locations within the transit peptide to cysteine, we performed crosslinking reactions with both psToc34 and psToc159 and the single cysteine mutants of transit peptide. We presented evidence that psToc34 interacted primarily with the C-terminus while psToc159 interacted primarily with the N-terminus. Additionally, the use of three fluorescently labeled transit peptides allowed us to confirm the C-terminal preference of psToc34.

The GTPase Activating Protein, or GAP, for the Toc GTPases was recently revealed by our laboratory (Chapter II and IV, Figures 2-11 and 4-4) and (53). However, identification of a GEF for psToc34 has remained elusive. Many putative GEFs have

been suggested, such as the soluble guidance complex (Figure 1-6) or even the preprotein itself, however none have been shown to be the GEF. We hypothesized that the Toc translocon could be its own regulational unit, and therefore one of the members of the Toc core complex may function as the GEF. Upon testing, this was not shown to be the case (data not shown). However, when psToc159G was incubated with and crosslinked to the S3C transit peptide, the psToc159G-transit peptide adduct did, in fact, stimulate the nucleotide exchange of psToc34 (Figure 4-11). This represented the first time a GEF protein has been identified for the Toc GTPases. Furthermore, the identification of both a GAP and a GEF allowed us to design a model to explain the kinetic and biophysical phenomena we observed. The Toc Clock model represents the reconciliation of enzymatic and biophysical data presented in this dissertation (Figure 5-4).

6.2 Future Directions

As mentioned above, the C-terminus of the transit peptide was shown in both crosslinking and fluorescence assays to primarily interact with psToc34. However, biophysical data on psToc159G is lacking and in need of further analysis. The crosslinking and fluorescence assays are macroscopic observations and the actual residue interactions are still unknown. Further structural work is needed, however the inherently unstructured nature of the peptide makes it recalcitrant to crystallization. In lieu of crystallography, molecular dynamics simulations and/or docking studies may represent good alternatives.

The Toc159G protein used in this study is the central GTPase domain of Toc159. Constructs including the A and M domain have limited or poor solubility (35). Further

study of the A and M domains of this protein are needed. A recent publication has shown with the use of hydrophobic clustering analysis (HCA) that the A and M domains of psToc159 are related to the G domain, however are now no longer capable of binding GTP. Whether this is important for heterodimeric interactions and/or targeting remains to be seen, *e.g.* can psToc34 heterodimerize with psToc159A (180). There have also been reports that the A domain serves as an anchor to the actin cytoskeleton and thereby functions as a terminal destination for preproteins being guided upon the actin network (150). Finally, since both psToc34 and psToc159G come together to form the heterodimer, it will be interesting to see the contributions of each protein to the overall GTPase cycle of the Toc complex. The XTPase sensitive mutants, discussed in Chapter II (Figure 2-12), will aid in this analysis.

Further characterization of the Toc proteins as well as the transit peptide can be aided by mutagenesis. For instance, by mutating cysteines at various locations on both the peptide and the Toc protein, then labeling each with a maleimide-nitroxide spin label, EPR coupling measurements will aid in determining the distances. With enough labeling, one could map the distances related to binding and further refine the interaction. However, our attempts to conservatively mutate the natural cysteine in psToc34 (C215S) have routinely resulted in protein insolubility (data not shown). Also of interest is the orientation of psToc34 on the membrane. We have hypothesized that the protein may orient itself differently depending on its bound nucleotide in order to more readily bind the transit peptide. It has been shown that the galactolipid character of the outer membrane aids in the induction of transit peptide secondary structure (17,21,33,105), which may facilitate Toc protein recognition. Mentioned briefly in Chapter III, the use of

benzophenone labeled liposomes may provide a way to assay the orientation of psToc34 on the membrane.

It was observed that isolated chloroplasts hydrolyzed *less* GTP when presented with high concentrations of preprotein. Naïvely, it was hypothesized that for each preprotein imported through the Toc complex that multiple rounds of GTP hydrolysis would occur. Thus, the incubation of preproteins with isolated chloroplasts would result in the observation of significantly more hydrolytic activity. This was not observed to be the case. Instead, incubation of preproteins with isolated chloroplasts reduced the overall hydrolysis rate: incubation of 0.1 μM and 1.0 μM preprotein resulted in titratable reductions of hydrolysis. More work will be required to understand this enigmatic process.

References

1. Margulis, L. (1975) *Symp Soc Exp Biol*, 21-38
2. Whatley, J. M., John, P., and Whatley, F. R. (1979) *Proc R Soc Lond B Biol Sci* **204**, 165-187
3. Reumann, S., Davila-Aponte, J., and Keegstra, K. (1999) *Proc Natl Acad Sci U S A* **96**, 784-789
4. Reumann, S., Inoue, K., and Keegstra, K. (2005) *Mol Membr Biol* **22**, 73-86
5. Jarvis, P., and Soll, J. (2001) *Biochim Biophys Acta* **1541**, 64-79
6. Karlin-Neumann, G. A., and Tobin, E. M. (1986) *EMBO J* **5**, 9-13
7. Smeekens, S., Bauerle, C., Hageman, J., Keegstra, K., and Weisbeek, P. (1986) *Cell* **46**, 365-375
8. Archer, E. K., and Keegstra, K. (1990) *J Bioenerg Biomembr* **22**, 789-810
9. Cline, K., and Henry, R. (1996) *Annual Review of Cell and Developmental Biology* **12**, 1-26
10. Bolter, B., Soll, J., Schulz, A., Hinnah, S., and Wagner, R. (1998) *Proceedings of the National Academy of Sciences of the United States of America* **95**, 15831-15836
11. Bruce, B. D. (2001) *Biochim Biophys Acta* **1541**, 2-21
12. Martin, W., Stoebe, B., Goremykin, V., Hapsmann, S., Hasegawa, M., and Kowallik, K. V. (1998) *Nature* **393**, 162-165
13. Blanchard, J. L., and Lynch, M. (2000) *Trends Genet* **16**, 315-320
14. Kuchler, M., and Soll, J. (2001) *Plant Science* **161**, 379-389
15. Emanuelsson, O., Nielsen, H., Brunak, S., and von Heijne, G. (2000) *J Mol Biol* **300**, 1005-1016
16. Richly, E., and Leister, D. (2004) *Gene* **329**, 11-16
17. Bruce, B. D. (2000) *Trends Cell Biol* **10**, 440-447
18. Bhushan, S., Kuhn, C., Berglund, A. K., Roth, C., and Glaser, E. (2006) *FEBS Lett* **580**, 3966-3972
19. Kleffmann, T., Russenberger, D., von Zychlinski, A., Christopher, W., Sjolander, K., Gruissem, W., and Baginsky, S. (2004) *Curr Biol* **14**, 354-362
20. Radhamony, R. N., and Theg, S. M. (2006) *Trends Cell Biol* **16**, 385-387
21. Perry, S. E., and Keegstra, K. (1994) *Plant Cell* **6**, 93-105
22. Schnell, D. J., Kessler, F., and Blobel, G. (1994) *Science* **266**, 1007-1012
23. Schnell, D. J., Kessler, F., Blobel, G., Patel, H. A., Hirsch, S., Muckel, E., Heemeyer, F., von Heijne, G., Soll, J., Wu, C., Seibert, S. S., and Ko, K. (1995) *Trends Cell Biol* **5**, 153
24. Kouranov, A., and Schnell, D. J. (1997) *Journal of Cell Biology* **139**, 1677-1685
25. Schleiff, E., Soll, J., Kuchler, M., Kuhlbrandt, W., and Harrer, R. (2003) *J Cell Biol* **160**, 541-551
26. Kouranov, A., Chen, X. J., Fuks, B., and Schnell, D. J. (1998) *Journal of Cell Biology* **143**, 991-1002
27. Stahl, T., Glockmann, C., Soll, J., and Heins, L. (1999) *Journal of Biological Chemistry* **274**, 37467-37472
28. Kovacheva, S., Bedard, J., Patel, R., Dudley, P., Twell, D., Rios, G., Koncz, C., and Jarvis, P. (2005) *Plant Journal* **41**, 412-428

29. Miras, S., Salvi, D., Piette, L., Seigneurin-Berny, D., Grunwald, D., Reinbothe, C., Joyard, J., Reinbothe, S., and Rolland, N. (2007) *Journal of Biological Chemistry* **282**, 29482-29492
30. May, T., and Soll, J. (1999) *Febs Letters* **452**, 52-56
31. Wallas, T. R., Smith, M. D., Sanchez-Nieto, S., and Schnell, D. J. (2003) *J Biol Chem* **278**, 44289-44297
32. Qbadou, S., Becker, T., Mirus, O., Tews, I., Soll, J., and Schleiff, E. (2006) *Embo Journal* **25**, 1836-1847
33. Pinnaduwage, P., and Bruce, B. D. (1996) *J Biol Chem* **271**, 32907-32915
34. Wienk, H. L., Wechselberger, R. W., Czisch, M., and de Kruijff, B. (2000) *Biochemistry* **39**, 8219-8227
35. Smith, M. D., Rounds, C. M., Wang, F., Chen, K., Afitlhile, M., and Schnell, D. J. (2004) *J Cell Biol* **165**, 323-334
36. Chen, K., Chen, X., and Schnell, D. J. (2000) *Biochem Soc Trans* **28**, 485-491
37. Olsen, L. J., Theg, S. M., Selman, B. R., and Keegstra, K. (1989) *J Biol Chem* **264**, 6724-6729
38. Kessler, F., Blobel, G., Patel, H. A., and Schnell, D. J. (1994) *Science* **266**, 1035-1039
39. Ma, Y., Kouranov, A., LaSala, S. E., and Schnell, D. J. (1996) *J Cell Biol* **134**, 315-327
40. Nielsen, E., Akita, M., Davila-Aponte, J., and Keegstra, K. (1997) *EMBO J* **16**, 935-946
41. Olsen, L. J., and Keegstra, K. (1992) *J Biol Chem* **267**, 433-439
42. Young, M. E., Keegstra, K., and Froehlich, J. E. (1999) *Plant Physiol* **121**, 237-244
43. Theg, S. M., Bauerle, C., Olsen, L. J., Selman, B. R., and Keegstra, K. (1989) *J Biol Chem* **264**, 6730-6736
44. Jackson-Constan, D., Akita, M., and Keegstra, K. (2001) *Biochim Biophys Acta* **1541**, 102-113
45. Richter, S., and Lamppa, G. K. (1999) *J Cell Biol* **147**, 33-44
46. Bhushan, S., Stahl, A., Nilsson, S., Lefebvre, B., Seki, M., Roth, C., McWilliam, D., Wright, S. J., Liberles, D. A., Shinozaki, K., Bruce, B. D., Boutry, M., and Glaser, E. (2005) *Plant Cell Physiol* **46**, 985-996
47. Bolter, B., May, T., and Soll, J. (1998) *FEBS Lett* **441**, 59-62
48. Bauer, J., Chen, K., Hiltbunner, A., Wehrli, E., Eugster, M., Schnell, D., and Kessler, F. (2000) *Nature* **403**, 203-207
49. Clantin, B., Delattre, A. S., Rucktooa, P., Saint, N., Meli, A. C., Locht, C., Jacob-Dubuisson, F., and Villeret, V. (2007) *Science* **317**, 957-961
50. Qbadou, S., Becker, T., Bionda, T., Reger, K., Ruprecht, M., Soll, J., and Schleiff, E. (2007) *Journal of Molecular Biology* **367**, 1330-1346
51. Kikuchi, S., Hirohashi, T., and Nakai, M. (2006) *Plant and Cell Physiology* **47**, 363-371
52. Bourne, H. R., Sanders, D. A., and McCormick, F. (1991) *Nature* **349**, 117-127
53. Reddick, L. E., Vaughn, M. D., Wright, S. J., Campbell, I. M., and Bruce, B. D. (2007) *J Biol Chem* **282**, 11410-11426

54. Sveshnikova, N., Soll, J., and Schleiff, E. (2000) *Proc Natl Acad Sci U S A* **97**, 4973-4978
55. Becker, T., Jelic, M., Vojta, A., Radunz, A., Soll, J., and Schleiff, E. (2004) *Embo J* **23**, 520-530
56. Voigt, A., Jakob, M., Klosgen, R. B., and Gutensohn, M. (2005) *FEBS Lett* **579**, 1343-1349
57. Jarvis, P., Chen, L. J., Li, H. M., Pete, C. A., Fankhauser, C., and Chory, J. (1998) *Science* **282**, 100-103
58. Gutensohn, M., Schulz, B., Nicolay, P., and Flugge, U. I. (2000) *Plant J* **23**, 771-783
59. Jelic, M., Soll, J., and Schleiff, E. (2003) *Biochemistry* **42**, 5906-5916
60. Kubis, S., Baldwin, A., Patel, R., Razzaq, A., Dupree, P., Lilley, K., Kurth, J., Leister, D., and Jarvis, P. (2003) *Plant Cell* **15**, 1859-1871
61. Sun, Y. J., Forouhar, F., Li Hm, H. M., Tu, S. L., Yeh, Y. H., Kao, S., Shr, H. L., Chou, C. C., Chen, C., and Hsiao, C. D. (2002) *Nat Struct Biol* **9**, 95-100
62. Yeh, Y. H., Kesavulu, M. M., Li, H. M., Wu, S. Z., Sun, Y. J., Konozy, E. H., and Hsiao, C. D. (2007) *J Biol Chem* **282**, 13845-13853
63. Kessler, F., and Schnell, D. J. (2002) *Nat Struct Biol* **9**, 81-83
64. Chen, K., Chen, X., and Schnell, D. J. (2000) *Plant Physiol* **122**, 813-822
65. Hiltbrunner, A., Bauer, J., Vidi, P. A., Infanger, S., Weibel, P., Hohwy, M., and Kessler, F. (2001) *J Cell Biol* **154**, 309-316
66. Lee, K. H., Kim, S. J., Lee, Y. J., Jin, J. B., and Hwang, I. (2003) *J Biol Chem* **278**, 36794-36805
67. Schleiff, E., Jelic, M., and Soll, J. (2003) *Proc Natl Acad Sci U S A* **100**, 4604-4609
68. Smith, M. D., Hiltbrunner, A., Kessler, F., and Schnell, D. J. (2002) *J Cell Biol* **159**, 833-843
69. Hofmann, N. R., and Theg, S. M. (2005) *Trends in Plant Science* **10**, 450-457
70. Wang, F., Agne, B., Kessler, F., and Schnell, D. J. (2008) *J Cell Biol* **183**, 87-99
71. Sveshnikova, N., Grimm, R., Soll, J., and Schleiff, E. (2000) *Biol Chem* **381**, 687-693
72. America, T., Hageman, J., Guera, A., Rook, F., Archer, K., Keegstra, K., and Weisbeek, P. (1994) *Plant Mol Biol* **24**, 283-294
73. Hinnah, S. C., Wagner, R., Sveshnikova, N., Harrer, R., and Soll, J. (2002) *Biophysical Journal* **83**, 899-911
74. Bourne, H. R., Sanders, D. A., and McCormick, F. (1990) *Nature* **348**, 125-132
75. Subramanian, C., Ivey, R., and Bruce, B. D. (2001) *Plant Journal* **25**, 349-363
76. Bos, J. L., Rehmann, H., and Wittinghofer, A. (2007) *Cell* **129**, 865-877
77. Weibel, P., Hiltbrunner, A., Brand, L., and Kessler, F. (2003) *J Biol Chem* **278**, 37321-37329
78. Jelic, M., Sveshnikova, N., Motzkus, M., Horth, P., Soll, J., and Schleiff, E. (2002) *Biol Chem* **383**, 1875-1883
79. Cline, K., Keegstra, K., and Staehelin, L. A. (1985) *Protoplasma* **125**, 111-123
80. Schnell, D. J., and Blobel, G. (1993) *J Cell Biol* **120**, 103-115
81. Scott, S. V., and Theg, S. M. (1996) *J Cell Biol* **132**, 63-75

82. Akita, M., Nielsen, E., and Keegstra, K. (1997) *J Cell Biol* **136**, 983-994
83. Heins, L., Mehrle, A., Hemmler, R., Wagner, R., Kuchler, M., Hormann, F., Sveshnikov, D., and Soll, J. (2002) *EMBO J* **21**, 2616-2625
84. Inaba, T., Alvarez-Huerta, M., Li, M., Bauer, J., Ewers, C., Kessler, F., and Schnell, D. J. (2005) *Plant Cell* **17**, 1482-1496
85. Inaba, T., Li, M., Alvarez-Huerta, M., Kessler, F., and Schnell, D. J. (2003) *J Biol Chem* **278**, 38617-38627
86. Wu, C., Seibert, F. S., and Ko, K. (1994) *J Biol Chem* **269**, 32264-32271
87. Chou, M. L., Fitzpatrick, L. M., Tu, S. L., Budziszewski, G., Potter-Lewis, S., Akita, M., Levin, J. Z., Keegstra, K., and Li, H. M. (2003) *EMBO J* **22**, 2970-2980
88. Chen, X., Smith, M. D., Fitzpatrick, L., and Schnell, D. J. (2002) *Plant Cell* **14**, 641-654
89. Ivey, R. A., 3rd, Subramanian, C., and Bruce, B. D. (2000) *Plant Physiol* **122**, 1289-1299
90. Waegemann, K., and Soll, J. (1996) *J Biol Chem* **271**, 6545-6554
91. Jarvis, P. (2008) *New Phytologist* **179**, 257-285
92. Moreau, P., Bessoule, J., S, M., E, T., P, V., and C, C. (1998) *Prog Lipid Res* **37**, 371-391
93. Andersson, M. X., Kjellberg, J. M., and Sandelius, A. S. (2004) *Biochim Biophys Acta* **1684**, 46-53
94. Wienk, H. L., Czisch, M., and de Kruijff, B. (1999) *FEBS Lett* **453**, 318-326
95. Chen, L., and Li, H. (1998) *Plant Journal* **16**, 33-39
96. Dabney-Smith, C., van Den Wijngaard, P. W., Treece, Y., Vredenberg, W. J., and Bruce, B. D. (1999) *J Biol Chem* **274**, 32351-32359
97. Lee, D. W., Lee, S., Lee, G. J., Lee, K. H., Kim, S., Cheong, G. W., and Hwang, I. (2006) *Plant Physiology* **140**, 466-483
98. Ambroggio, E. E., Austen, B., and Fidelio, G. D. (2007) *Journal of Peptide Science* **13**, 245-252
99. Buvinger, W. E., Michel, H., and Bennett, J. (1989) *J Biol Chem* **264**, 1195-1202
100. Reddick, L. E., Chotewutmontri, P., Crenshaw, W., Dave, A., Vaughn, M., and Bruce, B. D. (2008) *Methods Cell Biol* **90**, 365-398
101. Wienk, H. L., and de Kruijff, B. (1999) *Protein Expr Purif* **17**, 345-350
102. von Heijne, G., Steppuhn, J., and Herrmann, R. G. (1989) *Eur J Biochem* **180**, 535-545
103. Pilon, M., Wienk, H., Sips, W., de Swaaf, M., Talboom, I., van 't Hof, R., de Korte-Kool, G., Demel, R., Weisbeek, P., and de Kruijff, B. (1995) *J Biol Chem* **270**, 3882-3893
104. Krimm, I., Goyer, A., Issakidis-Bourguet, E., Miginiac-Maslow, M., and Lancelin, J. M. (1999) *J Biol Chem* **274**, 34539-34542
105. Lancelin, J. M., Bally, I., Arlaud, G. J., Blackledge, M., Gans, P., Stein, M., and Jacquot, J. P. (1994) *FEBS Lett* **343**, 261-266
106. Aronsson, H., Combe, J., and Jarvis, P. (2003) *FEBS Lett* **544**, 79-85
107. Kessler, F., and Schnell, D. J. (2006) *Traffic* **7**, 248-257

108. Schleiff, E., Soll, J., Sveshnikova, N., Tien, R., Wright, S., Dabney-Smith, C., Subramanian, C., and Bruce, B. D. (2002) *Biochemistry* **41**, 1934-1946
109. Bauer, J., Hiltbrunner, A., Weibel, P., Vidi, P. A., Alvarez-Huerta, M., Smith, M. D., Schnell, D. J., and Kessler, F. (2002) *J Cell Biol* **159**, 845-854
110. Shan, S. O., Stroud, R. M., and Walter, P. (2004) *PLoS Biol* **2**, e320
111. Sreerama, N., and Woody, R. W. (2000) *Anal Biochem* **287**, 252-260
112. Schweins, T., Scheffzek, K., Assheuer, R., and Wittinghofer, A. (1997) *J Mol Biol* **266**, 847-856
113. Scheffzek, K., Ahmadian, M. R., Kabsch, W., Wiesmuller, L., Lautwein, A., Schmitz, F., and Wittinghofer, A. (1997) *Science* **277**, 333-338
114. Nassar, N., Hoffman, G. R., Manor, D., Clardy, J. C., and Cerione, R. A. (1998) *Nat Struct Biol* **5**, 1047-1052
115. Graham, D. L., Lowe, P. N., Grime, G. W., Marsh, M., Rittinger, K., Smerdon, S. J., Gamblin, S. J., and Eccleston, J. F. (2002) *Chem Biol* **9**, 375-381
116. Schmidt, G., Lenzen, C., Simon, I., Deuter, R., Cool, R. H., Goody, R. S., and Wittinghofer, A. (1996) *Oncogene* **12**, 87-96
117. Liu, X., Choudhury, S., and Roy, R. (2003) *J Biol Chem* **278**, 50061-50069
118. Lu, G., Westbrooks, J. M., Davidson, A. L., and Chen, J. (2005) *Proc Natl Acad Sci U S A* **102**, 17969-17974
119. Raimo, G., Masullo, M., and Bocchini, V. (1995) *J Biol Chem* **270**, 21082-21085
120. Bhushan, S., Kuhn, C., Berglund, A. K., Roth, C., and Glaser, E. (2006) *FEBS Letters* **580**, 3966-3972
121. Bedard, J., and Jarvis, P. (2005) *J Exp Bot* **56**, 2287-2320
122. Chen, K. Y., and Li, H. M. (2007) *Plant Journal* **49**, 149-158
123. Oreb, M., Hofle, A., Mirus, O., and Schleiff, E. (2008) *Journal of Experimental Botany* **59**, 2309-2316
124. Keana, J. F., and Roman, R. B. (1978) *Membr Biochem* **1**, 323-327
125. le Maire, M., Champeil, P., and Moller, J. V. (2000) *Biochim Biophys Acta* **1508**, 86-111
126. Collins, M. L., and Salton, M. R. (1979) *Biochim Biophys Acta* **553**, 40-53
127. Schagger, H., and von Jagow, G. (1987) *Anal Biochem* **166**, 368-379
128. Qbadou, S., Tien, R., Soll, J., and Schleiff, E. (2003) *J Cell Sci* **116**, 837-846
129. Koenig, P., Oreb, M., Hofle, A., Kaltofen, S., Rippe, K., Sinning, I., Schleiff, E., and Tews, I. (2008) *Structure* **16**, 585-596
130. Koenig, P., Oreb, M., Rippe, K., Muhle-Goll, C., Sinning, I., Schleiff, E., and Tews, I. (2008) *J Biol Chem* **283**, 23104-23112
131. Egea, P. F., Shan, S. O., Napetschnig, J., Savage, D. F., Walter, P., and Stroud, R. M. (2004) *Nature* **427**, 215-221
132. Focia, P. J., Shepotinovskaya, I. V., Seidler, J. A., and Freymann, D. M. (2004) *Science* **303**, 373-377
133. Wright, S. J. (2006) *Master of Science Thesis*
134. Peluso, P., Shan, S. O., Nock, S., Herschlag, D., and Walter, P. (2001) *Biochemistry* **40**, 15224-15233
135. Agne, B., and Kessler, F. (2009) *FEBS J* **276**, 1156-1165
136. Cline, K., Henry, R., Li, C., and Yuan, J. (1993) *EMBO J* **12**, 4105-4114

137. Zhang, X. P., and Glaser, E. (2002) *Trends Plant Sci* **7**, 14-21
138. May, T., and Soll, J. (2000) *Plant Cell* **12**, 53-64
139. de Castro Silva Filho, M., Chaumont, F., Leterme, S., and Boutry, M. (1996) *Plant Mol Biol* **30**, 769-780
140. Rudhe, C., Chew, O., Whelan, J., and Glaser, E. (2002) *Plant J* **30**, 213-220
141. Roise, D., and Schatz, G. (1988) *J Biol Chem* **263**, 4509-4511
142. McWilliams, D. R. (2007)
143. Krieg, U. C., Walter, P., and Johnson, A. E. (1986) *Proc Natl Acad Sci U S A* **83**, 8604-8608
144. Inoue, H., and Akita, M. (2008) *Arch Biochem Biophys*
145. Ahmadian, M. R., Mittal, R., Hall, A., and Wittinghofer, A. (1997) *FEBS Lett* **408**, 315-318
146. Inoue, K., Demel, R., de Kruijff, B., and Keegstra, K. (2001) *European Journal of Biochemistry* **268**, 4036-4043
147. Inoue, K., and Keegstra, K. (2003) *Plant Journal* **34**, 661-669
148. Gutensohn, M., Fan, E., Frielingsdorf, S., Hanner, P., Hou, B., Hust, B., and Klosgen, R. B. (2006) *Journal of Plant Physiology* **163**, 333-347
149. Hiltbrunner, A., Bauer, J., Alvarez-Huerta, M., and Kessler, F. (2001) *Biochem Cell Biol* **79**, 629-635
150. Jouhet, J., and Gray, J. C. (2009) *J Biol Chem* **284**, 19132-19141
151. Sharom, F. J., Russell, P. L., Qu, Q., and Lu, P. (2003) *Methods Mol Biol* **227**, 109-128
152. Kohda, D. (2005)
153. Li, H. M., Kesavulu, M. M., Su, P. H., Yeh, Y. H., and Hsiao, C. D. (2007) *J Biomed Sci* **14**, 505-508
154. Bange, G., Petzold, G., Wild, K., Parlitz, R. O., and Sinning, I. (2007) *Proc Natl Acad Sci U S A* **104**, 13621-13625
155. Gasper, R., Scrima, A., and Wittinghofer, A. (2006) *J Biol Chem* **281**, 27492-27502
156. Kosloff, M., and Selinger, Z. (2003) *J Mol Biol* **331**, 1157-1170
157. Vetter, I. R., and Wittinghofer, A. (2001) *Science* **294**, 1299-1304
158. Stengel, A., Soil, J., and Bolter, B. (2007) *Biological Chemistry* **388**, 765-772
159. Inaba, T., and Schnell, D. J. (2008) *Biochemical Journal* **413**, 15-28
160. Gray, M. W., and Doolittle, W. F. (1982) *Microbiol Rev* **46**, 1-42
161. Giovannoni, S. J., Turner, S., Olsen, G. J., Barns, S., Lane, D. J., and Pace, N. R. (1988) *J Bacteriol* **170**, 3584-3592
162. Inoue, K., and Potter, D. (2004) *Plant J* **39**, 354-365
163. Reumann, S., and Keegstra, K. (1999) *Trends in Plant Science* **4**, 302-307
164. Alto, N. M. (2008) *Cell Microbiol* **10**, 566-575
165. Alto, N. M., and Dixon, J. E. (2008) *Methods Enzymol* **439**, 131-143
166. Dong, J. H., Wen, J. F., and Tian, H. F. (2007) *Gene* **396**, 116-124
167. Vojta, L., Soll, J., and Bolter, B. (2007) *Febs Letters* **581**, 2621-2624
168. Cline, K., Keegstra, K., and Staehelin, L. A. (1985) *Protoplasma* **125**, 111-123
169. Simpson, D. J. (1983) *Eur J Cell Biol* **31**, 305-314
170. Staehelin, L. A., and DeWit, M. (1984) *J Cell Biochem* **24**, 261-269

171. Oreb, M., Tews, I., and Schleiff, E. (2008) *Trends Cell Biol* **18**, 19-27
172. Papanikou, E., Karamanou, S., and Economou, A. (2007) *Nat Rev Microbiol* **5**, 839-851
173. Bauer, J., Chen, K. H., Hiltbunner, A., Wehrli, E., Eugster, M., Schnell, D., and Kessler, F. (2000) *Nature* **403**, 203-207
174. Hirsch, S., Muckel, E., Heemeyer, F., von Heijne, G., and Soll, J. (1994) *Science* **266**, 1989-1992
175. Yu, T. S., and Li, H. (2001) *Plant Physiol* **127**, 90-96
176. Soll, J., and Schleiff, E. (2004) *Nat Rev Mol Cell Biol* **5**, 198-208
177. Chigri, F., Sippel, C., Kolb, M., Vothknecht, U. (2009) *Molecular Plant* **2**, 1373-1383
178. Hoffman, N. E., and Franklin, A. E. (1994) *Plant Physiol* **105**, 295-304
179. Wang, F., Zhong, N. Q., Gao, P., Wang, G. L., Wang, H. Y., and Xia, G. X. (2008) *Plant Cell Environ* **31**, 982-994
180. Hernandez Torres, J., Maldonado, M. A., and Chomilier, J. (2007) *Biochem Biophys Res Commun* **364**, 325-331

Vita

Lovett Evan Reddick was born in Chattanooga in 1978, growing up in Kingsport, Tennessee. He graduated Dobyns-Bennett High School in 1996 and the University of Tennessee in 2001. During college he worked as a molecular and cellular biology laboratory technician at ORNL. In the spring of 2003, he joined the Graduate Program in Biochemistry, Cellular and Molecular Biology at the University of Tennessee. His research interests involved post-translational transport of proteins across the chloroplast double membrane - a system that has proved challenging in the past. His dissertation research uncovered several mechanistic steps and afforded him the ability to create a "Unified Model of Chloroplast Protein Import" which seeks to reconcile his and others' biochemical and biophysical evidence. He has published papers in the *Journal of Biological Chemistry*, *Nano Letters*, *Methods in Cell Biology*, *Biomedical Concepts*, and will submit three papers the year of his graduation to *Plant Cell*, *The EMBO Journal*, and *Biochemistry*. During graduate school, Evan was the two-time recipient of the UT Knoxville Science Alliance Award, he received a 2008 Chancellor's Award for Professional Promise and was inducted into the scientific research society Sigma Xi, where he was recently awarded 1st prize in the University of Tennessee Sigma Xi lecture series. He has given invited lectures at the Univ. Pennsylvania, Vanderbilt Univ. Medical Center and the National Cancer Institute at the National Institutes of Health. He has served on the BCMB Department Graduate Recruiting Committee and the Retreat Planning Committee. Evan defended his dissertation in October of 2009 and graduated in December of the same year. In January of 2010, Evan will begin a Postdoctoral Fellowship at the University of Texas Southwestern Medical Center in Dallas Texas where his research will seek to understand the structure/function relationship between enteropathogenic bacterial effector proteins and GTP-binding proteins present in human intestinal cells, the goal of which will be to design novel therapeutics to combat the diseases caused by a wide variety of malicious bacteria.